

©[2012]

Qiang Zhang

ALL RIGHTS RESERVED

REGULATION OF DRUG TRANSPORTERS

By

QIANG ZHANG

A dissertation submitted to the Graduate School-New Brunswick

Rutgers, The State University of New Jersey

In partial fulfillment of the requirements

For the degree of

Doctor of Philosophy

Graduate Program in Pharmaceutical Sciences

Written under the direction of

Professor Guofeng You, Ph.D.

And approved by

New Brunswick, New Jersey

May, 2012

ABSTRACT OF THE DISSERTATION

Regulation of Drug Transporters

By QIANG ZHANG

Dissertation Director:

Guofeng You

Organic anion transporters (OATs) are of great importance in the body disposition of a variety of clinical drugs, including anti-cancer, anti-HIV, antibiotics and anti-inflammatory drugs. Long-term regulations of OATs are mainly mediated by gene expression, and short-term regulations are mainly post-translational modifications such as phosphorylation and glycosylation.

In the present study, we investigate the constitutive and PKC-regulated trafficking of both hOAT1 and hOAT4 in COS-7 cells. We observed that the internalization of both transporters was accelerated by PKC activation in COS-7 cells. However, the recycling rate of hOAT1 was not affected by PMA treatment. Using approaches of pharmacology and molecular biology, hOAT1 and hOAT4 transporters have been demonstrated to internalize partly via a dynamin- and clathrin-dependent pathway.

We observed that overexpression of NHERF1 significantly delayed the internalization of hOAT4 and this observation suggests that the interaction between the PDZ-binding motif of hOAT4 and NHERF1 is involved in the regulation of hOAT4 trafficking by NHERF1. The simultaneous mutations of both leucine residues (L6A/L7A) of hOAT1 resulted in a complete loss of function and the complete loss of function of L6A/L7A hOAT1 was due to the absence of mature form of this mutant at the cell surface and in total cellular

extract. It seems that the L6L7 motif does not play a role in the hOAT1 trafficking from the cell surface, and may be involved in its stability.

Ubiquitination of membrane proteins has been shown to regulate internalization, postinternalization sorting and degradation of other membrane proteins. Our current investigation focuses on the internalization and degradation of OATs transporters. The major discoveries from our current study are 1) activation of PKC promotes OAT1 ubiquitination both in vitro and in vivo. 2) OAT1 ubiquitination mainly occurs through K48-linked polyubiquitin chains. 3) K48-linked polyubiquitination plays an essential role in PKC-regulated internalization and degradation of OAT1.

DEDICATION

To my wonderful parents,

Who always gave me moral support and instilled the importance of hard work and
commitment to research into my mind.

To my supervisor, Professor Guofeng You,

Who has always given me valuable suggestions, encouragement, and continued support.

To my beloved wife, Min,

Whose love has supported me and encouraged me to complete this work.

To my beloved son, Aiden,

Whose smile gives me happiness, courage, and patience.

ACKNOWLEDGEMENTS

First, I would like to express my gratitude to my supervisor, Dr. Guofeng You, who has supported me throughout my Ph.D. studies with her patience, guidance, support and valuable suggestions. Without her encouragement and enormous effort this dissertation would not have been possible to be completed.

I would like to thank my committee members: Dr. Tamara Minko, Dr. Bozena Michniak-Kohn, and Dr. Zui Pan for their helpful suggestions and valuable time.

I would like to thank Dr. Zui Pan for helping me with the confocal microscopy, which made my research possible to complete. I also want to thank Dr. Xiaoping Zhang for his helpful suggestions to my research.

I am grateful to many of my former and present colleagues in Dr. You's group who help me with my research. They are Dr. Mei Hong, Dr. Fanfan Zhou, Dr. Weinan Du, Dr. Xingxiang Peng, Ms. Jinwei Wu, Dr. Peng Duan, Shanshan Li, Wonmo Suh, and Da Xu. I would also like to thank them for their support and help.

I am also grateful to Marianne Shen, Hui Pung, Sharana Taylor and other colleagues in the Department of Pharmaceutics for their kind help and patience.

I wish to express my deepest love and gratitude to my beloved families. I am so grateful to my parents for their love, support and encouragement in my life. In particular, to my wife, Min, I greatly appreciate what she has done for me in my research and life. She always gives me her endless support and helped me with her heart whenever I need her. I also want thank my adorable son, Aiden. Although he just became a member of my family in December of 2011, his smile has already made me stronger. Without their support, I could not make this dissertation possible.

I would also like to thank my parents-in-law for their love and support.

Lastly, I offer my regards and blessings to all of those who supported me in any respect during the completion of my dissertation.

TABLE OF CONTENTS

ABSTRACT OF THE DISSERTATION	ii
DEDICATION	iv
ACKNOWLEDGEMENTS	v
TABLE OF CONTENTS.....	vii
LIST OF FIGURES	x
1 Overview	1
2 Regulation of OATs by membrane trafficking.....	3
2.1 Introduction	3
2.2 Materials and methods	4
2.2.1 Materials and instruments	4
2.2.2 Experimental procedures	6
2.3 Results	17
2.3.1 Constitutive internalization of OAT proteins	17
2.3.2 Constitutive recycling of OAT proteins.....	23
2.3.3 PKC-regulated membrane trafficking of OAT1	29
2.3.4 PKC-regulated membrane trafficking of OAT4	37
2.3.5 Endocytosis pathway of OAT1	40
2.3.6 Endocytosis pathway of OAT4.....	52
2.4 Discussion	60
3 Regulation of OATS by structure motives	66
3.1 Introduction	66
3.2 Materials and Methods	67

3.2.1	Materials and Instruments	67
3.2.2	Experimental Procedures	69
3.3	Results	82
3.3.1	Regulation of hOAT4 internalization by NHERF1	82
3.3.2	Role of the dileucine motif (L6L7) at the amino terminus of hOAT1.....	86
3.4	Discussion	94
3.4.1	PDZ-binding motif and NHERF1	94
3.4.2	Dileucine motif	96
4	Regulation of OATs by ubiquitination	99
4.1	Introduction	99
4.2	Materials and Methods	100
4.2.1	Materials and Instruments	100
4.2.2	Experimental Procedures	101
4.3	Results	126
4.3.1	<i>In vitro</i> PMA-induced ubiquitination of OAT1	126
4.3.2	PMA-induced ubiquitination of rat OAT1 in rat kidney slices.....	129
4.3.3	PMA-induced ubiquitination of OAT1 is sensitive to PKC inhibitor treatment	130
4.3.4	PMA-induced ubiquitination of cell surface OAT1.....	131
4.3.5	Affinity purification and mass spectrometric analysis of ubiquitinated OAT1 proteins	133
4.3.6	Effects of ubiquitin mutants on PMA-induced ubiquitination of OAT1 ..	134

4.3.7	Effect of K48R ubiquitin mutant on PMA-induced reduction of cell surface OAT1	135
4.3.8	Effect of K48R ubiquitin mutant on PKC-regulated internalization of OAT1	137
4.3.9	Multiple lysine substitutions of OAT1 inhibit PMA-induced ubiquitination	138
4.3.10	Down-regulation of OAT1 by PKC activation is decreased by multilycine mutation	140
4.3.11	Multiple lysine substitutions of OAT1 inhibit PMA-induced internalization	141
4.3.12	Effect of PKC activation on the degradation of surface OAT1	143
4.3.13	Effect of K48R ubiquitin mutant on PKC-regulated degradation of surface OAT1	145
4.3.14	Multiple lysine substitutions of OAT1 inhibit PMA-induced degradation of surface hOAT1	147
4.4	Discussion	148
5	References	152
6	Curriculum Vitae	160

LIST OF FIGURES

Figure 2-1 Constitutive internalization of human OAT1 in COS-7 cells.	18
Figure 2-2 Total expression of human OAT1 in cell lysate of COS-7 cells as a loading control..	19
Figure 2-3 Densitometry plot of three independent experiments of COS-7 cells.....	19
Figure 2-4 Constitutive internalization of human OAT1 in LLC-PK1 cells.	20
Figure 2-5 Total expression of human OAT1 in cell lysate of LLC-PK1 cells as a loading control..	20
Figure 2-6 Densitometry plot of three independent experiments of LLC-PK1 cells.....	21
Figure 2-7 Constitutive internalization of human OAT4 in COS-7 cells	22
Figure 2-8 Densitometry plot of three independent experiments of COS-7 cells.....	23
Figure 2-9 Constitutive recycling of transferrin receptor in COS-7 cells.....	24
Figure 2-10 Constitutive recycling of Na/K-ATPase in COS-7 cells.....	25
Figure 2-11 Constitutive recycling of human OAT1 in COS-7 cells.	26
Figure 2-12 Densitometry plot of three independent recycling experiments of human OAT1 in COS-7 cells.....	27
Figure 2-13 Effect of cycloheximide treatment on the total and surface expression levels of hOAT1 in COS-7 cells	27
Figure 2-14 Constitutive recycling of transferrin receptor (TfR) in COS-7 cells.....	28
Figure 2-15 Constitutive recycling of human OAT4 (hOAT4) in COS-7 cells.	28
Figure 2-16 Densitometry plot of three independent recycling experiments of human OAT4 in COS-7 cells.....	29
Figure 2-17 Characterization of hOAT1 in COS-7 cells.	30

Figure 2-18 PKC-activation induced cellular re-distribution of hOAT1 in COS-7 cells..	32
Figure 2-19 Internalization analysis of hOAT1 following PKC activation.....	34
Figure 2-20 Total expression of hOAT1 in cell lysate in parallel to internalization experiment as the loading control..	34
Figure 2-21 Densitometry plot of internalization analysis of hOAT1 following PKC activation.....	35
Figure 2-22 Recycling analysis of hOAT1 after PKC activation..	36
Figure 2-23 Densitometry plot of recycling analysis of hOAT1 following PKC activation in COS-7 cells.....	37
Figure 2-24 PKC-activation induced cellular redistribution of hOAT4 in COS-7 cells...	38
Figure 2-25 Internalization analysis of hOAT4 after PKC activation in COS-7 cells.....	39
Figure 2-26 Effect of dominant negative mutant of dynamin-2 on the distribution of hOAT1 in COS-7 cells.....	41
Figure 2-27 Effect of dominant negative mutant of dynamin-2 on the function of hOAT1 in COS-7 cells.....	42
Figure 2-28 Effect of dominant negative mutant of dynamin-2 on the constitutive and PKC-modulated internalization of hOAT1 in COS-7 cells..	43
Figure 2-29 Densitometry plot of results from effect of dynamin-2 mutant on OAT1 internalization..	44
Figure 2-30 Effect of ConA on the constitutive and PKC-modulated internalization of hOAT1 in COS-7 cells.....	45
Figure 2-31 Densitometry of internalization analysis of of hOAT1 in COS-7 cells treated with ConA.....	46

Figure 2-32 Effect of potassium depletion on the constitutive and PKC-modulated internalization of hOAT1 in COS-7 cells..	47
Figure 2-33 Densitometry of internalization analysis of hOAT1 in COS-7 cells treated with potassium depletion.	47
Figure 2-34 Effect of dominant negative mutant of Eps15 on the constitutive internalization of hOAT1 in COS-7 cells.	48
Figure 2-35 Effect of dominant negative mutant of Eps15 on the function of hOAT1 in COS-7 cells.	49
Figure 2-36 Immunolocalization of hOAT1 and transferrin in COS-7 cells.	52
Figure 2-37 Effect of dominant negative mutant of dynamin-2 on the internalization of hOAT4 in COS-7 cells.	53
Figure 2-38 Effect of dominant negative mutant of dynamin-2 on the steady-state surface expression of hOAT4 in COS-7 cells.	55
Figure 2-39 Effect of dominant negative mutant of dynamin-2 on the function of hOAT4 in COS-7 cells.	55
Figure 2-40 Effect of dominant negative mutant of Eps15 on the internalization of hOAT4 in COS-7 cells.	57
Figure 2-41 Effect of dominant negative mutant of Eps15 on the steady-state surface expression of hOAT4 in COS-7 cells.	58
Figure 2-42 Effect of dominant negative mutant of Eps15 on the function of hOAT4 in COS-7 cells.	58
Figure 2-43 Immunolocalization of hOAT4 and EEA1 in COS-7 cells.	59

Figure 3-1 Effect of NHERF1 transfection on the steady-state surface expression of hOAT4 in COS-7 cells.....	84
Figure 3-2 Effect of NHERF1 transfection on the internalization of hOAT4 in COS-7 cells.	85
Figure 3-3 Predicted transmembrane topology of hOAT1.	87
Figure 3-4 ³ H-labeled PAH uptake by hOAT1 wild type (Wt) and its alanine-substituted mutants L6A, L7A, and L6A/L7A.....	88
Figure 3-5 Cell surface and total cell expression of hOAT1 Wt and its mutant L6A/L7A.	89
Figure 3-6 Effect of protease inhibitors on the total expression of hOAT1 Wt and its mutant L6A/L7A.....	91
Figure 3-7 Immunolocalization of L6A/L7A hOAT1.	92
Figure 3-8 Effect of chemical chaperones on the expression of L6A/L7A.	94
Figure 4-1 PKC-dependent ubiquitination of hOAT1 in COS-7 cells.....	126
Figure 4-2 PKC-dependent ubiquitination of hOAT1 in COS-7 cells following transfection of empty vector and HA-tagged ubiquitin..	128
Figure 4-3 Time-dependence of ubiquitination of hOAT1 in COS-7 cells.	129
Figure 4-4 PMA-induced ubiquitination of rat OAT1 in vivo.....	130
Figure 4-5 Blocking of PMA-induced ubiquitination of hOAT1 by staurosporine treatment. a. Endogenous ubiquitin. b. Transfected HA-ubiquitin.	131
Figure 4-6 PKC-dependent ubiquitination of hOAT1 occurs at the plasma membrane..	132
Figure 4-8 Effects of ubiquitin mutants on PMA-induced ubiquitination of hOAT1. ...	135

Figure 4-9 Effect of K48R ubiquitin mutant on PMA-induced reduction of cell surface hOAT1.	136
Figure 4-10 Effect of K48R ubiquitin mutant on PKC-regulated internalization of hOAT1.	138
Figure 4-11 Effect of multiple lysine mutation on PKC-induced ubiquitination of hOAT1..	139
Figure 4-12 Effect of multiple lysine mutation on PKC-induced down-regulation of surface hOAT1.....	141
Figure 4-13 Effect of multiple lysine mutation on PKC-induced endocytosis of hOAT1.	143
Figure 4-14 Effect of PKC activation on the degradation of surface hOAT1.	144
Figure 4-15 Effect of PKC activation on the degradation of surface hOAT3	145
Figure 4-16 Effect of K48R ubiquitin mutant on PKC-regulated degradation of surface hOAT1.	146
Figure 4-17 Effect of multiple lysine substitutions on PKC-induced degradation of surface hOAT1.	148

1 Overview

A large number of in vitro and in vivo studies have documented that drug transporters are one of the determinant factors controlling drug disposition (1, 2). In human body, drug transporters are expressed in a range of tissues and organs involved in drug disposition, such as the intestine, brain, liver and kidney. Present in these important organs, drug transporters play critical roles in drug absorption, distribution, and elimination. It has been also shown that some significant drug-drug interactions in the clinic are mediated by drug transporters. Therefore, a better understanding of the regulation of drug transporters in vitro and in vivo will facilitate the research of pharmacokinetics and pharmacodynamics of drug candidates, and the process of drug discovery and development.

Organic anion transporters (OAT) are of great importance in the body disposition of a variety of clinical drugs, including anti-cancer, anti-HIV, antibiotics and anti-inflammatory drugs (3, 4). All the members of OAT family share some important structural features (5). First, they have similar molecular sizes; second, they all have twelve transmembrane domains with both amino and carboxyl termini locating intracellularly; third, they all have a large extracellular loop between transmembrane domain 1 and 2, and a large intracellular loop between transmembrane domain 6 and 7; in addition, they have glycosylation sites present in the extracellular loop and putative phosphorylation sites located in the intracellular loop (5).

As the first cloned member of OAT family, OAT1 is predominantly expressed in the kidney and weakly expressed in the brain. In the kidney, OAT1 protein is primarily

localized at the basolateral membrane of proximal tubular cells. With weak expression in the kidney, OAT2 is predominantly expressed in the liver. OAT3 is expressed in the kidney, liver and brain. In the kidney, like OAT1, OAT3 is localized at the basolateral membrane of proximal tubular cells. In the brain, OAT3 is present in the brush-border member of choroid plexus cells and capillary endothelial cells (3). In addition to being expressed in the kidney, OAT4 is also localized at the fetal side of syncytiotrophoblast cells in the placenta (3).

Under different conditions, OAT proteins can be regulated in a long-term or short-term manner. Long-term regulations of OAT are mainly mediated by gene expression, and short-term regulations are accomplished mainly through post-translational modifications such as phosphorylation and glycosylation (3, 5). There is several lines of evidence (5) suggesting that OAT functions might be regulated through membrane trafficking mechanisms (including endocytosis and recycling) like other transporters such as dopamine transporter (6), norepinephrine transporter (7), and glucose transporter (8).

2 Regulation of OATs by membrane trafficking

2.1 Introduction

A great number of plasma membrane proteins have been demonstrated to traffic to and from the plasma membrane constitutively, such as neurotransmitter transporters (6, 7, 9), chloride transporter (10, 11), glucose transporter (8). Under basal condition, there are a considerable amount of mature hOAT1 proteins in the intracellular compartments, which suggests that hOAT1 proteins may traffic to and from the plasma membrane constitutively. To determine whether hOAT1 undergoes constitutive membrane trafficking between the plasma membrane and the intracellular compartments, a biotinylation-based internalization method was used to study the kinetics of the possible internalization of hOAT1, and a biotinylation-based recycling method was also used for the recycling kinetics of the recycling of hOAT1 in cell lines.

It has been well documented that membrane trafficking of plasma membrane proteins can be regulated by protein kinase C (PKC) activation. These membrane proteins include dopamine transporter (6), gamma-aminobutyric acid transporter (12), and norepinephrine transporter (7).

Our results showed that acute treatment with PKC activator, phorbol 12 myristate 13-acetate (PMA), down-regulated the transport of PAH (OAT1 substrate) mediated by OAT1. To investigate the mechanism by which PKC activation reduced the OAT1-mediated PAH transport, we used diverse approaches from transport measurements, surface protein biotinylation to internalization assay.

By means of endocytosis, cells internalize extracellular materials, ligands, proteins and lipids in plasma membrane, and the compositions of plasma membrane is governed by the balance of endocytic uptake and recycling of membrane proteins and lipids (13). A variety of cellular processes are regulated to the balance between endocytosis and recycling, including nutrient uptake, cell adhesion, cell junction, cell migration, cell polarity and signal transduction (13).

In general, endocytosis pathways can be divided into those that are clathrin dependent and those that are independent of clathrin (13-15). In clathrin-dependent endocytosis, adaptor proteins in the cytoplasm specifically recognize the cytoplasmic domains of plasma membrane proteins, and the membrane proteins are packaged into clathrin-coated vesicles that move into the cell (13). Clathrin-dependent endocytosis has been widely studied, but clathrin-independent endocytosis has not been well understood. Recently scientists have paid more and more attention to clathrin-independent endocytosis (13).

By means of endocytosis, cells internalize extracellular materials, ligands, proteins and lipids in plasma membrane, and the compositions of plasma membrane is governed by the balance of endocytic uptake and recycling of membrane proteins and lipids (13). A variety of cellular processes are regulated to the balance between endocytosis and recycling, including nutrient uptake, cell adhesion, cell junction, cell migration, cell polarity and signal transduction (13).

2.2 Materials and methods

2.2.1 Materials and instruments

2.2.1.1 Cell

COS-7 cell was purchased from American Type Culture Collection (Manassas, VA).

2.2.1.2 Chemicals

Dulbecco's modified Eagle's medium was purchased from Cellgro (Manassas, VA). Fetal bovine serum, protease inhibitor cocktail, Triton X-100 and Sodium 2-mercaptoethanesulfonate (MesNa) were purchased from Sigma (St. Louis, MO). LipofectAmine 2000™ reagent, 1 M Tris-HCl (pH 7.5 and pH 8.0) and geneticin (G418) were purchased from Invitrogen (Carlsbad, CA). SuperSignal West Dura extended duration substrate kit, NHS-SS-biotin and streptavidin-agarose beads were purchased from Thermo Scientific (Waltham, MA). p-[³H]Aminohippuric acid (PAH) was from NEN Life Science Products (Hercules, CA). [³H] estrone sulfate was purchased from Perkin-Elmer Life and Analytical Sciences (Boston, MA). 7.5% ready gel, glycine and protein assay reagent were purchased from Bio-Rad (Hercules, CA).

2.2.1.3 Antibodies

Mouse anti-c-Myc monoclonal antibody (9E10) was purchased from Hybridoma Center, Mount Sinai School of Medicine (New York, NY). Goat anti-mouse IgG conjugated to horseradish peroxidase was purchased from Thermo Scientific (Waltham, MA). Rabbit anti-transferrin receptor (TfR) polyclonal antibody and mouse anti-Na⁺/K⁺-ATPase monoclonal antibody were purchased from Santa Cruz (Santa Cruz, CA). Goat anti-mouse IgG conjugated to horseradish peroxidase was purchased from Thermo Scientific (Waltham, MA). Mouse anti-EEA1 monoclonal antibody was purchased from BD Biosciences. Transferrin-tetramethylrhodamine conjugate, Alexa Fluor® 488 goat anti-mouse IgG (H+L), and Alexa Fluor® 350 goat anti-rabbit IgG (H+L) were from Molecular Probes (Eugene, OR). Rabbit anti-c-Myc polyclonal antibody was purchased from Sigma (St. Louis, MO).

2.2.1.4 Plasmids

Dynamin-2/K44A mutant was purchased from American Type Culture Collection (Manassas, VA). Eps15 mutant (D95/295) was generously provided by Dr. Jennifer Lippincott-Schwartz from NICHD, National Institutes of Health (Bethesda, MD).

2.2.1.5 Buffers

- (1) Phosphate-buffered saline (PBS)/Ca²⁺ and Mg²⁺: 137 mM NaCl, 2.7 mM KCl, 4.3 mM Na₂HPO₄, 1.4 mM KH₂PO₄, 0.1 mM CaCl₂, and 1 mM MgCl₂, pH 7.4.
- (2) Regular lysis buffer (biotinylation): 10mM Tris-HCl (pH7.5), 150mM NaCl, 1mM EDTA, 0.1% SDS, 1% Triton X-100.
- (3) NT buffer: 20 mM Tris-HCl (pH8.0), 150mM NaCl, 1mM EDTA, 0.2% BSA, adjust pH to 8.5 with NaOH.
- (4) Hypotonic shock solution: serum-free Dulbecco's modified Eagle's medium and distilled water in 1:1 ratio.
- (5) KCl depletion buffer: 50mM HEPES, 100mM NaCl, pH 7.4; 1 mM CaCl₂; 1 mM MgCl₂
- (6) 5 × Laemmli loading Buffer: 28.5% glycerol, 175mM Tris-HCl (pH6.8), 7.5% SDS, 0.03% BPB dye, 12.5% β-mercaptoethanol (freshly added).

2.2.1.6 Instruments

Fluorchem® 8800 system (Alpha Innotech, USA), BioPhotometer (Eppendorf, Germany), Zeiss LSM-510 laser-scanning microscope (Carl Zeiss Inc., Thornwood, NY).

2.2.2 Experimental procedures

(1) Cell culture

COS-7 cells and COS-7 cells stably expressing hOAT1-C-myc are grown at 37 °C and 5% CO₂ in Dulbecco's modified Eagle's medium (Cellgro, USA) supplemented with 10% fetal bovine serum (Sigma), 100 units/ml penicillin, and 100 mg/ml streptomycin.

(2) Transfection

1. Plate 5×10^5 COS-7 cells in a 35 mm dish and grow for 24 h;
2. For each 35 mm dish, mix 4 µg of plasmid DNA in 250 µl of Opti-MEM®I reduce serum medium in a sterile EP tube, and mix 10 µl of Lipofectamine 2000 transfection reagent in 250 µl of Opti-MEM®I reduce serum medium in a sterile EP tube. Incubate for 5 min at room temperature;
3. Combine the diluted DNA and diluted Lipofectamine 2000, mix gently and incubate for 20 min at room temperature;
4. Mix the DNA-Lipofectamine 2000 complexes with culture medium by adding 100 µl of complexes to 2 ml of culture medium for each 35 mm dish, and mix gently;
5. Remove the medium in the dish containing cells and add the medium with the DNA- Lipofectamine 2000 complexes into the dish.
6. Incubate the cells for 24 ~ 72 h in a cell culture incubator at 37 °C.

Note: To reduce the toxicity of Lipofectamine 2000, the medium with the DNA-Lipofectamine 2000 complexes may be replaced by the medium without the complexes 4 ~ 6 h after transfection.

(3) Internalization assay

A. Cell surface biotinylation

1. Plate 5×10^5 cells on each well of a 6-well plate or a 35 mm dish, and grow for 24 hours;
2. Place the 6-well plate on ice for a couple of minutes;
3. Aspirate the medium and wash cells with 2 ml of cold PBS(+) (pH8.0) [supplemented with both 1mM Ca^{2+} (CaCl_2) and 1mM Mg^{2+} (MgCl_2)] two times to remove any proteins in the culture medium and cool down the cells rapidly;
4. Add 1ml of freshly prepared 0.5 mg/ml NHS-SS-Biotin (Pierce) in PBS(+) (pH8.0);
5. Incubate the cells on ice for 20 min with gently shaking on an orbital shaker;
6. Remove biotin solution and wash cells with 2 ml of 100mM Glycine in PBS(+) (pH8.0) once;
7. Incubate the cells with 2 ml of cold 100mM Glycine in PBS(+) (pH8.0) for 20 ~ 30 min, with gently shaking on a orbital shaker;
8. Extensively wash the cells twice with 2ml of cold PBS (+) (pH8.0);
9. After quenching of Glycine, each 35mm-dish is incubated in prewarmed PBS(+), pH7.4 or serum-free medium at 37°C for a designated period of time. (Based on my experience, 3 minutes is enough for a 35mm-dish to reach the endocytosis-allowable temperature, so the actual time is 3 minutes longer than the designated time, eg. if 5 min is the designated time, the actual time of incubation is 8 min.);

B. Internalization and stripping

10. After 37°C incubation, put the dishes on ice immediately and wash twice with cold PBS (+), pH 7.4 to stop endocytosis;
11. Add 2ml Stripping Buffer (MesNa, 30 min X 2 times, 50mM in NT buffer) to strip the membrane-bound biotin with gentle shaking.
12. Wash cells twice with cold PBS, pH 7.4. (For some highly-expressed proteins, concentration of MesNa and incubation times may be increased for desired stripping efficiency through optimization.) ;

C. Cell lysis and binding to streptavidin-agarose

13. Add 400 ~ 500 µl of regular lysis buffer with freshly added Proteinase Inhibitor Cocktail (Sigma);
14. Vigorously shake the plate on ice for 10-15 min, harvest cells to an Eppendorf (EP) tube by using a cell scraper. Squeeze cells with a pipet tip by pipetting in order to help break down cell membrane;
15. Rotate the EP tubes for 40 min at 4°C for further lysis;
16. Centrifuge the tubes at 13200 rpm for 20 min at 4°C;
17. Transfer the supernatant to a new EP tube;
18. Measure protein concentrations to normalize loading amount of proteins.
300 ~ 500 µg of proteins may be applied to bind streptavidin-agarose beads;
19. 40 µl of Streptavidin-Agarose beads (Pierce) is added to each tube. Rotate for 1.5 ~ 4 h at 4°C;

20. After rotation, centrifuge at 13,200 rpm for 1 min at 4°C. Wash the beads with 1ml of regular lysis buffer for 3 times (don't lose beads);
21. Wash the beads with 1ml of PBS (pH7.4).
22. Now all the membrane proteins are bound to beads, so the target protein has to be released for the following immunoblot detection. The remaining volume of PBS in beads is estimated and add 10 µl of 5X Laemmli sample buffer with freshly added beta-mercaptomethanol (reducing agent, final concentration is 5%);
23. Incubate the mixture for 30min at 50°C to denature the released proteins. During the incubation, tap the bottom of tubes 3 times to make sure that all beads are accessible to the Laemmli sample buffer;
24. After denaturing is done, spin down the samples. Then Western Blot is followed.

D. Data analysis

Relative OAT1 internalized is calculated as % of the total initial cell-surface hOAT1 or hOAT4 pool.

(4) Recycling assay

A. Cell surface biotinylation and recycling

1. Plate 5×10^5 cells on each well of a 6-well plate or a 35 mm dish, and grow for 24 hours;
2. Place the 6-well plate on ice for a couple of minutes;

3. Aspirate the medium and wash cells with 2 ml of cold PBS(+) (pH8.0) [supplemented with both 1mM Ca^{2+} (CaCl_2) and 1mM Mg^{2+} (MgCl_2)] two times to remove any proteins in the culture medium and cool down the cells rapidly;
4. Add 1ml of freshly prepared 1.0 mg/ml NHS-SS-Biotin (Pierce) in PBS(+) (pH8.0);
5. Incubate the cells on ice for 30 min with gently shaking on an orbital shaker ;
6. Subsequently, one set of cells are continuously biotinylated at 4 °C with 1.0 mg/ml NHS-SS-Biotin for a designated period of time;
7. Cells in the duplicate plate are warmed to 37 °C and continuously biotinylated at 37 °C with 1.0 mg/ml NHS-SS-Biotin for a designated period of time;
8. After 37°C incubation, put the dishes on ice immediately and wash the both set of cells twice with cold PBS (+), pH 7.4 to stop membrane trafficking;
9. Remove biotin solution and wash cells with 2 ml of 100mM Glycine in PBS(+) (pH 8.0) once;
10. Incubate the cells with 2 ml of cold 100mM Glycine in PBS(+) (pH8.0) for 20 ~ 30 min, with gently shaking on a orbital shaker;
11. Extensively wash the cells twice with 2ml of cold PBS (+) (pH 8.0);

B. Cell lysis and binding to streptavidin-agarose

12. Add 400 ~ 500 μ l of regular lysis buffer with freshly added Proteinase Inhibitor Cocktail (Sigma);
13. Vigorously shake the plate on ice for 10-15 min, harvest cells to an Eppendorf (EP) tube by using a cell scraper. Squeeze cells with a pipet tip by pipetting in order to help break down cell membrane;
14. Rotate the EP tubes for 40 min at 4°C for further lysis;
15. Centrifuge the tubes at 13200 rpm for 20 min at 4°C;
16. Transfer the supernatant to a new EP tube;
17. Measure protein concentrations to normalize loading amount of proteins.
300 ~ 500 μ g of proteins may be applied to bind streptavidin-agarose beads;
18. 40 μ l of Streptavidin-Agarose beads (Pierce) is added to each tube. Rotate for 1.5 ~ 4 h at 4°C;
19. After rotation, centrifuge at 13,200 rpm for 1 min at 4°C. Wash the beads with 1ml of regular lysis buffer for 3 times (don't lose beads);
20. Wash the beads with 1ml of PBS (pH7.4).
21. Now all the membrane proteins are bound to beads, so the target protein has to be released for the following immunoblot detection. The remaining volume of PBS in beads is estimated and add 10 μ l of 5X Laemmli sample buffer with freshly added beta-mercaptoethanol (reducing agent, final concentration is 5%);

22. Incubate the mixture for 30min at 50°C to denature the released proteins.
During the incubation, tap the bottom of tubes 3 times to make sure that all beads are accessible to the Laemmli sample buffer;
23. After denaturing is done, spin down the samples. Then Western Blot is followed.

C. Data analysis

Relative OAT1 recycled was calculated as the difference between transporter biotin-labeled at 37 °C and transporter biotin-labeled at 4 °C.

(5) SDS- polyacrylamide gel electrophoresis (PAGE) and immunoblotting

A. Gel Running

1. At least 400 ml of 1x running buffer is used and can be re-used.
2. Set 200V to run 30 min for 7.5% gel, running time can be adjusted by purpose.

B. Transfer

1. Use 100% methanol to pre-wet the PVDF membrane for 30 seconds, and transfer to Transfer buffer for at least 30min;
2. Use 1200-1500 ml of transfer buffer;
3. Set 100V to transfer for at least 30min (for large proteins, transfer time should be longer).

C. Primary antibody incubation

1. After transfer step, transfer the PVDF membrane to a small container and block with 5 % non-fat milk in PBST keeping the protein side up for 1hour at room temperature with gently shaking;
2. Rinse the membrane with PBST once, add primary antibody (in 2.5 % milk in PBST), and incubate overnight;
3. Wash membrane three times with PBST, 5 min each time;
4. Incubate with secondary antibody (anti-mouse or rat IgG) at a ratio of 1:5000 ~ 1:10000 for 1 h at RT;
5. Extensively wash with PBST for more than three times, each time 10 ~ 15 min.

D. Development of membrane

1. Adjust the focus of the FluorChem 8800 imaging system;
2. Open the software on the computer, click “Acquire”, click “Movie setup”, set “Sensitivity” as Medium;, set Exposure time at 3 ~ 5 seconds, total frames at 30, click “copy to next” until the frame is 30. Then click “GO”;
3. For the marker, take another photo by choosing “reflective”, the exposure time is typically 18 milliseconds.

E. Reprobe with another primary antibody

1. The membrane can be re-probed by stripping the antibody on the membrane with Restore® Western Blot Stripping Buffer (Pierce). Incubate the membrane with stripping buffer for 40 min at 37°C;
2. Wash three times with PBST, 5 ~ 10min each time;

3. Incubate the membrane with another primary antibody overnight.

(6) Co-localization analysis

A. Cell fixation

4. 1×10^5 COS-7 Cells expressing hOAT1-C-myc are cultured on cover glass (thickness 0.15, suitable for laser) in a 24-well plate;
5. Incubate cells with 1 μ M transferrin-tetramethylrhodamine conjugate (Molecular Probes) in DMEM medium at 4 $^{\circ}$ C for 1 h;
6. Incubate cells at 37 $^{\circ}$ C for a designated period of time (allow internalization to occur);
7. Wash cells with PBS twice;
8. Add freshly prepared 4% paraformaldehyde in PBS, and incubate for 20 min at room temperature avoiding light.

B. Cell permeabilization

3. Incubate the cells with freshly prepared 0.1 % Triton X-100 in PBS for 5 min at room temperature;
4. Wash once with PBS;
5. Incubate the cells with 0.1 % Triton X-100 in PBS for 5 min at room temperature;
6. Wash once with PBS;
7. Incubate the cells with 0.1 % Triton X-100 in PBS for 5 min at room temperature;
8. Wash twice with PBS.

C. Fluorescent probe labeling

9. Incubate the cells with freshly prepared 5% goat serum in PBS for 1 ~ 2 h at room temperature;
10. Incubate the cells with primary antibodies in freshly prepared 2.5% goat serum in PBS for 2h at room temperature or overnight at 4 °C;

Note: Two antibodies against two antigens must be from different species. Use 2 µg/ml of 9E10 mAb, 1.5 µg/ml of rabbit anti-myc pAb (Sigma), and 1:250 dilution of anti-EEA1 mAb (BD Biosciences) for co-localization analysis.

11. Wash four times with PBS;
12. Incubate the cells with fluorescence-labelled secondary antibodies in 2.5% goat serum in PBS for 2 h at room temperature;

Note: Two fluorescence-labelled antibodies must recognize two different immunoglobulins, such as mouse IgG and rabbit IgG. Use anti-mouse and anti-rabbit IgG at 1:1000 dilution for hOAT1 detection, and anti-mouse IgG at 1:500 dilution for EEA1 detection.

13. Wash four times with PBS for 5 min each time with gentle rotation.

D. Anti-fading reagents and mounting

14. Put a small drop of anti-fading reagent on the microscope slide, and transfer the glass cover on which the cells grow to the drop of anti-fading reagent on the microscope slide with the side of cells facing down;

Note: Slowly lay down glass cover to prevent air bubbles.

15. Dry the microscope slides covered with foil for 15 ~ 20 min at room temperature in a chemical hood with strong air flow;
16. Seal the glass cover with a small amount of nail polish;
17. Dry the microscope slides covered with foil for 10 ~ 15 min at room temperature in a chemical hood with strong air flow.

E. Confocal microscopy

18. Check the immunostaining efficiency of specimens under a fluorescent microscope;
19. Samples are visualized with a Zeiss LSM-510 laser-scanning microscope (Carl Zeiss Inc., Thornwood, NY).

2.3 Results

2.3.1 Constitutive internalization of OAT proteins

A biotinylation-based internalization method has been employed by several groups to determine the constitutive internalization of different membrane proteins, such as dopamine transporter (6), gamma-aminobutyric acid transporter (12), and chloride transporter (11). We used this method to measure the rates of constitutive internalization of human OAT proteins including hOAT1, hOAT4 and hOAT3.

2.3.1.1 Constitutive internalization of OAT1

In figure 2-1, hOAT1 undergoes constitutive internalization robustly after initiation of membrane trafficking under trafficking-permissive condition (37 °C). With densitometry analysis shown in figure 2-3, our result indicates that around 10%, 20%, and 30% of

surface labeled hOAT1 proteins were present in the intracellular compartments at 5, 10, and 15 min respectively.

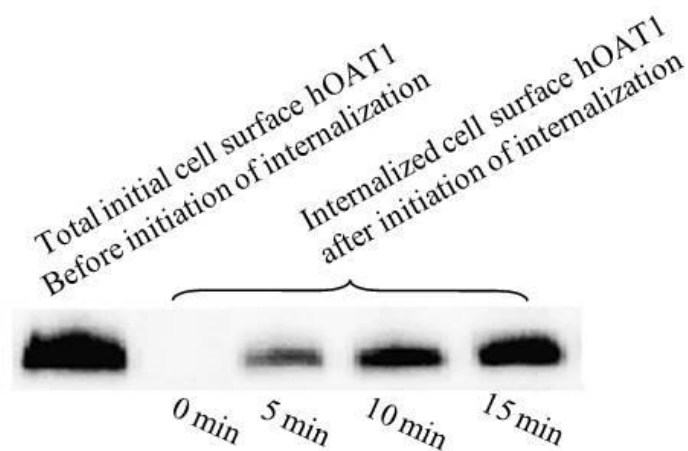


Figure 2-1 Constitutive internalization of human OAT1 in COS-7 cells using biotinylation-based internalization assay. OAT1 internalization was analyzed as described under “Materials and Methods” followed by Western blotting using anti-myc antibody (1:100). (*Journal of Biological Chemistry*, 2008, 283 (47): 32570~32579).

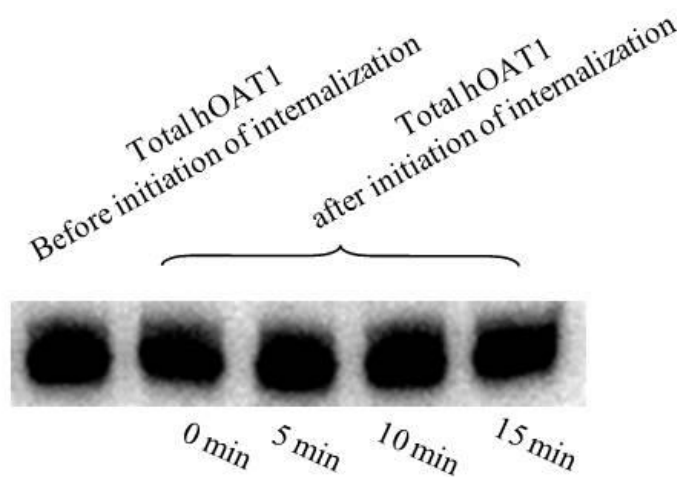


Figure 2-2 Total expression of human OAT1 in cell lysate of COS-7 cells as a loading control. Total expression of OAT1 in cell lysate was measured in parallel to experiments shown in a by Western blotting using anti-myc antibody (1:100). (*Journal of Biological Chemistry*, 2008, 283 (47): 32570~32579).

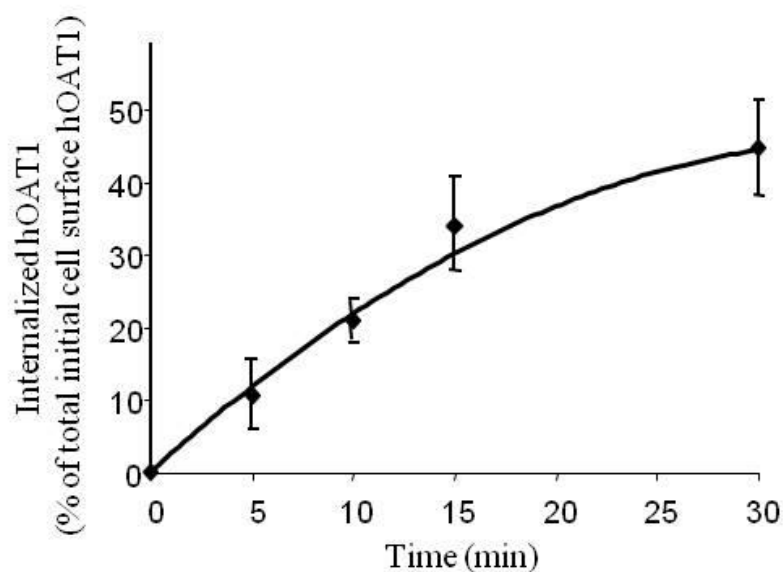


Figure 2-3 Densitometry plot of three independent experiments of COS-7 cells. Internalization of human OAT1 is expressed as % of total initial cell surface human OAT1 pool. Values are mean \pm S.E. (n = 3). (*Journal of Biological Chemistry*, 2008, 283 (47): 32570~32579).

To determine whether the constitutive internalization of hOAT1 is cell-type dependent, we also evaluated the constitutive internalization of hOAT1 in another cell line, LLC-PK1 cell. As shown in figures 2-4 and 2-6, hOAT1 proteins also constitutively internalize rapidly in hOAT1-expression LLC-PK1 cells. This result reveals that the constitutive internalization of hOAT1 is not cell-type specific and is a general property of this transporter protein.

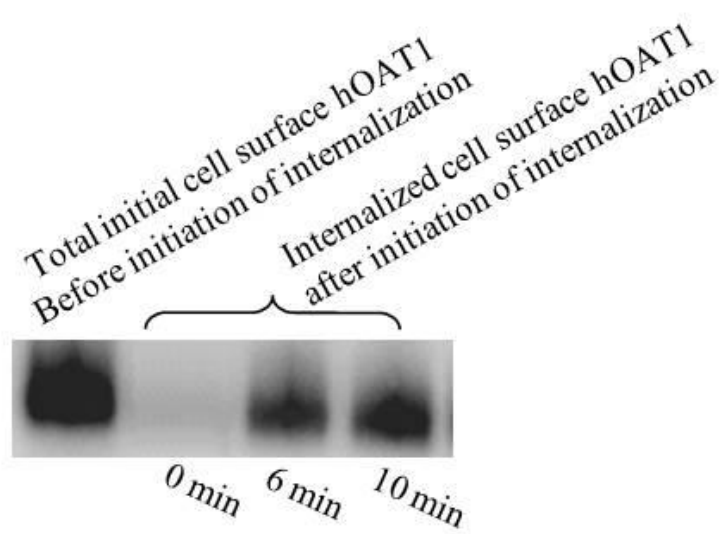


Figure 2-4 Constitutive internalization of human OAT1 in LLC-PK1 cells using biotinylation-based internalization assay OAT1 internalization was analyzed as described under “Materials and Methods” followed by Western blotting using anti-myc antibody (1:100). (*Journal of Biological Chemistry*, 2008, 283 (47): 32570~32579).

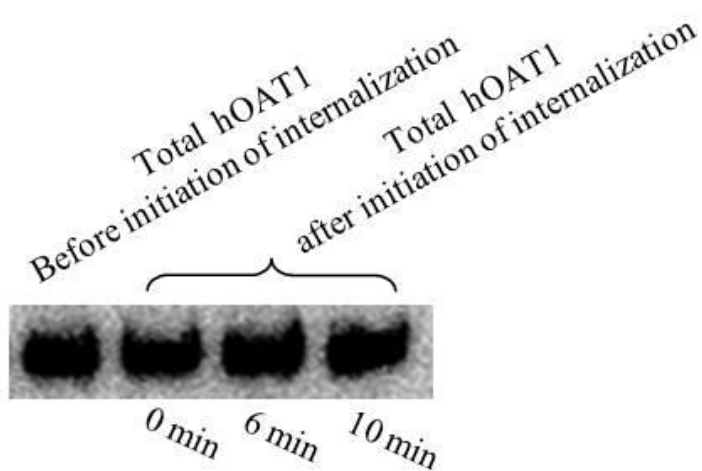


Figure 2-5 Total expression of human OAT1 in cell lysate of LLC-PK1 cells as a loading control. Total expression of OAT1 in cell lysate was measured in parallel to experiments

shown in a by Western blotting using anti-myc antibody (1:100). (*Journal of Biological Chemistry*, 2008, 283 (47): 32570~32579).

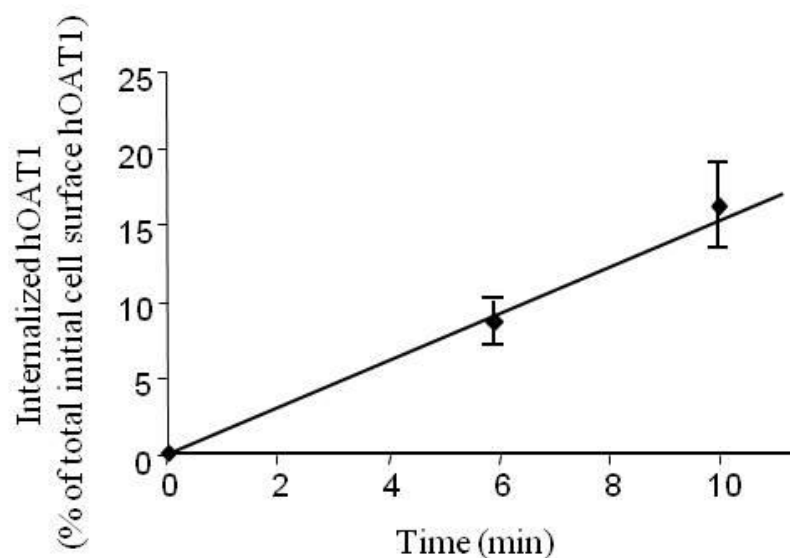


Figure 2-6 Densitometry plot of three independent experiments of LLC-PK1 cells. Internalization of human OAT1 is expressed as % of total initial cell surface human OAT1 pool. Values are mean \pm S.E. (n = 3). (*Journal of Biological Chemistry*, 2008, 283 (47): 32570~32579).

2.3.1.2 Constitutive internalization of OAT4

It is attempting to look at other members of OAT family after we discovered that hOAT1 proteins undergo constitutive internalization. Therefore, we first investigated the internalization of hOAT4 under basal condition in COS-7 cells. Interestingly, hOAT4 proteins also constitutively internalize in COS-7 cells, as demonstrated in figures 2-7 and 2-8.

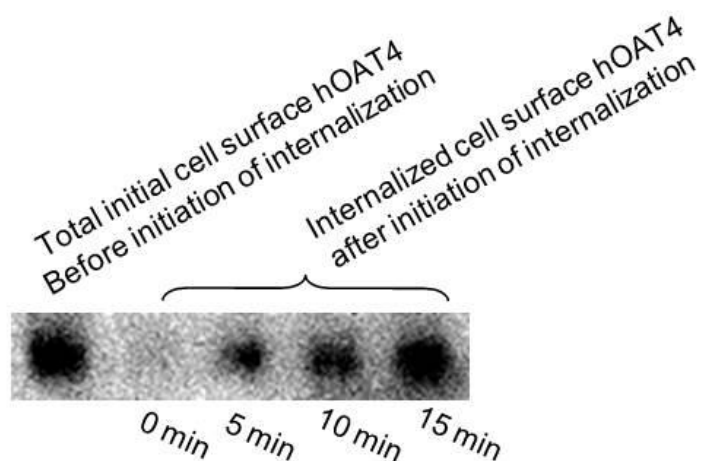


Figure 2-7 Constitutive internalization of human OAT4 in COS-7 cells using biotinylation-based internalization assay. hOAT4 internalization was analyzed as described in “Materials and Methods” section followed by Western blotting using anti-myc antibody (1:100). (*Pharmaceutical Research*. 2010, 27 (4): 589~596)

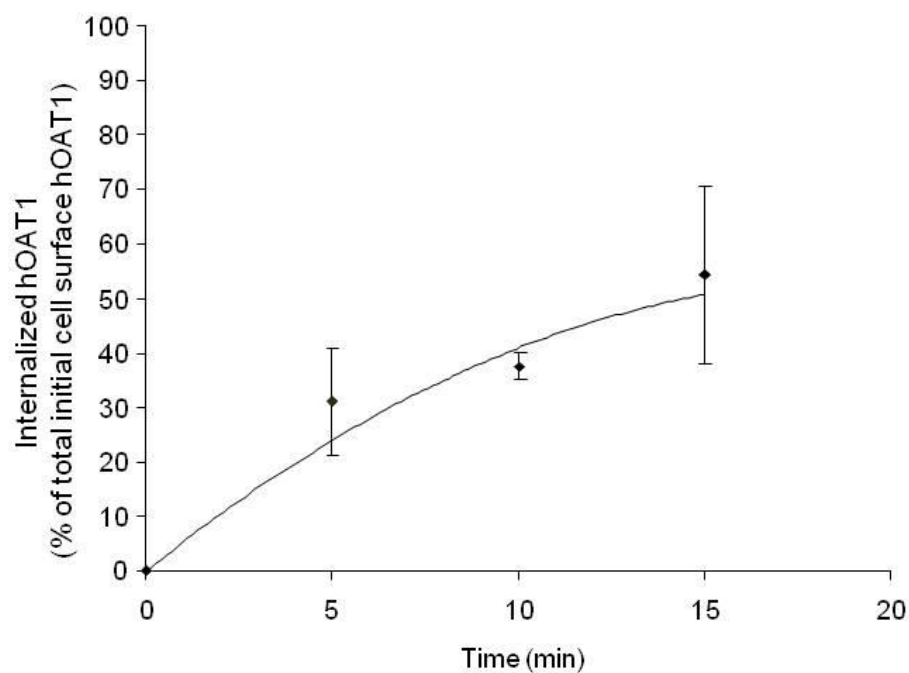


Figure 2-8 Densitometry plot of three independent experiments of COS-7 cells. Internalization of human OAT4 is expressed as % of total initial cell surface human OAT1 pool. Values are mean \pm S.E. (n = 3). (*Pharmaceutical Research*. 2010, 27 (4): 589~596)

2.3.2 Constitutive recycling of OAT proteins

To directly determine whether OAT proteins recycle back to the plasma membrane after internalization, we used a biotinylation-based method to examine the kinetics of constitutive recycling of OAT proteins in COS-7 cells. This recycling assay has been utilized by other researchers to characterize the recycling of other membrane proteins including dopamine transporter (6), gamma-aminobutyric acid transporter (12), and chloride transporter (11).

The mechanism of this biotinylation-based recycling assay is that if OAT proteins constitutively traffic to and from the cell surface, then biotinylation with membrane impermeable biotin reagent NHS-SS-biotin under trafficking-permissive condition (37 °C) should significantly increase the amount of biotin-labeled OAT proteins as compared with biotinylation under trafficking-restrictive condition (4 °C). To validate our experimental procedure, we chose transferrin receptor (TfR) as a positive control protein and Na⁺/K⁺ ATPase as a negative control protein, because TfR is known to recycle back to the plasma membrane after constitutive internalization and Na⁺/K⁺ ATPase is known not to considerably participate in constitutive membrane trafficking (6, 11).

2.3.2.1 Constitutive recycling of OAT1

As shown in Figure 2-9, the amount of biotinylated TfR was increased significantly after initiation of recycling without any difference in total expression before and after initiation of recycling. In contrast, the amount of biotinylated Na⁺/K⁺ ATPase did not change before and after initiation of recycling as shown in Figure 2-10. Hence, these results of control proteins validated our experimental procedure. We then used the same experimental conditions to investigate the constitutive recycling of hOAT1 proteins.

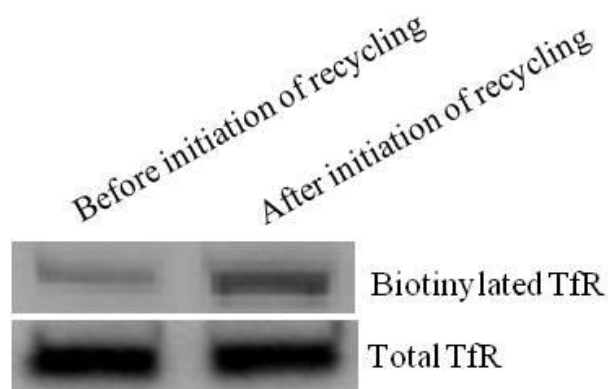


Figure 2-9 Constitutive recycling of transferrin receptor in COS-7 cells. Top panel: 30-min recycling of transferrin receptor (TfR) was analyzed as described under “Materials and Methods” followed by Western blotting using anti-TfR antibody (1:100). Bottom panel: as a loading control for top panel, total expression of TfR in cell lysate was measured in parallel to experiments shown in the top panel by Western blotting using anti-TfR antibody (1:100). (*Journal of Biological Chemistry*, 2008, 283 (47): 32570~32579).

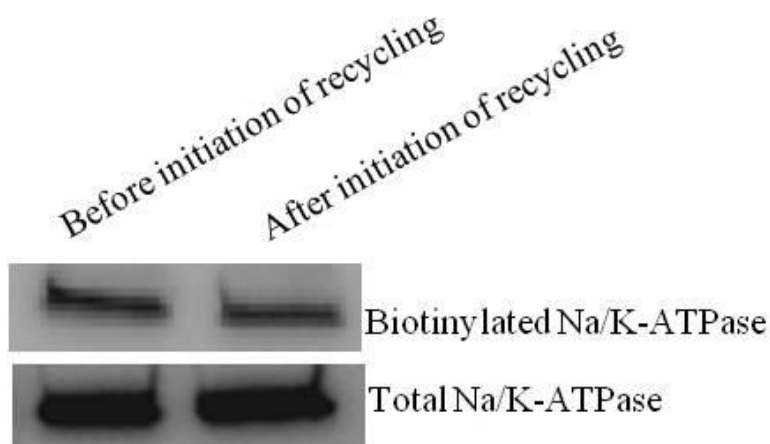


Figure 2-10 Constitutive recycling of Na/K-ATPase in COS-7 cells. Top panel: 30-min recycling of Na⁺/K⁺-ATPase was analyzed followed by Western blotting using anti-Na⁺/K⁺ ATPase antibody (1:100). Bottom panel: as a loading control for top panel, total expression of Na⁺/K⁺ ATPase in cell lysate was measured in parallel to experiments shown in the top panel by Western blotting using anti-Na/K ATPase antibody (1:100). (*Journal of Biological Chemistry*, 2008, 283 (47): 32570~32579).

It is demonstrated in Figures 2-11 and 2-12 that the amount of biotinylated hOAT1 proteins at 37 °C was increased remarkably compared to that at 4 °C since 5 min after initiation of recycling. To rule out the possibility of the contribution of newly-synthesized hOAT1 proteins to the increase in biotinylated hOAT1 proteins in the recycling assay, we blocked proteins synthesis by treating cells with cycloheximide (10 μM) over a time span of 2 h. Figure 2-13 indicates that the treatment of cycloheximide for 2h did not alter either the surface or total expression of hOAT1 proteins. Therefore, the contribution of biosynthesis of hOAT1 to the cell surface hOAT1 is not significant over the time frames in which our recycling experiments were conducted.

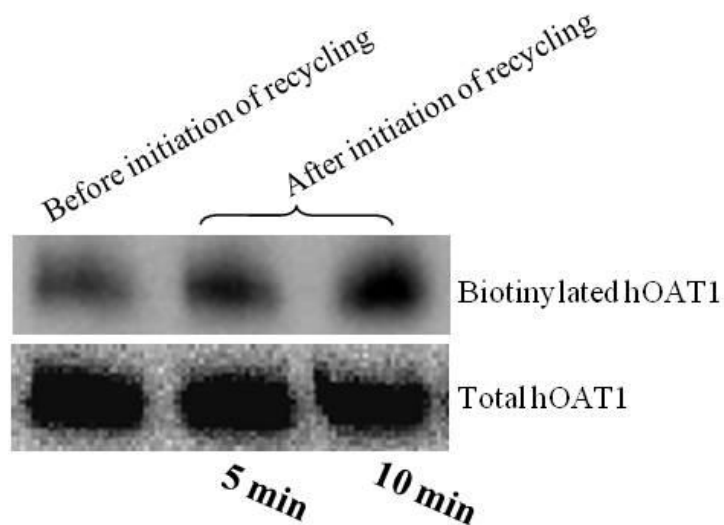


Figure 2-11 Constitutive recycling of human OAT1 in COS-7 cells. Top panel: OAT1 recycling was analyzed at time points 5 min and 10 min followed by Western blotting using anti-myc antibody (1:100). Bottom panel: as a loading control for the top panel, total expression of OAT1 in cell lysate was measured in parallel to experiments shown in the top panel by Western blotting using anti-myc antibody (1:100). (*Journal of Biological Chemistry*, 2008, 283 (47): 32570~32579).

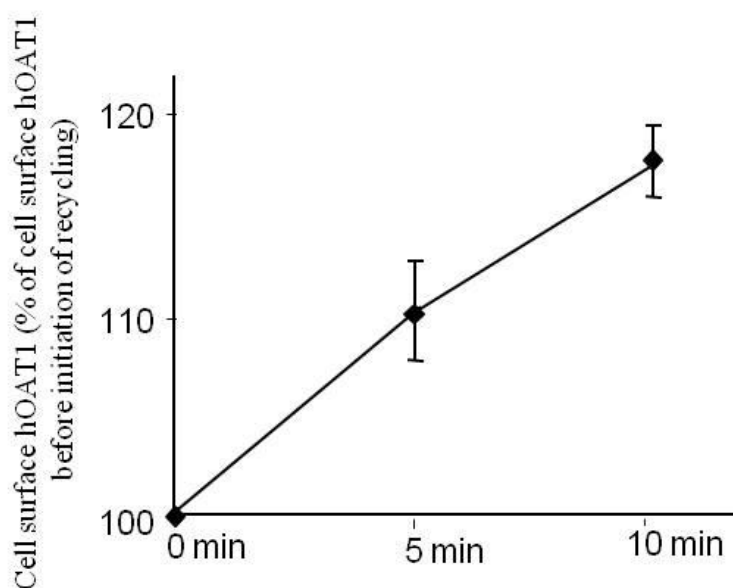


Figure 2-12 Densitometry plot of three independent recycling experiments of human OAT1 in COS-7 cells. Total biotin-labeled human OAT1 is expressed as % of human OAT1 biotinylated at 4 °C. Values are mean \pm S.E. (n = 3). (*Journal of Biological Chemistry*, 2008, 283 (47): 32570~32579).

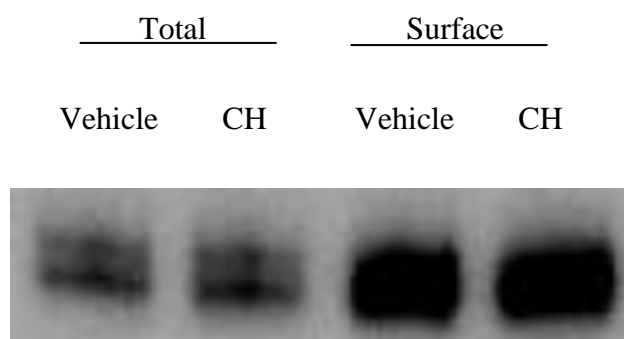


Figure 2-13 Effect of cycloheximide treatment on the total and surface expression levels of hOAT1 in COS-7 cells stably expressing hOAT1. Vehicle is DMSO, and CH denotes cycloheximide.

2.3.2.2 Constitutive recycling of OAT4

Similar to the recycling study of hOAT1 protein in COS-7 cell, we examined the constitutive recycling of TfR as a positive control, and then the recycling of hOAT4 protein under steady state using the same biotinylation-based recycling assay as that for hOAT1. As shown in Figure 2-14, transferring receptor (TfR) recycles back to the plasma membrane constitutively. Figures 2-15 and 2-16 indicate that hOAT4 proteins also constitutively recycle back to the plasma membrane following internalization in COS-7 cells.

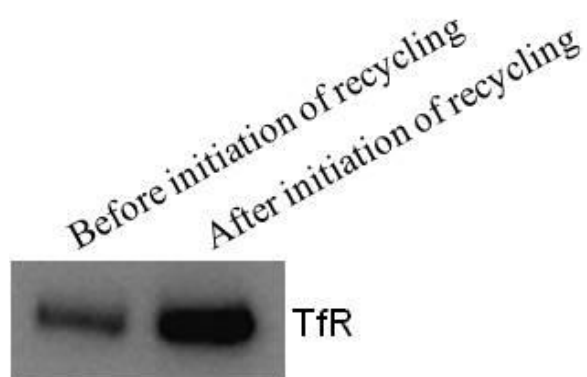


Figure 2-14 Constitutive recycling of transferrin receptor (TfR) in COS-7 cells Thirty-minute recycling of TfR was analyzed by recycling assay. 30-min recycling of transferrin receptor (TfR) was analyzed as described in “Materials and Methods” section followed by Western blotting using anti-TfR antibody (1:100). (*Pharmaceutical Research*. 2010, 27 (4): 589~596)

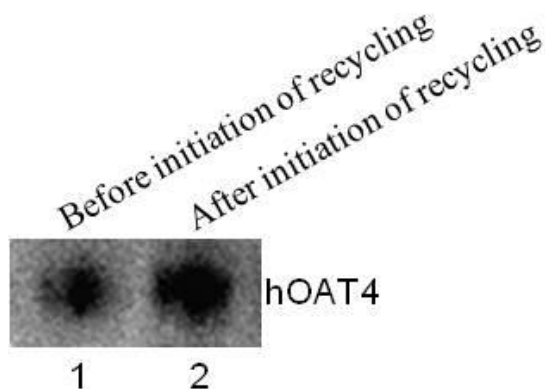


Figure 2-15 Constitutive recycling of human OAT4 (hOAT4) in COS-7 cells. Five-minute recycling of hOAT4 was analyzed by recycling assay. (*Pharmaceutical Research*. 2010, 27 (4): 589~596)

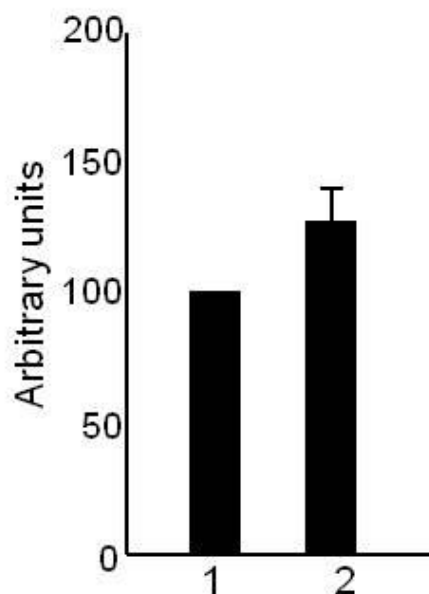


Figure 2-16 Densitometry plot of three independent recycling experiments of human OAT4 in COS-7 cells. Total biotin-labeled human OAT4 is expressed as % of human OAT4 biotinylated at 4 °C. Values are mean \pm S.E. ($n = 3$). (*Pharmaceutical Research*. 2010, 27 (4): 589~596)

2.3.3 PKC-regulated membrane trafficking of OAT1

2.3.3.1 Down-regulation of hOAT1 activity by PKC activation

We first established COS-7 cells stably expressing hOAT1-C-myc in order to study the underlying mechanism of regulation of hOAT1-mediated drug transport. In [Fig. 3-1a](#), the kinetic analysis of hOAT1-mediated PAH (a prototypical organic anion) transport indicated that the hOAT1-mediated transport of PAH across the plasma membrane in the COS-7 cells stably expressing hOAT1-C-myc was saturable. The Eadie–Hofstee transformation analysis ([Fig. 31a](#), inset) showed that the K_m value for PAH was 112.7 μM and V_{max} was 1070 pmol/mg/3 min.

It has been documented that acute PKC activation down-regulated OAT1 activity in transfected cells and kidney proximal tubules, therefore we studied whether down-regulation of hOAT1 activity by acute PKC activation also occurred in the hOAT1-COS-7 cells. As shown in Fig. 2-17b, treatment of hOAT1-COS-7 cells with phorbol 12-myristate 13-acetate (PMA), a commonly used PKC activator, at 1 μ M for 30 min led to a significant reduction in hOAT1-mediated PAH transport. This result is similar to our previous report. These results demonstrate that all the functional properties of hOAT1 that were reported in other cell systems were shown in hOAT1-COS-7 cells, and hOAT1-COS-7 cells are suitable for investigating the regulation of this drug transporter.

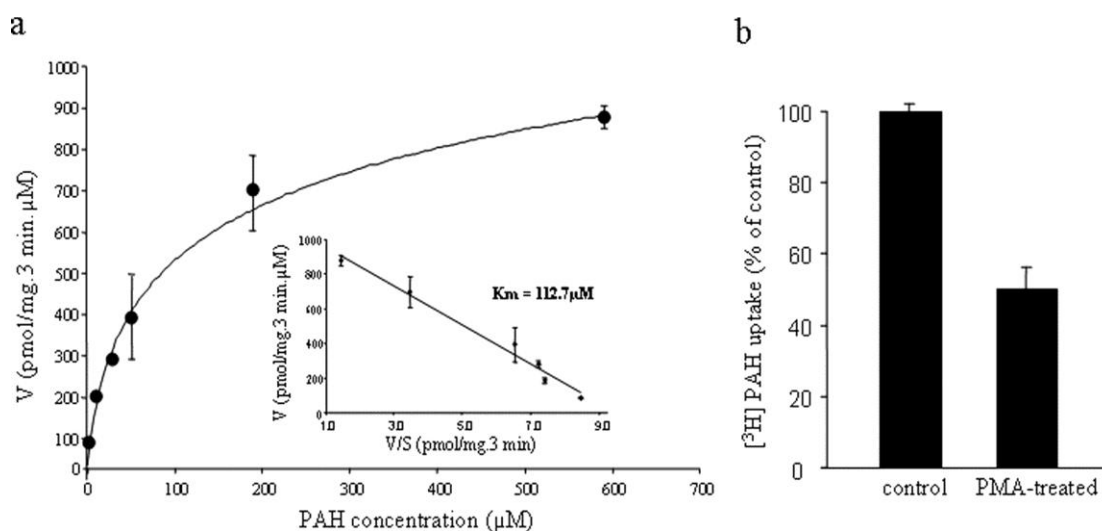


Figure 2-17 Characterization of hOAT1 in COS-7 cells. a, kinetic analysis of hOAT1-mediated PAH uptake. Kinetic characteristics were determined at substrate concentration ranging from 10 to 600 μ M (3-min uptake). The data represent uptake into OAT1-expressing cells minus uptake into mock cells. Values are mean \pm S.E. (n = 3). Inset,

transport kinetic values were calculated using the Eadie–Hofstee transformation. b, activation of PKC by PMA inhibits OAT1 activity. COS-7 cells stably expressing OAT1 were incubated for 30 min with or without 1 μ M PMA added directly to the culture media. After washing the cells, 3-min uptake of [3 H] PAH (20 μ M) was measured. Uptake activity was expressed as a percentage of the uptake measured in cells without treatment with PMA. Values are mean \pm S.E. (n = 3). (*Journal of Biological Chemistry*, 2008, 283 (47): 32570~32579).

2.3.3.2 Cellular redistribution of OAT1 following PKC activation

Our previous study demonstrated (16) that the down-regulation of OAT1 activity by acute PKC activation resulted from a remarkable decrease in the maximum transport velocity (V_{max}) of OAT1 without a change in the substrate affinity (K_m) of this transporter. There are two possibilities for the decrease in V_{max} . One is a decrease in the density of OAT1 at the cell surface, and the other is a decrease in the transport turnover rates of OAT1.

To find out which possibility is the reason causing the decrease in the maximum transport velocity, we used a cell surface biotinylation approach to determine the cellular distribution of hOAT1 in hOAT1-COS-7 cells treated with or without PMA. Fig. 2-18 showed that treatment with PMA resulted in a substantial reduction in hOAT1 at the cell surface (Fig. 2-18a) and an increase in hOAT1 in the intracellular compartments (Fig. 2-18b), and that the total expression levels of hOAT1 did not change following PMA treatment (Fig. 2-18c). Hence, PMA treatment induced re-distribution of hOAT1 from the cell surface to the intracellular compartments. These findings support that the decrease in

the maximum transport velocity of hOAT1 after PMA treatment is due to the loss of hOAT1 from the cell surface.

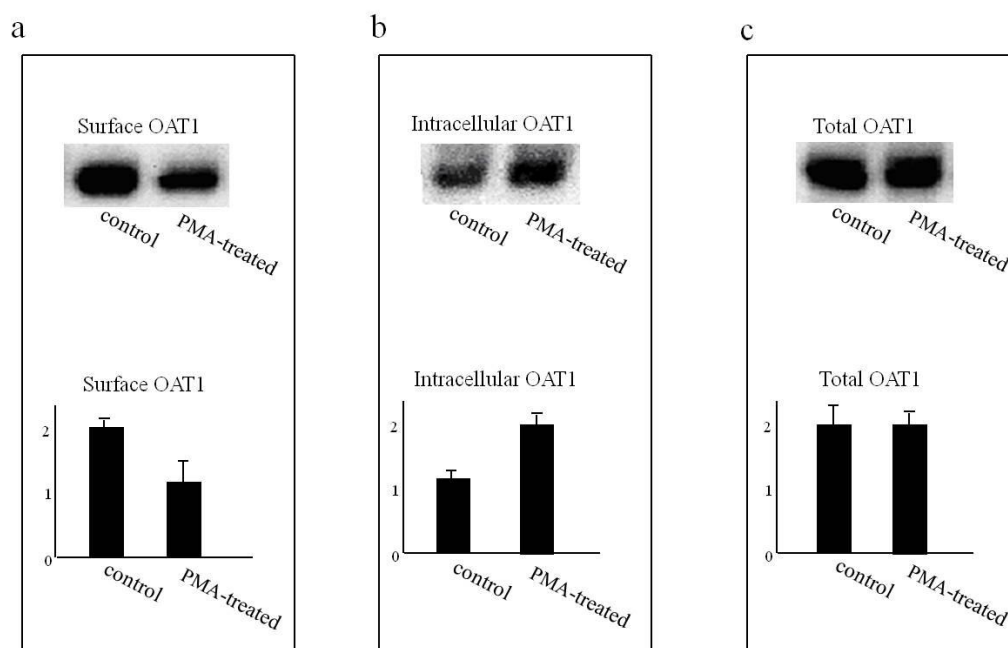


Figure 2-18 PKC-activation induced cellular re-distribution of hOAT1 in COS-7 cells. Cell surface biotinylation of OAT1-COS-7 cells were performed after 30-min treatment with either vehicle or 1 μ m PMA. Biotinylated (cell surface) and nonbiotinylated (intracellular) proteins were separated with streptavidin beads and analyzed together with total cell proteins by immunoblotting with an anti-myc antibody (1:100) as described under “Materials and Methods.” a, cell surface OAT1; b, intracellular OAT1; c, total cellular OAT1. Top panel: representative immunoblots. Bottom panel: quantitation of data from top panel as well as from other experiments. (*Journal of Biological Chemistry*, 2008, 283 (47): 32570~32579).

2.3.3.3 PKC-regulated internalization of OAT1

As discussed above in chapter 1, we observed that hOAT1 traffics from and back to the plasma membrane constitutively in COS-7 cells. And because PKC activation by PMA treatment induced redistribution of hOAT1 proteins from the cell surface to the intracellular compartments, we hypothesized that the increase in intracellular hOAT1 after PMA treatment may be due to an increase in the internalization of hOAT1 at the cell surface, a decrease in the recycling of hOAT1 back to the cell surface, or a combination of both.

To determine the effect of PKC activation on the membrane trafficking of hOAT1 in COS-7 cells, we used the same biotinylation methods as we employed to study the constitutive trafficking of hOAT1. From Fig. 2-19, we can see that the amount of biotinylated hOAT1 internalized in the presence of PMA was greater than that in the absence of PMA at each time point, which suggested that activation of PKC accelerated the endocytosis of hOAT1 from the cell surface. The kinetic analysis of the hOAT1 internalization shown in Fig. 2-21 revealed that the internalization rate of hOAT1 in the presence of PMA was significantly faster than that in the absence of PMA.

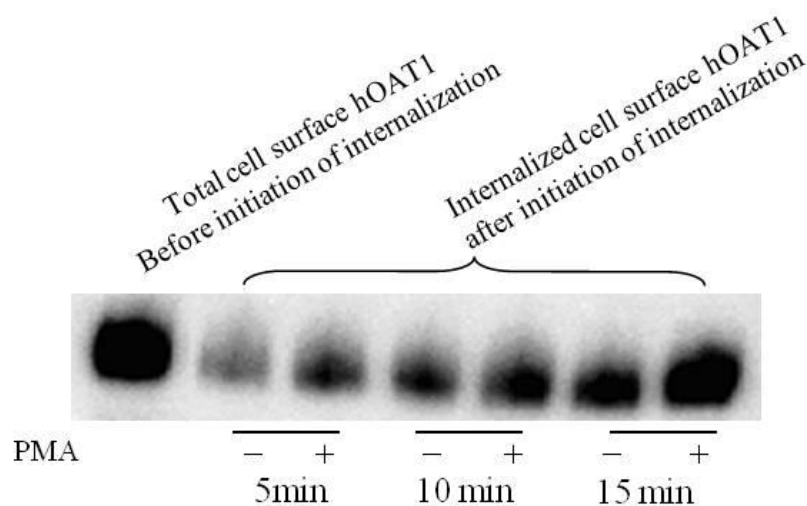


Figure 2-19 Internalization analysis of hOAT1 following PKC activation. OAT1 internalization (5, 10, and 15 min) was analyzed as described under “Materials and Methods” in the presence and the absence of PMA followed by Western blotting using anti-myc antibody (1:100). (*Journal of Biological Chemistry*, 2008, 283 (47): 32570~32579).

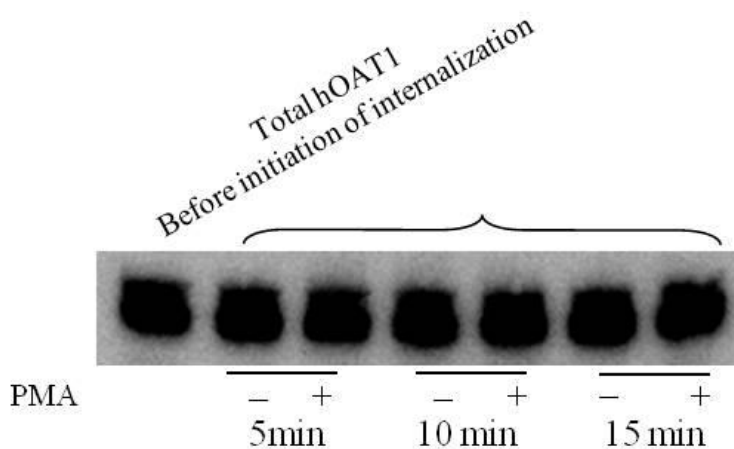


Figure 2-20 Total expression of hOAT1 in cell lysate in parallel to internalization experiment as the loading control. Total expression of OAT1 in cell lysate was measured

in parallel to experiments shown in a by Western blotting using anti-myc antibody (1:100). (*Journal of Biological Chemistry*, 2008, 283 (47): 32570~32579).

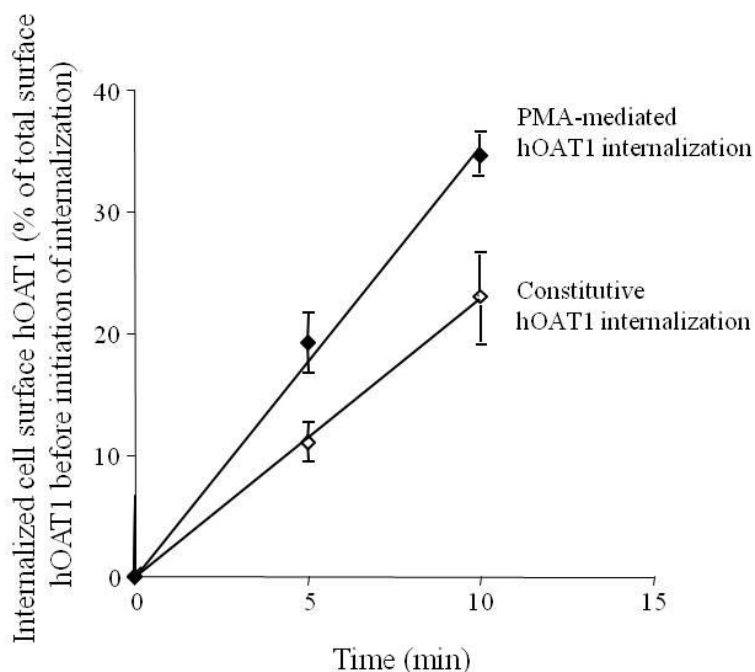


Figure 2-21 Densitometry plot of internalization analysis of hOAT1 following PKC activation. Internalization of hOAT1 is expressed as % of total initial cell surface hOAT1 pool. Values are mean \pm S.E. ($n = 3$). (*Journal of Biological Chemistry*, 2008, 283 (47): 32570~32579).

2.3.3.4 Effect of PKC activation on OAT1 recycling

Because the decreased surface hOAT1 after PMA treatment may be also due to a decrease in the recycling of hOAT1, we examined the effect of PKC activation on the recycling of hOAT1 in hOAT1-COS-7 cells using the same biotinylation method as we used to study the constitutive recycling of hOAT1. Our results shown in Fig. 2-22 and Fig. 2-23 indicated that the recycling rate of hOAT1 in the presence of PMA was not significantly different from that in the absence of PMA in hOAT1-COS-7 cells.

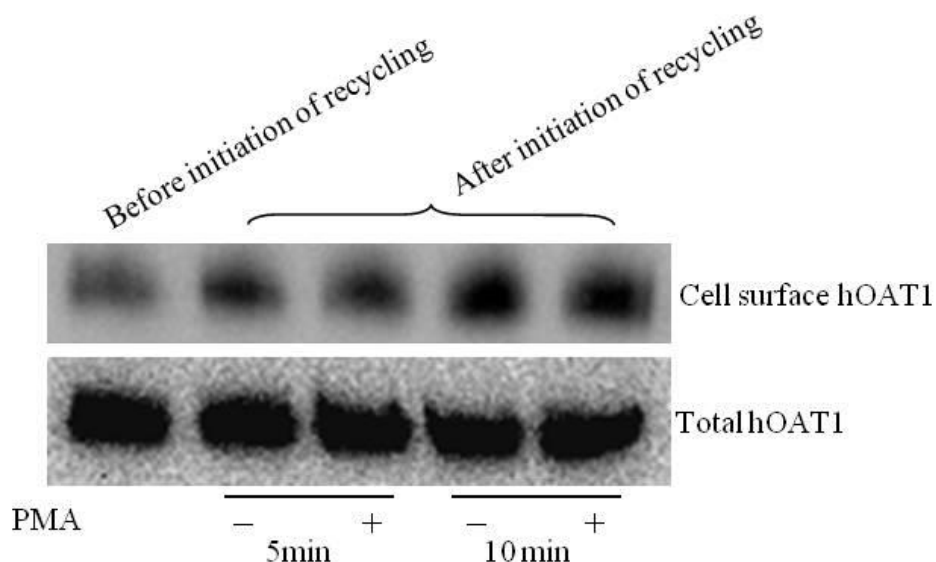


Figure 2-22 Recycling analysis of hOAT1 after PKC activation. Total expression of hOAT1 in cell lysate in parallel to recycling experiment as the loading control. Top panel: OAT1 recycling (5 min and 10 min) was analyzed as described under “Materials and Methods” in the presence and the absence of PMA followed by Western blotting using anti-myc antibody (1:100). Bottom panel: as a loading control for top panel, total expression of OAT1 in cell lysate was measured in parallel to experiment shown in the top panel by Western blotting using anti-myc antibody (1:100). (*Journal of Biological Chemistry*, 2008, 283 (47): 32570~32579).

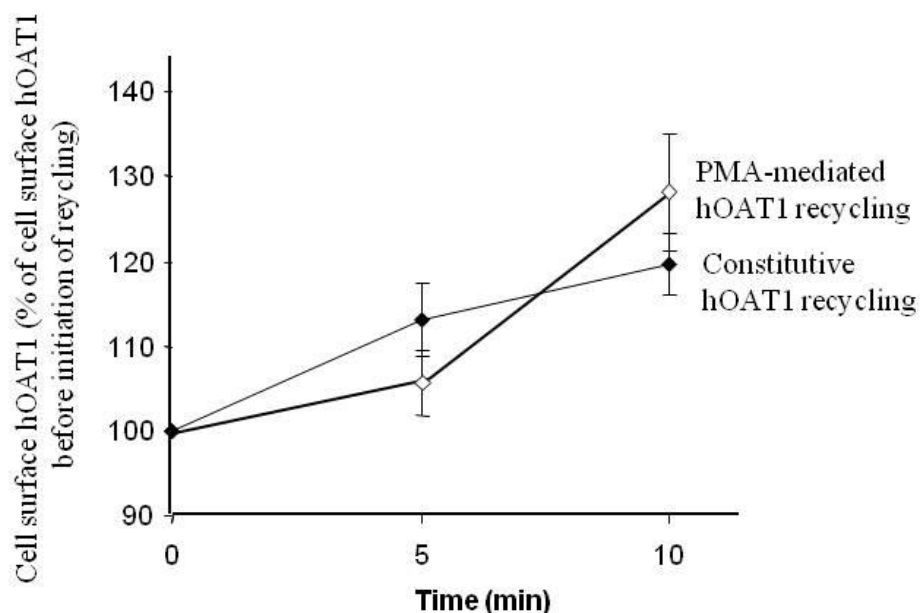


Figure 2-23 Densitometry plot of recycling analysis of hOAT1 following PKC activation in COS-7 cells. Total biotin-labeled hOAT1 is expressed as % of hOAT1 biotinylated at 4 °C. Values are mean \pm S.E. (n = 3). (*Journal of Biological Chemistry*, 2008, 283 (47): 32570~32579).

2.3.4 PKC-regulated membrane trafficking of OAT4

We previously reported (17) that activation of PKC by PMA treatment down-regulated hOAT4 activity, decreased the cell surface expression of this transporter, and resulted in a decrease in V_{max} without a significant change in K_m . To further investigate the mechanism underlying the regulation of hOAT4 by PKC activation, we measured the distribution and endocytosis rate of hOAT4 in COS-7 cells after PMA treatment.

2.3.4.1 Cellular redistribution of OAT4 following PKC activation

It is shown in Fig. 2-24 that treatment of COS-7 cells expressing hOAT4 with 1 μ M PMA for 30 min remarkably reduced the density of hOAT4 at the cell surface, suggesting

that PKC activation induced redistribution of hOAT4 proteins from the cell surface to the intracellular compartments.

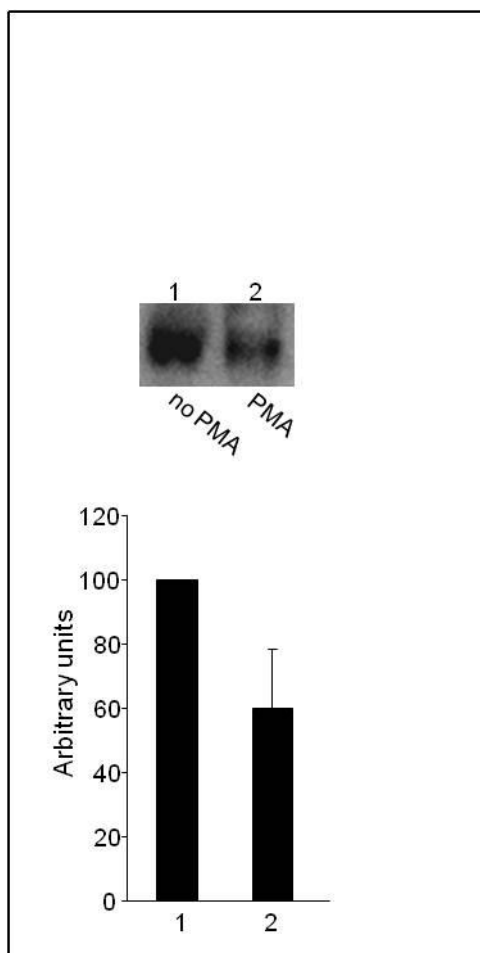


Figure 2-24 PKC-activation induced cellular redistribution of hOAT4 in COS-7 cells. Top panel: The effect of PMA on the steady-state expression of hOAT4 at cell surface was analyzed by biotinylation approach. Bottom panel: Densitometry analyses of results from top panel as well as from other experiments. The cell surface expression of hOAT4 in the presence of PMA was expressed as % of the cell surface hOAT4 in the absence of PMA. Values are mean \pm S.E. ($n = 3$). (*Pharmaceutical Research*. 2010, 27 (4): 589~596)

2.3.4.2 PKC-regulated internalization of OAT4

After we observed the decreased hOAT4 at the cell surface following PMA treatment, we determined the internalization of hOAT4 in the absence and presence of 1 μ M PMA to see whether the hOAT4 internalization is modulated by PKC activation. Fig. 2-25 showed that the amount of biotinylated hOAT4 internalized in the presence of PMA was significantly greater than that in the absence of PMA. This result demonstrated that the down-regulation of hOAT4 activity and reduced surface hOAT4 by PKC activation was due to an increase in hOAT4 internalization by activation of PKC.

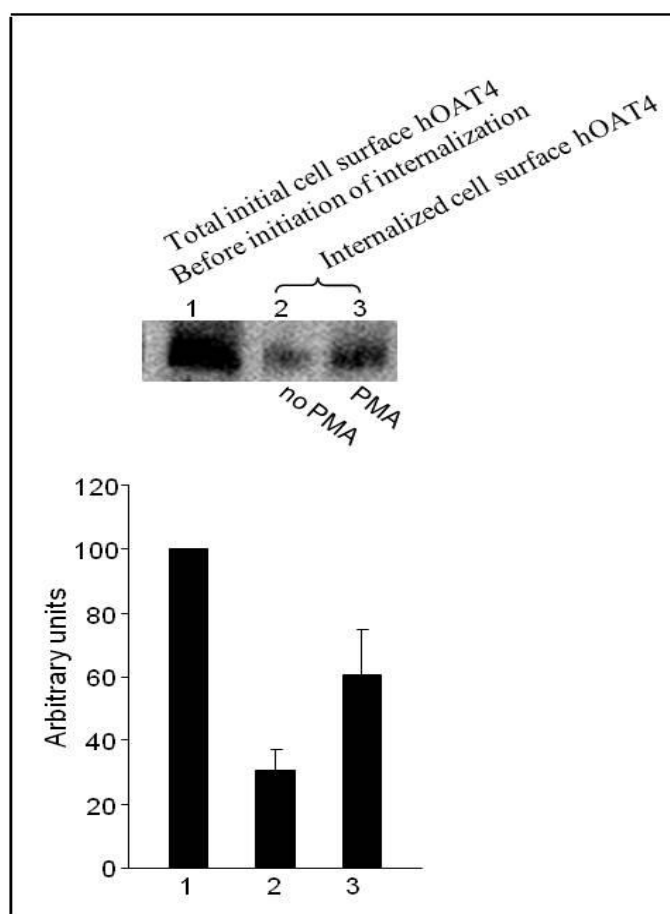


Figure 2-25 Internalization analysis of hOAT4 after PKC activation in COS-7 cells. Top panel: hOAT4 internalization (15 min) was analyzed as described in “Materials and

Methods” section in the presence and the absence of 1 μ M PMA followed by Western blotting using anti-myc antibody (1:100). Bottom panel: Densitometry analyses of results from top panel as well as from other experiments. Internalized hOAT4 was expressed as % of total initial cell surface hOAT4 pool. Values are mean \pm S.E. (n = 3). (*Pharmaceutical Research*. 2010, 27 (4): 589~596)

2.3.5 Endocytosis pathway of OAT1

In the processes of both clathrin-dependent and clathrin-independent endocytosis, a GTPase called dynamin plays important roles in the scission of clathrin-coated vesicles from the plasma membrane (18). There three isoforms of dynamin identified. Dynamin-1 is exclusively expressed in neurons, dynamin-2 is expressed ubiquitously in different tissues, and dynamin-3 is expressed in the testes, neurons and the lung.

2.3.5.1 Internalization of OAT1 is dynamin dependent

To determine whether the internalization of hOAT1 is dynamin dependent, we transfected the hOAT1-COS-7 cells with a dominant negative mutant of dynamin, K44A, and examined the effect of this dynamin-2 mutant on the cellular distribution, transport activity, and internalization of hOAT1. This K44A dynamin mutant has been widely used to investigate endocytosis mechanisms of numerous receptors and transporters localized in the plasma membrane (7, 19, 20)

If the internalization of hOAT1 is inhibited by dynamin-2 mutant, the surface hOAT1 would be increased and the intracellular hOAT1 would be decreased after the over-expression of dynamin-2 mutant. In Fig. 2-26, our result showed an increased hOAT1 at the cell surface and a concomitant decreased hOAT1 in the intracellular compartments

without a change in the total expression levels of this transporter following transfection of dynamin-2 mutant. The hOAT1-mediated PAH transport in hOAT1-COS-7 cells was also increased by over-expression of dynamin-2 mutant, as indicated in Fig. 2-26. These results revealed that over-expression of dynamin-2 mutant induced an accumulation of hOAT1 proteins at the cell surface leading to an increase in hOAT1-mediated PAH transport.

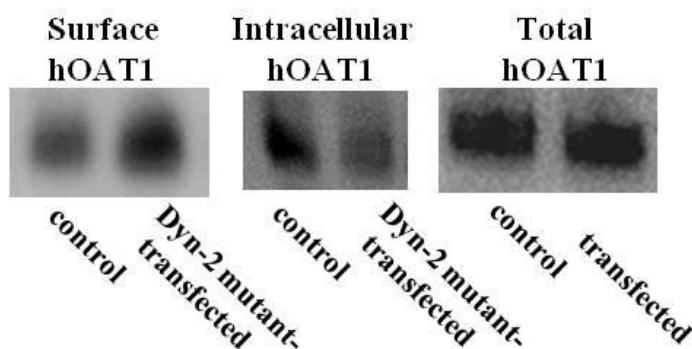


Figure 2-26 Effect of dominant negative mutant of dynamin-2 on the distribution of hOAT1 in COS-7 cells. The effect of Dyn-2 mutant on the expression of OAT1 at cell surface, in intracellular compartments, as well as in total cell lysates. (*Journal of Biological Chemistry*, 2008, 283 (47): 32570~32579).

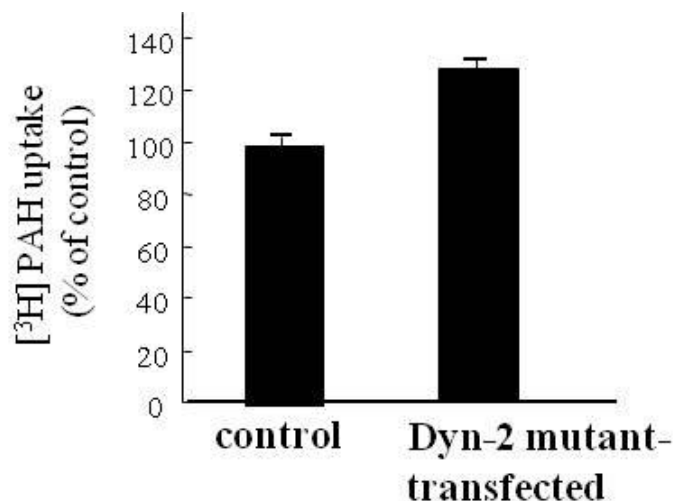


Figure 2-27 Effect of dominant negative mutant of dynamin-2 on the function of hOAT1 in COS-7 cells. [³H]PAH uptake into cells transfected with Dyn-2 mutant. Uptake activity was expressed as a percentage of the uptake measured in control cells. Values are mean \pm S.E. (n = 3). (*Journal of Biological Chemistry*, 2008, 283 (47): 32570~32579).

In order to directly determine the involvement of dynamin in constitutive and PKC-regulated internalization of hOAT1, we conducted internalization experiments with hOAT1-COS-7 cells. Consistent with the results of distribution and transport described above, our internalization result shown in Fig. 2-28 demonstrated that the amount of biotinylated hOAT1 internalized in the presence and absence of PMA was reduced after over-expression of dynamin-2 mutant, suggesting that the constitutive and PKC-regulated internalization of hOAT1 in COS-7 cells were inhibited by over-expression of dynamin-2 mutant. Therefore, the endocytic pathway of hOAT1 is dependent on dynamin.

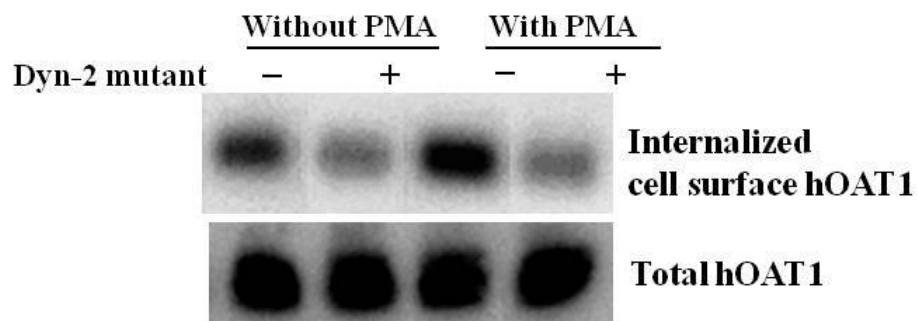


Figure 2-28 Effect of dominant negative mutant of dynamin-2 on the constitutive and PKC-modulated internalization of hOAT1 in COS-7 cells. Top panel: cells were transfected with cDNA encoding dominant negative mutant of dynamin-2 (Dyn-2 mutant). 48 h later, OAT1 internalization (15 min) was analyzed as described under “Materials and Methods” in the presence and the absence of 1 μ M PMA followed by Western blotting using anti-myc antibody (1:100). Bottom panel: as a loading control for the top panel, total expression of OAT1 in cell lysate was measured in parallel to experiment shown in the top panel by Western blotting using anti-myc antibody (1:100). (*Journal of Biological Chemistry*, 2008, 283 (47): 32570~32579).

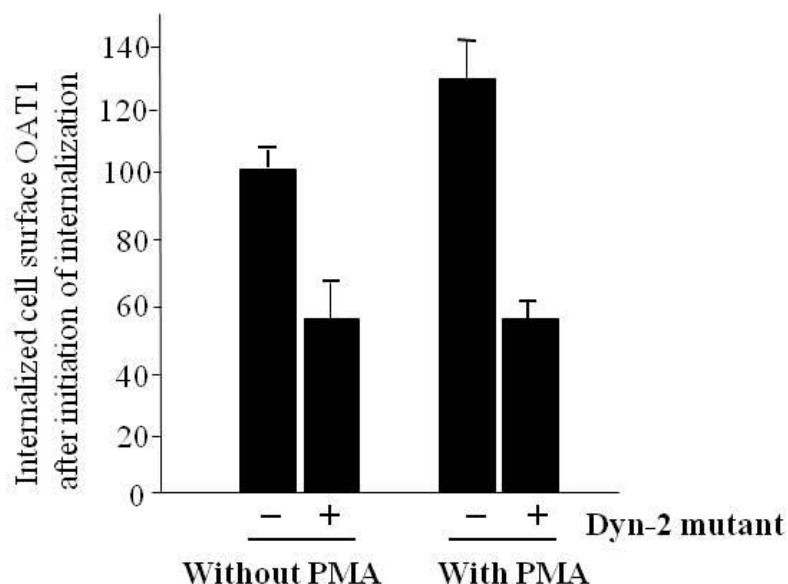


Figure 2-29 Densitometry plot of results from effect of dynamin-2 mutant on OAT1 internalization. Internalized OAT1 was expressed as % of total initial cell surface OAT1 pool. Values are mean \pm S.E. (n = 3). (*Journal of Biological Chemistry*, 2008, 283 (47): 32570~32579).

2.3.5.2 OAT1 internalization is clathrin-dependent

To determine whether the internalization of hOAT1 is dependent on clathrin, we used different approaches to block clathrin-dependent endocytosis, including chemical inhibition, potassium depletion, and over-expression of a dominant negative mutant of Eps15, an important adaptor protein for the formation of clathrin-coated vesicle.

Concanavalin A (ConA) is commonly used to inhibit clathrin-dependent endocytosis (7, 21-26). As shown in Fig. 2-30 and Fig. 2-31, both constitutive and PKC-regulated internalization of hOAT1 was significantly inhibited after treatment of 250 μ g/ml of ConA.

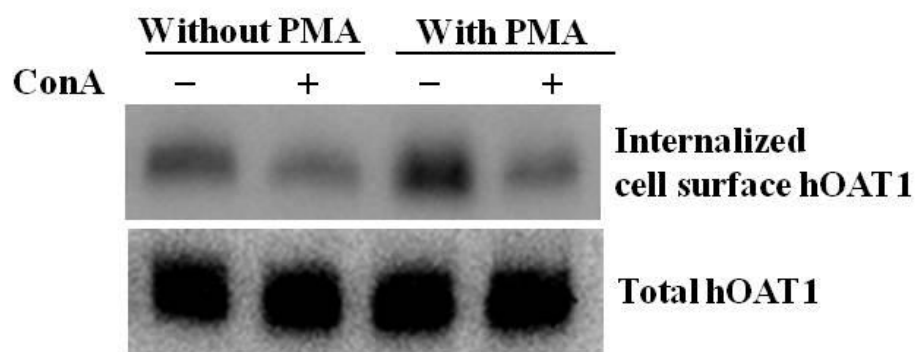


Figure 2-30 Effect of ConA on the constitutive and PKC-modulated internalization of hOAT1 in COS-7 cells. Top panel: cells were treated with ConA (250 $\mu\text{g/ml}$) for 30 min (45). OAT1 internalization (15 min) was then analyzed as described under “Materials and Methods” in the presence and the absence of 1 μM PMA followed by Western blotting using anti-myc antibody (1:100). Bottom panel: as a loading control for the top panel, total expression of OAT1 in cell lysate was measured in parallel to the experiment shown in the top panel by Western blotting using anti-myc antibody (1:100). (*Journal of Biological Chemistry*, 2008, 283 (47): 32570~32579).

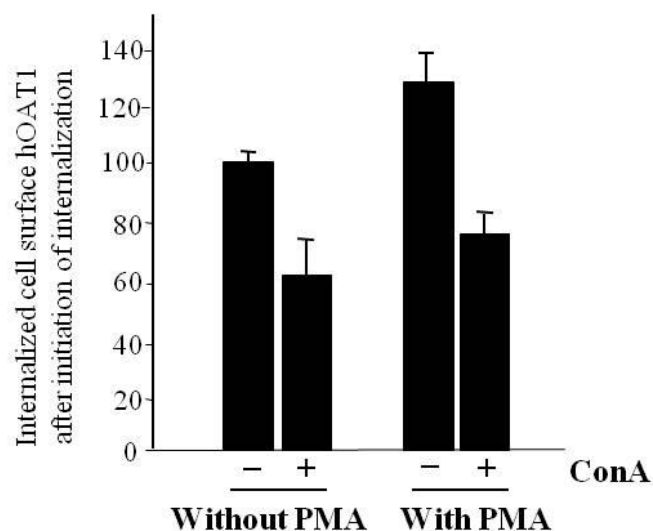


Figure 2-31 Densitometry of internalization analysis of of hOAT1 in COS-7 cells treated with ConA. Internalized OAT1 was expressed as % of total initial cell surface OAT1 pool. Values are mean \pm S.E. (n = 3). (*Journal of Biological Chemistry*, 2008, 283 (47): 32570~32579).

It has been established that clathrin-dependent endocytosis is inhibited by depletion of cellular potassium (27-29). In this study, we treated hOAT1-COS-7 cells with K^+ depletion buffer to examine whether hOAT1 endocytosis was affected by inhibiting clathrin-dependent endocytosis. Similar to ConA treatment, Fig. 2-33 indicates that both constitutive and PKC-regulated internalization of hOAT1 was significantly inhibited by depletion of intracellular K^+ .

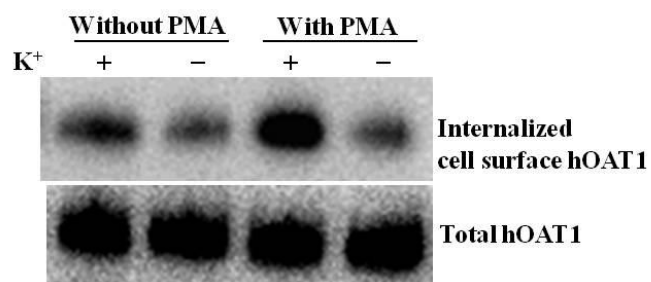


Figure 2-32 Effect of potassium depletion on the constitutive and PKC-modulated internalization of hOAT1 in COS-7 cells. Top panel: cells were incubated at 37 °C for 5 min in hypotonic shock solution (serum-free Dulbecco's modified Eagle's medium and distilled water in 1:1 ratio) and then rinsed and incubated with K⁺ depletion buffer (50mM HEPES; 100mM NaCl, pH 7.4; 1 mM CaCl₂; 1 mM MgCl₂) for 30 min (45). OAT1 internalization (15 min) was then analyzed as described under "Materials and Methods" in the presence and the absence of 1 μM PMA followed by Western blotting using anti-myc antibody (1:100). Bottom panel: as a loading control for the top panel, total expression of OAT1 in cell lysate was measured in parallel to the experiment shown in the top panel by Western blotting using anti-myc antibody (1:100). (*Journal of Biological Chemistry*, 2008, 283 (47): 32570~32579).

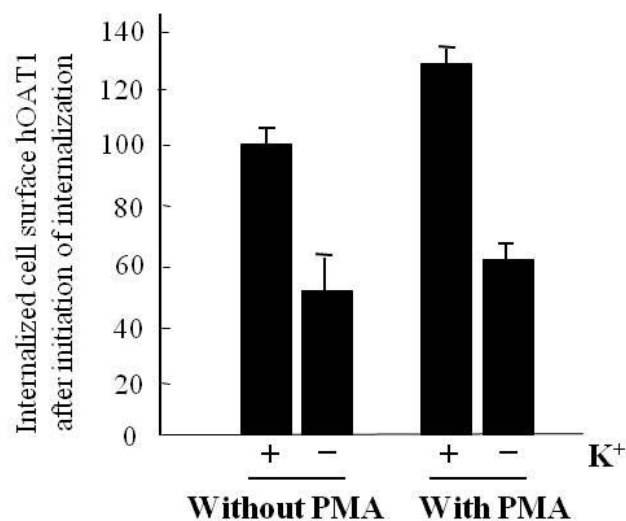


Figure 2-33 Densitometry of internalization analysis of hOAT1 in COS-7 cells treated with potassium depletion. Internalized OAT1 was expressed as % of total initial cell surface OAT1 pool. Values are mean ± S.E. (n = 3). (*Journal of Biological Chemistry*, 2008, 283 (47): 32570~32579).

In addition to chemical inhibition of clathrin-dependent endocytosis, transfection of a dominant negative mutant of Eps15 ($\Delta 95/295$), an adaptor protein involved in the formation of clathrin-coated pits, has been frequently used to block clathrin-dependent endocytosis (30-32).

After 48h transfection of a dominant negative mutant of Eps15, we measured the internalization of hOAT1 in COS-7 cells. In Fig. 2-34, our result indicated that over-expression of Eps15 mutant reduced the internalization of hOAT1 to a significant extent. We also conducted a PAH-transport study in hOAT1-COS-7 cells after transfection of Eps15 mutant. As shown in Fig. 2-35, the hOAT1-mediated PAH transport across the plasma membrane was enhanced by over-expression of Eps15 mutant. These data demonstrated that the internalization of hOAT1 in COS-7 cells is partially through a clathrin-dependent pathway.

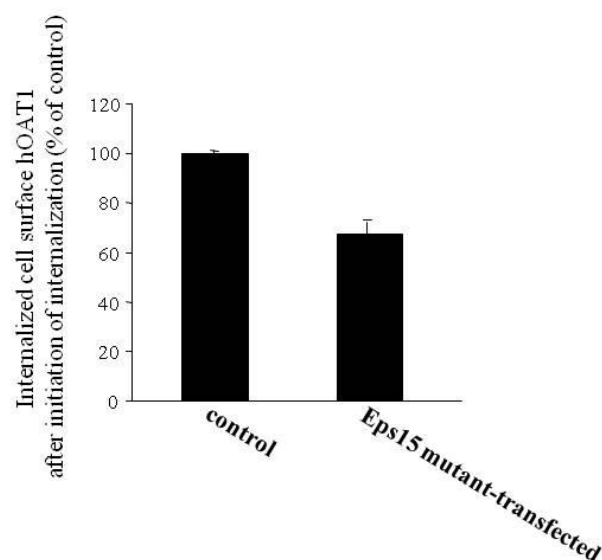


Figure 2-34 Effect of dominant negative mutant of Eps15 on the constitutive internalization of hOAT1 in COS-7 cells. Densitometry analyses of OAT1 internalization. Cells were transfected with cDNA encoding dominant negative mutant of Eps15. 48 h

later, OAT1 internalization (15 min) was analyzed as described under “Materials and Methods” followed by Western blotting using anti-myc antibody (1:100). Densitometry analyses of such Western blots were then performed. Internalized OAT1 was expressed as % of total initial cell surface OAT1 pool. Values are mean \pm S.E. (n = 3). (*Journal of Biological Chemistry*, 2008, 283 (47): 32570~32579).

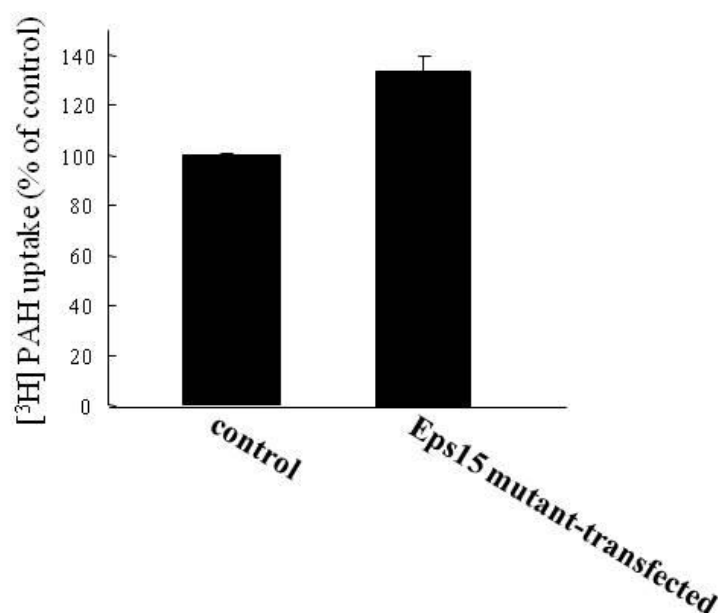


Figure 2-35 Effect of dominant negative mutant of Eps15 on the function of hOAT1 in COS-7 cells. [³H]PAH uptake into cells transfected with Eps15 mutant. Uptake activity was expressed as a percentage of the uptake measured in control cells. Values are mean \pm S.E. (n = 3). (*Journal of Biological Chemistry*, 2008, 283 (47): 32570~32579).

2.3.5.3 Immunolocalization of OAT1

Immunolocalization is an important approach to investigate endocytosis mechanism of a plasma membrane protein. By using some well established markers of clathrin-mediated endocytosis, numerous proteins have been discovered to internalize through

clathrin-mediated endocytosis, as indicated by colocalization with the markers in the intracellular compartments.

Transferrin has been commonly used as a marker of clathrin-mediated endocytosis, because the complex of transferrin and transferrin receptor internalizes via a clathrin-mediated pathway after binding of transferrin to transferrin receptor at the cell surface (33). After endocytosis from the plasma membrane, transferrin-transferrin receptor complex is targeted to the EEA1-positive early endosome (33). EEA1 is a marker of early endosome, because it is located in the membrane of early endosome.

We determined the cellular distribution of hOAT1 in COS-7 cells using confocal microscopy. hOAT1-COS-7 cells were incubated with rhodamine-conjugated transferrin for 1h on ice allowing the formation of transferrin-transferrin receptor complex at the plasma membrane. After incubation on ice, the cells were incubated at 37 °C to initiate internalization of the transferrin-transferrin receptor complex into the cell. The cells were fixed at various time points after 37 °C incubation. Fig. 2-36a-c showed that hOAT1 proteins were partially colocalized with transferrin at the cell surface after 10 min of 37 °C incubation, and Fig. 2-36d-f showed that after 45 min of 37 °C incubation hOAT1 proteins were colocalized with transferrin in the intracellular compartments. The intracellular compartments were confirmed as the EEA1-positive early endosomes, as demonstrated by the colocalization of hOAT1 and EEA1 (Fig. 2-36g-i) as well as colocalization of transferrin and EEA1 (Fig. 2-36j-l).

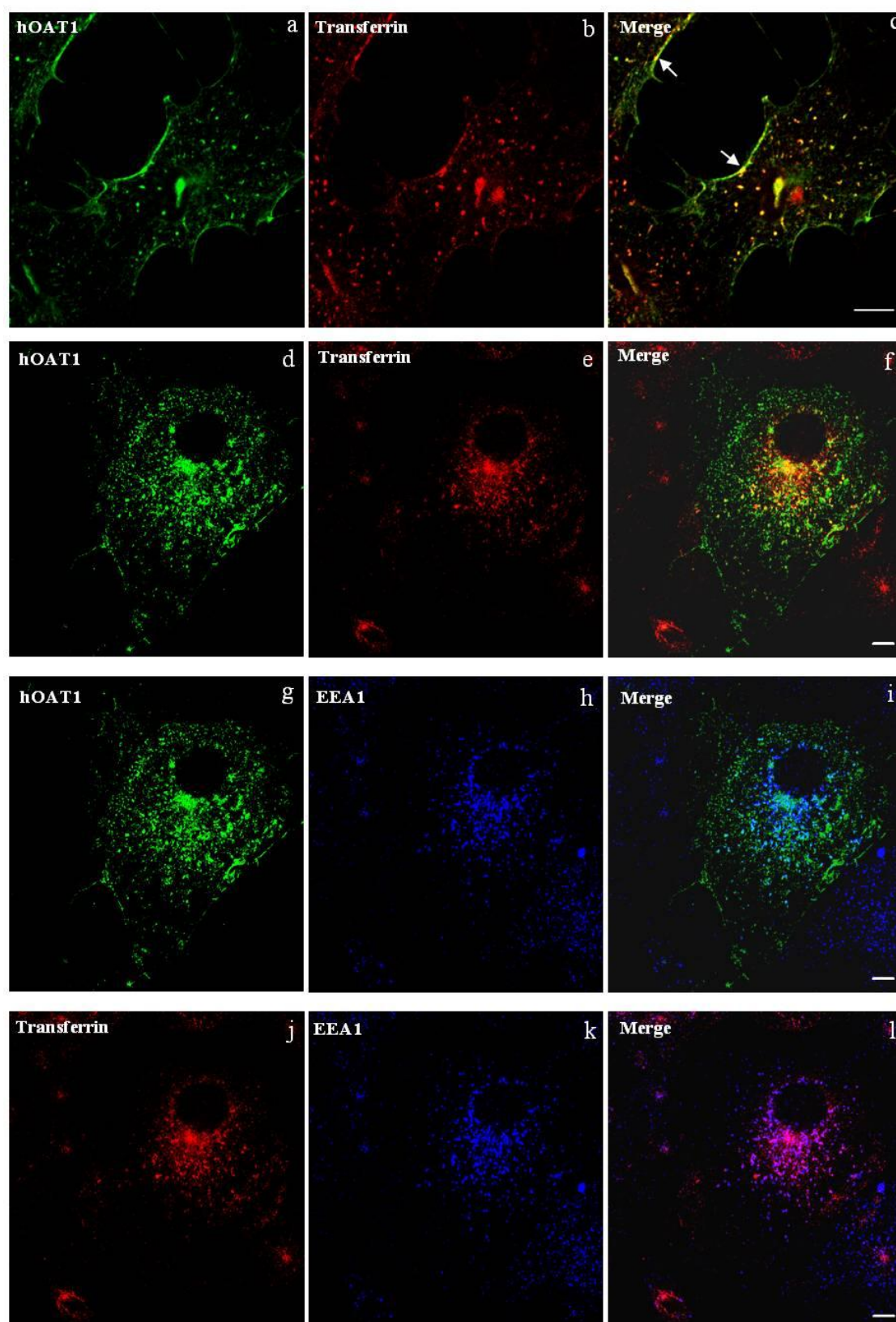


Figure 2-36 Immunolocalization of hOAT1 and transferrin in COS-7 cells. Cells were incubated with rhodamine-conjugated transferrin for 1 h at 4 °C to allow the formation of transferrin-transferrin receptor complex, followed by incubation at 37 °C to allow the internalization of transferrin-transferrin receptor complex. The cells were then fixed and immunostained for OAT1, and early endosome marker EEA1. a–c, fluorescence images of OAT1 (green), transferrin (red), taken 10 min after 37 °C incubation, and their merged image (orange/yellow). d–f, fluorescence images of OAT1 (green), transferrin (red), taken 45 min after 37 °C incubation, and their merged image (orange/yellow). g–i, fluorescence images of OAT1 (green), EEA1 (dark blue), taken 45 min after 37 °C incubation, and their merged image (light blue). j–l, fluorescence images of transferrin (red), EEA1 (dark blue), taken 45 min after 37 °C incubation, and their merged image (purple). Bar, ~10 µm. (*Journal of Biological Chemistry*, 2008, 283 (47): 32570~32579).

2.3.6 Endocytosis pathway of OAT4

2.3.6.1 Internalization of OAT4 is dynamin dependent

To further examine the effect of the dynamin-2 mutant-induced decrease in hOAT4 internalization on steady-state surface expression of this transporter, a cell surface biotinylation study was conducted after transfection of the dominant negative mutant of dynamin-2. We observed that the steady-state surface expression of hOAT4 in COS-7 cells was dramatically increased to more than 2 fold after overexpression of the dominant negative dynamin-2 (Fig. 2-38).

We also determined the effect of transfection of the dominant negative mutant of dynamin-2 on hOAT4 function using an uptake assay. It is shown in Fig. 2-39 that the

hOAT4-mediated estrone sulfate uptake was enhanced by transfection of the dominant negative dynamin-2 because of the increased hOAT4 at the cell surface.

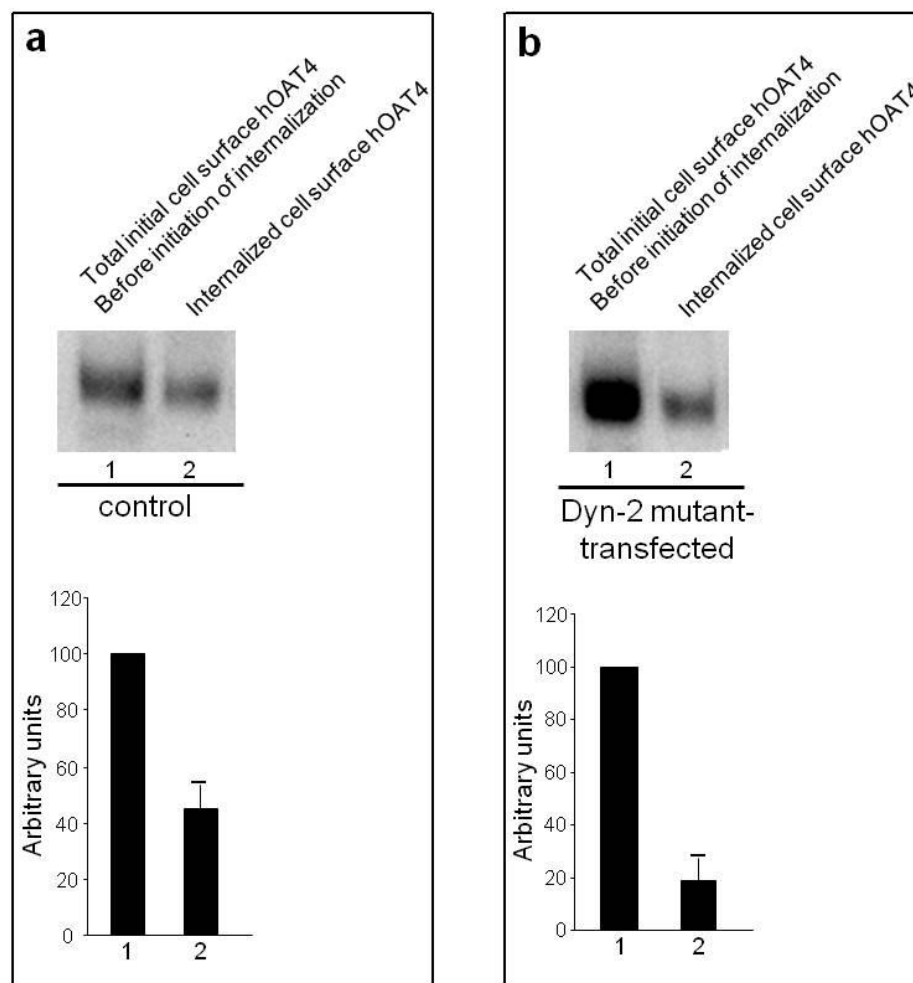


Figure 2-37 Effect of dominant negative mutant of dynamin-2 on the internalization of hOAT4 in COS-7 cells. a. Top panel: cells were transfected with control plasmid (pcDNA vector). 48 h later, hOAT4 internalization (15 min) was analyzed as described in “Materials and Methods” section followed by Western blotting using anti-myc antibody (1:100). Bottom panel: Densitometry analysis of results from top panel as well as other experiments. Internalized hOAT4 was expressed as % of total initial cell surface hOAT4 pool. Values are mean \pm S.E. (n=3). b. Top panel: Cells were transfected with cDNA

encoding dominant negative mutant of dynamin-2 (Dyn-2 mutant). 48 h later, hOAT4 internalization (15 min) was analyzed as described in “Materials and Methods” section followed by Western blotting using anti-myc antibody (1:100). Bottom panel: Densitometry analysis of results from top panel as well as other experiments. Internalized hOAT4 was expressed as % of total initial cell surface hOAT4 pool. Values are mean \pm S.E. (n=3). (*Pharmaceutical Research*. 2010, 27 (4): 589~596)

Therefore, our data revealed that the internalization of hOAT4 in COS-7 cells is dependent on dynamin, and inhibition of hOAT4 endocytosis by a dominant negative dynamin-2 resulted in an increased levels of hOAT4 in the plasma membrane and an increase in the hOAT4 –mediated estrone sulfate transport across the plasma membrane.

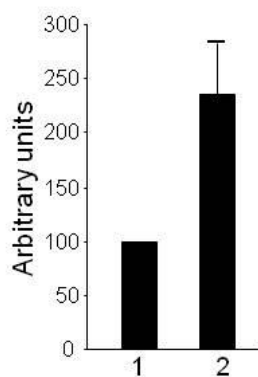
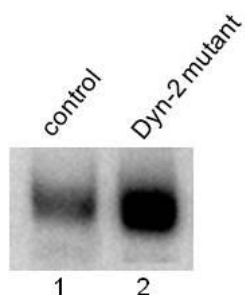


Figure 2-38 Effect of dominant negative mutant of dynamin-2 on the steady-state surface expression of hOAT4 in COS-7 cells. Top panel: Steady-state surface expression of hOAT4 in cells transfected with or without Dyn-2 mutant was determined by biotinylation analyses. Bottom panel: Densitometry analysis of results from top panel as well as other experiments. Surface expression of hOAT4 in cell transfected with Dyn-2 mutant was expressed as % of total cell surface hOAT4 pool in control cells. Values are mean \pm S.E. (n=3). (*Pharmaceutical Research*. 2010, 27 (4): 589~596)

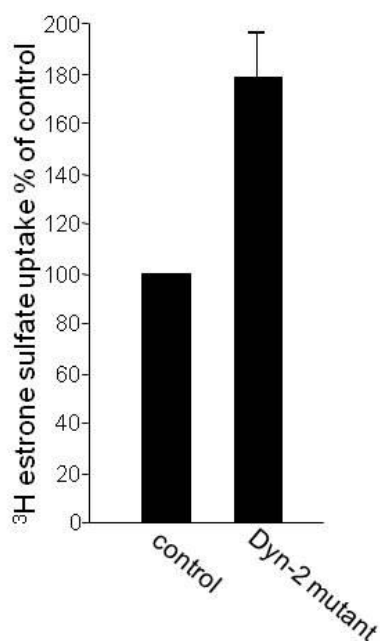


Figure 2-39 Effect of dominant negative mutant of dynamin-2 on the function of hOAT4 in COS-7 cells. Four-min uptake of [³H] estrone sulfate (100 nM) into cells transfected with Dyn-2 mutant. Uptake activity was expressed as a percentage of the uptake measured in control cells. Values are mean \pm S.E. (n = 3). (*Pharmaceutical Research*. 2010, 27 (4): 589~596)

2.3.6.2 OAT4 internalization is clathrin dependent

As we investigated the mechanism of hOAT1 internalization, the cDNA of dominant negative mutant of Eps15 was transfected in the COS-7 cells expressing hOAT4 to determine whether the hOAT4 internalization is through a clathrin-mediated pathway. Fig. 2-40 showed that the internalization of hOAT4 was decreased considerably after transfection of the dominant negative Eps15.

Using a cell surface biotinylation experiment, we observed shown in Fig. 2-41 that the steady-state surface expression of hOAT4 in COS-7 cells was significantly increased after overexpression of the dominant negative Eps15. With an increased surface hOAT4, the hOAT4-mediated uptake of estrone sulfate in COS-7 cells was also enhanced following transfection of the dominant negative Eps15 (Fig. 2-42).

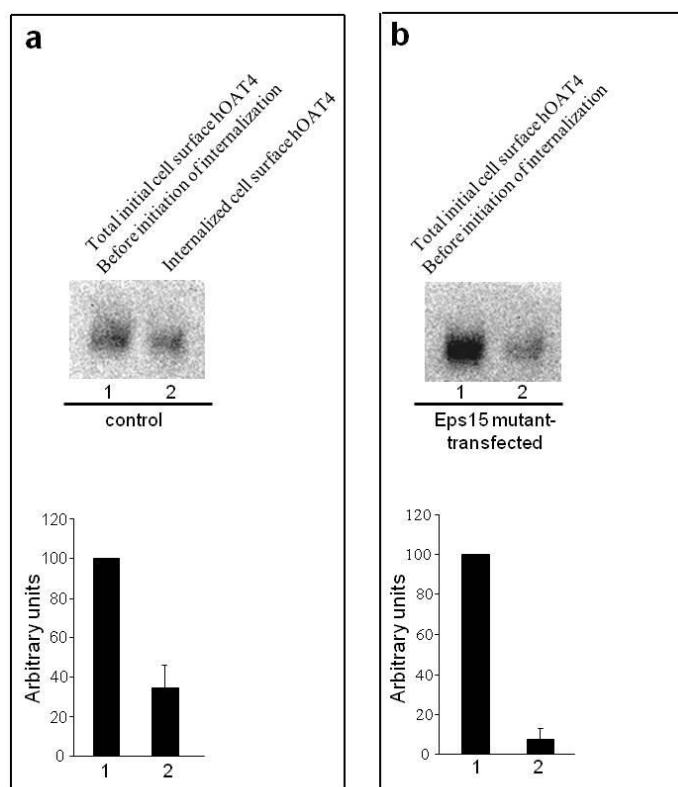


Figure 2-40 Effect of dominant negative mutant of Eps15 on the internalization of hOAT4 in COS-7 cells. **a.** Top panel: cells were transfected with control plasmid (pcDNAvector). 48 h later, hOAT4 internalization (15 min) was analyzed as described in “Materials and Methods” section followed by Western blotting using anti-myc antibody (1:100). Bottom panel: Densitometry analysis of results from top panel as well as other experiments. Internalized hOAT4 was expressed as % of total initial cell surface hOAT4 pool. Values are mean \pm S.E. (n = 3). **b.** Top panel: Cells were transfected with cDNA encoding dominant negative mutant of Eps15. 48 h later, hOAT4 internalization (15 min) was analyzed as described in “Materials and Methods” section followed by Western blotting using anti-myc antibody (1:100). Bottom panel: Densitometry analysis of results from top panel as well as other experiments. Internalized hOAT4 was expressed as % of total initial cell surface hOAT4 pool. Values are mean \pm S.E. (n = 3). (*Pharmaceutical Research*. 2010, 27 (4): 589~596)

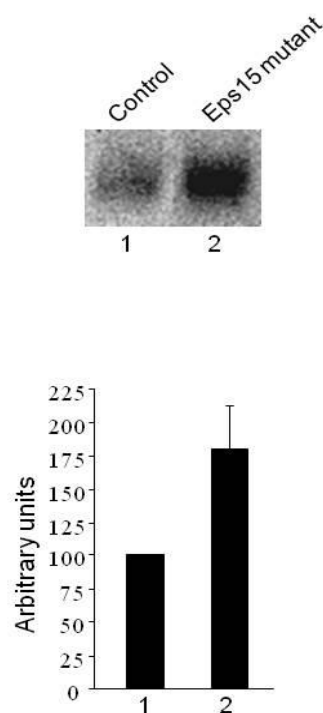


Figure 2-41 Effect of dominant negative mutant of Eps15 on the steady-state surface expression of hOAT4 in COS-7 cells. Top panel: Steady-state surface expression of hOAT4 in cells transfected with or without Eps15 mutant was determined by biotinylation analyses. Bottom panel: Densitometry analysis of results from top panel as well as other experiments. Surface expression of hOAT4 in cell transfected with Eps15mutant was expressed as% of total cell surface hOAT4 pool in control cells. Values are mean \pm S.E. (n = 3). (*Pharmaceutical Research*. 2010, 27 (4): 589~596)

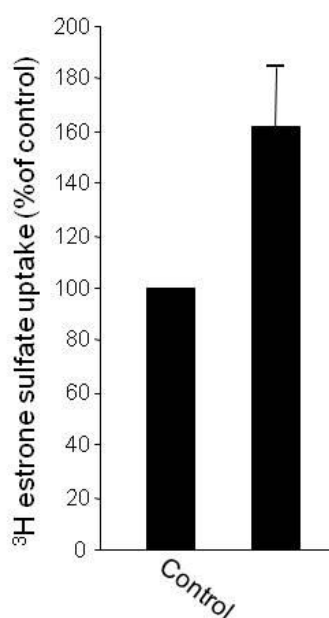


Figure 2-42 Effect of dominant negative mutant of Eps15 on the function of hOAT4 in COS-7 cells. Four-min uptake of [³H] estrone sulfate (100 nM) into cells transfected with Eps15 mutant was examined. Uptake activity was expressed as a percentage of the uptake measured in control cells. Values are mean \pm S.E. (n = 3). (*Pharmaceutical Research*. 2010, 27 (4): 589~596)

2.3.6.3 Immunolocalization of OAT4

The cellular distribution of hOAT4 in COS-7 cells was analyzed by using confocal microscopy. COS-7 cells expressing hOAT4 were fixed and labeled with antibodies specifically binding to hOAT4 and EEA1. As indicated in Fig. 2-43, hOAT4 proteins were partially colocalized with EEA1 in the EEA1-positive early endosomes.

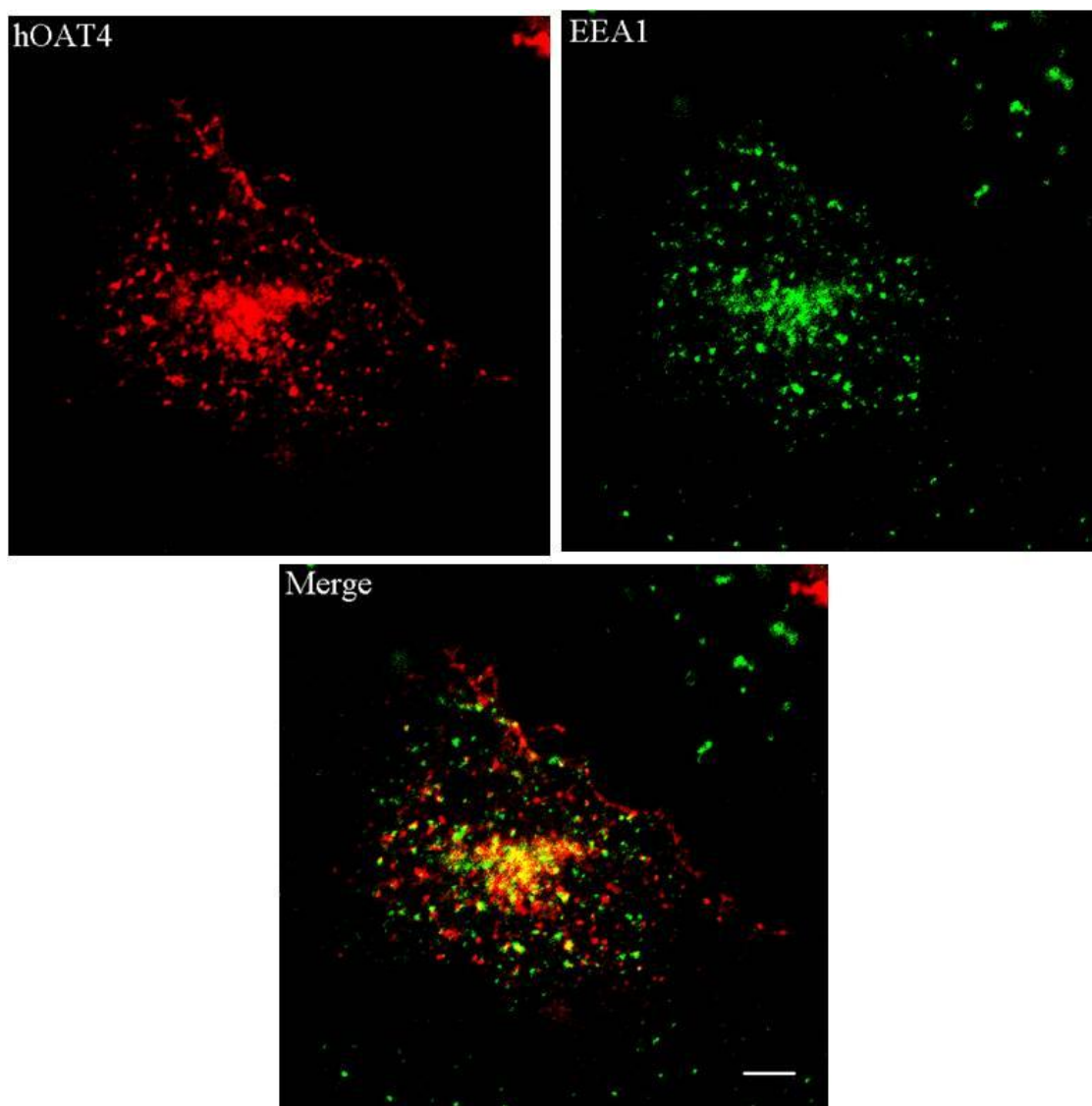


Figure 2-43 Immunolocalization of hOAT4 and EEA1 in COS-7 cells. The cells were immunostained for hOAT4, and early endosome marker EEA1. Fluorescence images were taken for hOAT4 (red), and EEA1 (green). The merged image of hOAT4 and EEA1

was shown as orange/yellow. Bar = ~10 μ m. (*Pharmaceutical Research*. 2010, 27 (4): 589~596)

2.4 Discussion

Organic anion transporters (OAT) are of great importance in the body disposition of a variety of clinical drugs, including anti-cancer, anti-HIV, antibiotics and anti-inflammatory drugs. Under different conditions, OAT proteins can be regulated in a long-term or short-term manner. Long-term regulations of OAT are mainly mediated by gene expression, and short-term regulations are mainly post-translational modifications such as phosphorylation and glycosylation (3, 5).

Endocytosis is one of the most important pathways for molecules internalized from the cell surface into the intracellular compartments. There are several lines of evidence (5) suggesting that OAT functions might be regulated through membrane trafficking mechanisms like other transporters such as dopamine transporter (6), norepinephrine transporter (7), and glucose transporter (8). Furthermore, as shown in Fig 4b, there is a sizable pool of intracellular OAT1 under basal condition, which implies that OAT1 may undergo constitutive internalization from and recycling back to the cell surface.

In the present study, we investigate the constitutive trafficking of both hOAT1 and hOAT4 in COS-7 cells. There are several advantages which COS-7 cells can provide as an important mammalian cell model system to study cloned organic anion transporters. First, COS-7 cells were directly derived from the kidney of the African green monkey, and have been used to study renal transport processes and cellular functions including

organic anion transport. Second, there are no endogenous PAH or estrone sulfate transporters in these cells. As a result, expression of hOAT1 or hOAT4 in COS-7 cells will allow us to investigate the transport characteristics of OATs proteins in a relevant mammalian cell system in the absence of possibly confounding effects of other organic anion transporters. Third, COS-7 cells possess endogenous PKC and PKA signaling pathways. COS-7 cells provide a good experimental system for investigating the regulatory mechanisms of various transport processes.

Among the approaches for analyzing kinetics of internalization of membrane proteins, the biotinylation-based approach is a good one to accurately describe the kinetic rates of internalization membrane proteins. In my study, the biotinylation-based endocytosis approach was chosen to analyze the kinetics of constitutive endocytosis of both hOAT1 and hOAT4 in COS-7 cells.

To directly determine whether OAT proteins recycle back to the plasma membrane after internalization, we used a biotinylation-based method to examine the kinetics of constitutive recycling of OAT proteins in COS-7 cells. This recycling assay has been utilized by other researchers to characterize the recycling of other membrane proteins including dopamine transporter (6), gamma-aminobutyric acid transporter (12), and chloride transporter (11). To validate our experimental procedure, we chose transferrin receptor (TfR) as a positive control protein and Na⁺/K⁺ ATPase as a negative control protein, because TfR is known to recycle back to the plasma membrane after constitutive internalization and Na⁺/K⁺ ATPase is known not to considerably participate in constitutive membrane trafficking (6, 11). To rule out the possibility of the contribution of newly-synthesized hOAT1 proteins to the increase in biotinylated hOAT1 proteins in

the recycling assay, we blocked proteins synthesis by treating cells with cycloheximide over a time span of 2 h. Figure 13 indicates that the treatment of cycloheximide for 2h did not alter either the surface or total expression of hOAT1 proteins. Therefore, the contribution of biosynthesis of hOAT1 to the cell surface hOAT1 is not significant over the time frames in which our recycling experiments were conducted.

The approaches we used for analyzing the kinetics of membrane trafficking of OATs proteins provide a proper platform for investigating the precise mechanism underlying the OATs trafficking in a mammalian cell system.

Our group has reported that PKC activation by PMA inhibited the function of mouse organic anion transporter (mOAT) in the pig proximal tubule-like cell line LLC-PK1 by decreasing the maximum transport velocity (V_{max}) of mOAT without directly phosphorylating the transporter (16).

In that study, the mOAT-mediated transport of radio-labeled PAH was decreased by 50% after treatment of 0.1 μ M PMA for 3 h compared to that of untreated cells. The inhibition of PAH transport by PKC activation was time- and concentration-dependent. To determine whether the PKC-dependent inhibition of PAH transport was mediated by phosphorylation of mOAT, LLC-PK1 cells were metabolically labeled with [32 P]orthophosphate and immunoprecipitated with anti-myc antibody. The results showed that no phosphorylated mOAT was detected in the presence of various concentrations of PMA, suggesting that the phosphorylation of mOAT is unlikely responsible for the PKC-dependent down-regulation of PAH transport.

We further conducted a transport kinetic study to elucidate the mechanism of the PMA-induced inhibition of PAH transport (16). An Eadie-Hofstee analysis of the kinetics data

indicated that PMA treatment gave rise to a remarkable decrease in the maximum velocity (V_{max}) of mOAT without a significant change of affinity for PAH (K_m).

Interestingly, Wolff et al reported that preincubation of oocytes expressing Flag-tagged hOAT1 with 1 μ M PMA for 1h induced substantial redistribution of hOAT1 from cell surface into the intracellular compartments under cell membrane based on an immunocytochemistry study (34). Recently, we also found that PKC-activation by PMA caused a remarkable decrease in cell surface hOAT1 with a concomitant increase in intracellular OAT1 in COS-7 cells stably expressing OAT1. And the total expression levels of OAT1 in the cells were unchanged. Hence, the PMA-induced loss of OAT1 from the cell surface is responsible for the decrease in V_{max} of OAT1 following PMA treatment. Given the experimental results, it is possible that the membrane trafficking of OAT1 is a possible mechanism underlying the down-regulation of OAT1 function by PKC-activation.

One of the advantages of using COS-7 cells for study of OATs proteins trafficking is that the cells possess endogenous PKC and PKA signaling pathways. COS-7 cells provide a good experimental system for investigating the regulatory mechanisms of various transport processes (35, 36). In the present study, we found that PKC activation induced a redistribution of hOAT1 and hOAT4 from the cell surface to the intracellular compartments in COS-7 cells. By looking at the effect of PKC activation on the endocytosis of these transporters, we observed that the endocytosis of both transporters was accelerated by PKC activation in COS-7 cells. However, the recycling rate of hOAT1 was not affected by PMA treatment, indicating that PKC activation enhanced the

endocytosis of hOAT1 without changing the recycling of hOAT1 back to the plasma membrane.

Other studies have shown that the endocytosis of other transporters can be accelerated by PKC activation, such as dopamine transporter (6), gamma-aminobutyric acid transporter (12), and norepinephrine transporter (7). Loder *et al* (6) reported that the recycling of dopamine transporter was also inhibited by PKC activation in rat pheochromocytoma cells. Taken together, the precise mechanism by which PKC regulates the membrane trafficking of OATs proteins remains unclear, and more studies will be needed to dissect the molecular mechanism of PKC-regulated endocytosis of OATs proteins.

Three different internalization pathways have been described for membrane proteins: (i) clathrin-mediated internalization, (ii) caveolae-mediated internalization, and (iii) clathrin- and caveolae-independent internalization. Dynamin is an important protein involved in pinching off of endocytic vesicles from the plasma membrane in both clathrin-dependent and caveolae-dependent pathways. During the process of formation of clathrin-coat on cell surface, a variety of adaptor proteins play essential roles, including adaptor protein complex 2 (AP2), epsin, and Eps15. On the other hand, the membrane protein caveolin is of importance for the formation of endocytic vesicles in caveolae-mediated internalization because this protein is an essential structural component of caveolae in most cells (15).

To determine whether OATs proteins internalize via a clathrin-dependent pathway, the constitutive and PKC-modulated internalization of OATs were determined under the manipulations that specifically block clathrin-dependent internalization: (i) treatment of the cells with ConA, (ii) depletion of potassium in the cells, (iii) transfection of a

dominant negative mutant of dynamin-2 (K44A Dyn-2), and (iv) transfection of a dominant negative mutant of Eps15 ($\Delta 95/295$). All of these methods significantly reduced hOAT1 internalization in hOAT1-expressing COS-7 cells. Transfection of dominant negative mutant of dynamin-2 or Eps15 also inhibited hOAT4 internalization in hOAT4-expressing COS-7 cells. Immunocolocalization study shows that hOAT1 and transferrin (a marker of clathrin-mediated endocytosis) were considerably colocalized both at the cell surface and in the early endosomes. The fact that blocking the clathrin-mediated endocytosis by chemical inhibitors or overexpression of dominant negative mutants of dynamin-2 and Eps15 did not completely block the constitutive and PKC-regulated hOAT1 endocytosis suggests that hOAT1 proteins internalize partly via a dynamin- and clathrin-dependent pathway. It is worth to note that hOAT1 is overexpressed in hOAT1-expressing COS-7 cells, and in the overexpression system, it is possible to see that hOAT1 proteins do not completely colocalize with transferrin.

It is interesting to ask why the cell spends energy to allow OATs proteins cycle between the cell surface and the intracellular compartments. Our speculation is that the transporters at the plasma membrane are in a dynamic rather than static state so that the cell can respond to environmental changes in a more rapid and efficient fine-tuning manner.

3 Regulation of OATS by structure motives

3.1 Introduction

Adaptor proteins that are capable to specifically bind to drug transporters may regulate the cell-surface expression, transport activity, and intracellular trafficking of drug transporters (37). Among these adaptor proteins, PDZ proteins have been shown to play important roles in regulation of drug transporters (37, 38). The name of PDZ proteins derives from the first identified three proteins containing PDZ domains: PSD-95, Discs-large, and ZO-1. Some drug transporters that belong to the SLC superfamily have been found to bear a PDZ-binding motif, such as OAT4, OCTN1, OCTN2, OATP-A, OATP-B, PEPT1, and PEPT2 (37).

The PDZ-binding motif (S-T-S-L) of hOAT4 is located at its carboxyl terminus. Interestingly, our and other group's previous reports have shown that hOAT4 function was enhanced by the interaction with PDZ proteins, PDZK1 and NHERF1 as a result of an increase in the cell-surface expression of this transporter (39, 40). In this study, we attempted to elucidate the mechanism underlying the regulation of hOAT4 function by PDZ proteins.

Dileucine (LL)-based motives have been demonstrated to play important roles in various cellular processes including endocytosis of transmembrane proteins (20, 41), transport of proteins from the ER to the plasma membrane (42), and sorting of transmembrane

proteins to the lysosome (41). Because the structural elements of hOAT1 that dictate the trafficking of this transporter have not been identified yet, we hypothesize that the dileucine (Leu6Leu7) located at the amino-terminus of hOAT1 may play a role in the membrane trafficking of hOAT1 protein.

3.2 Materials and Methods

3.2.1 Materials and Instruments

3.2.1.1 Cell

COS-7 cell was purchased from American Type Culture Collection (Manassas, VA).

3.2.1.2 Chemicals

Dulbecco's modified Eagle's medium was purchased from Cellgro (Manassas, VA). Fetal bovine serum, protease inhibitor cocktail, Triton X-100, leupeptin, pepstatin A, MG132, glycerol, goat serum, and Sodium 2-mercaptoethanesulfonate (MesNa) were purchased from Sigma (St. Louis, MO). 4PBA was purchased from EMD Chemicals (Gibbstown, NJ). Paraformaldehyde was purchased from Electron Microscopy Sciences (Hatfield, PA). LipofectAmine 2000™ reagent, 1 M Tris-HCl (pH 7.5 and pH 8.0) and geneticin (G418) were purchased from Invitrogen (Carlsbad, CA). SuperSignal West Dura extended duration substrate kit, NHS-SS-biotin and streptavidin-agarose beads were purchased from Thermo Scientific (Waltham, MA). p-[³H]Aminohippuric acid (PAH) was from NEN Life Science Products (Hercules, CA). [³H] estrone sulfate was purchased from Perkin-Elmer Life and Analytical Sciences (Boston, MA). 7.5% ready gel, glycine and

protein assay reagent were purchased from Bio-Rad (Hercules, CA). QuikChange II XL Site-Directed Mutagenesis Kit was purchased from Stratagene (La Jolla, CA).

3.2.1.3 Antibodies

Mouse anti-c-Myc monoclonal antibody (9E10) was purchased from Hybridoma Center, Mount Sinai School of Medicine (New York, NY). Mouse anti- β -actin monoclonal antibody was purchased from Thermo Scientific (Waltham, MA). Rabbit anti-calnexin polyclonal antibody was purchased from Enzo Life Sciences International (Plymouth Meeting, PA). Alexa Fluor® 488 goat anti-mouse IgG (H+L), and Alexa Fluor® 350 goat anti-rabbit IgG (H+L) were from Molecular Probes (Eugene, OR). Goat anti-mouse IgG conjugated to horseradish peroxidase was purchased from Thermo Scientific (Waltham, MA).

3.2.1.4 Plasmid

Human NHERF1 cDNA (accession number, BC011777) was purchased from Open Biosystems (Huntsville, AL).

3.2.1.5 Buffers

- (1) Phosphate-buffered saline (PBS)/Ca²⁺ and Mg²⁺: 137 mM NaCl, 2.7 mM KCl, 4.3 mM Na₂HPO₄, 1.4 mM KH₂PO₄, 0.1 mM CaCl₂, and 1 mM MgCl₂, pH 7.4.
- (2) Regular lysis buffer (biotinylation): 10mM Tris-HCl (pH7.5), 150mM NaCl, 1mM EDTA, 0.1% SDS, 1% Triton X-100.
- (3) NT buffer: 20 mM Tris-HCl (pH8.0), 150mM NaCl, 1mM EDTA, 0.2% BSA, adjust pH to 8.5 with NaOH.

- (4) 5 × Laemmli loading Buffer: 28.5% glycerol, 175mM Tris-HCl(pH6.8), 7.5% SDS, 0.03% BPB dye, 12.5% β-mercaptoethanol (freshly added).

3.2.1.6 Instruments

Fluorchem® 8800 system (Alpha Innotech, USA), BioPhotometer (Eppendorf, Germany, Zeiss LSM-510 laser-scanning microscope (Carl Zeiss Inc., Thornwood, NY).

3.2.2 Experimental Procedures

(1) Cell culture

COS-7 cells and COS-7 cells stably expressing hOAT1-C-myc are grown at 37 °C and 5% CO₂ in Dulbecco's modified Eagle's medium (Cellgro, USA) supplemented with 10% fetal bovine serum (Sigma), 100 units/ml penicillin, and 100 mg/ml streptomycin.

(2) Transfection

1. Plate 5×10^5 COS-7 cells in a 35 mm dish and grow for 24 h;
2. For each 35 mm dish, mix 4 µg of plasmid DNA in 250 µl of Opti-MEM®I reduce serum medium in a sterile EP tube, and mix 10 µl of Lipofectamine 2000 transfection reagent in 250 µl of Opti-MEM®I reduce serum medium in a sterile EP tube. Incubate for 5 min at room temperature;
3. Combine the diluted DNA and diluted Lipofectamine 2000, mix gently and incubate for 20 min at room temperature;
4. Mix the DNA-Lipofectamine 2000 complexes with culture medium by adding 100 µl of complexes to 2 ml of culture medium for each 35 mm dish, and mix gently;

5. Remove the medium in the dish containing cells and add the medium with the DNA-Lipofectamine 2000 complexes into the dish.
6. Incubate the cells for 24 ~ 72 h in a cell culture incubator at 37 °C.

Note: To reduce the toxicity of Lipofectamine 2000, the medium with the DNA-Lipofectamine 2000 complexes may be replaced by the medium without the complexes 4 ~ 6 h after transfection.

(3) Uptake assay

1. Plate 5 ~ 7 x 10⁴ COS-7 cells expressing hOAT1-C-myc into collagen-coated 48-well plate in triplicate evenly;
2. Preparation of uptake solution:
 - a. PAH: 19 µM cold PAH + 1 µM hot [³H] PAH, totally 20 µM. (long-time stored cold PAH may be degraded that lead to a lowered uptake value)
 - b. Stock solution: cold PAH: 50 mM, hot [³H] PAH: varies from batch to batch
 - c. Estrone sulfate: 50nM for both cold and hot [³H] Estrone sulfate
 - d. Stock solution: Cold estrone sulfate: 100 µM, hot estrone sulfate: varies from batch to batch.
3. Put the plate on bench for 5 min at room temperature (allow the media to reach room temperature);
4. Aspirate the medium, add 120 µl of uptake solution, for PAH let stand 3 min, or for Estrone Sulfate 3 or 4 min, rotating the plate slowly on a shaker at room temperature;

5. Stop uptake by adding 500 μ l of ice-cold PBS (+) (freshly add 1 mM CaCl_2 and 1 mM MgCl_2) at a rate of three wells/min. Aspirate the uptake solution and PBS (+), and wash each well once with 500 μ l of ice-cold PBS (+);
6. Aspirate PBS (+) completely, add 200 μ l of 0.2 N NaOH to lyse cells, rotating rigorously for more than 40 min at room temperature;
7. Label the scintillation vials, add 200 μ l of 0.2 N HCl for neutralization. Pipette up and down the cell lysate and transfer all the lysate into the scintillation vials;
8. Add 3 ml of scintillation liquid, mix and cap;
9. Insert 1.44M floating disk into machine, use program "01" label. The counting is carried out at a rate of approximately 75 seconds /vial;
10. Analyze data using Microsoft Excel software.

(4) Cell surface biotinylation

1. Plate 5×10^5 cells on each well of a 6-well plate or a 35 mm dish, and grow for 24 hours;
2. Place the 6-well plate on ice for a couple of minutes;
3. Aspirate the medium and wash cells with 2 ml of cold PBS(+) (pH8.0) [supplemented with both 1mM Ca^{2+} (CaCl_2) and 1mM Mg^{2+} (MgCl_2)] two times to remove any proteins in the culture medium and cool down the cells rapidly;
4. Add 1ml of freshly prepared 0.5 mg/ml NHS-SS-Biotin (Pierce) in PBS(+) (pH8.0);
5. Incubate the cells on ice for twice, each time for 20 min with gently shaking on an orbital shaker ;

6. Remove biotin solution and wash cells with 2 ml of 100mM Glycine in PBS(+) (pH8.0) once;
7. Incubate the cells with 2 ml of cold 100mM Glycine in PBS(+) (pH8.0) for 20 ~ 30 min, with gently shaking on a orbital shaker;
8. Extensively wash the cells twice with 2ml of cold PBS (+) (pH8.0);
9. Add 400 ~ 500 μ l of regular lysis buffer with freshly added Proteinase Inhibitor Cocktail (Sigma);
10. Vigorously shake the plate on ice for 10-15 min, harvest cells to an Eppendorf (EP) tube by using a cell scraper. Squeeze cells with a pipet tip by pipetting in order to help break down cell membrane;
11. Rotate the EP tubes for 40 min at 4°C for further lysis;
12. Centrifuge the tubes at 13200 rpm for 20 min at 4°C;
13. Transfer the supernatant to a new EP tube;
14. Measure protein concentrations to normalize loading amount of proteins. 300 ~ 500 μ g of proteins may be applied to bind streptavidin-agarose beads;
15. 40 μ l of Streptavidin-Agarose beads (Pierce) is added to each tube. Rotate for 1.5 ~ 4 h at 4°C;
16. After rotation, centrifuge at 13,200 rpm for 1 min at 4°C. Wash the beads with 1ml of regular lysis buffer for 3 times (don't lose beads);
17. Wash the beads with 1ml of PBS (pH7.4).

18. Now all the membrane proteins are bound to beads, so the target protein has to be released for the following immunoblot detection. The remaining volume of PBS in beads is estimated and add 10 μ l of 5X Laemmli sample buffer with freshly added beta-mercaptomethanol (reducing agent, final concentration is 5%);
19. Incubate the mixture for 30min at 50°C to denature the released proteins. During the incubation, tap the bottom of tubes 3 times to make sure that all beads are accessible to the Laemmli sample buffer;
20. After denaturing is done, spin down the samples. Then Western Blot is followed.

(5) Internalization assay

A. Cell surface biotinylation

1. Plate 5×10^5 cells on each well of a 6-well plate or a 35 mm dish, and grow for 24 hours;
2. Place the 6-well plate on ice for a couple of minutes;
3. Aspirate the medium and wash cells with 2 ml of cold PBS(+) (pH8.0) [supplemented with both 1mM Ca^{2+} (CaCl_2) and 1mM Mg^{2+} (MgCl_2)] two times to remove any proteins in the culture medium and cool down the cells rapidly;
4. Add 1ml of freshly prepared 0.5 mg/ml NHS-SS-Biotin (Pierce) in PBS(+) (pH8.0);
5. Incubate the cells on ice for 20 min with gently shaking on an orbital shaker;
6. Remove biotin solution and wash cells with 2 ml of 100mM Glycine in PBS(+) (pH8.0) once;

7. Incubate the cells with 2 ml of cold 100mM Glycine in PBS(+) (pH8.0) for 20 ~ 30 min, with gently shaking on a orbital shaker;
8. Extensively wash the cells twice with 2ml of cold PBS (+) (pH8.0);
9. After quenching of Glycine, each 35mm-dish is incubated in prewarmed PBS(+), pH7.4 or serum-free medium at 37°C for a designated period of time. (Based on my experience, 3 minutes is enough for a 35mm-dish to reach the endocytosis-allowable temperature, so the actual time is 3 minutes longer than the designated time, eg. if 5 min is the designated time, the actual time of incubation is 8 min.);

B. Internalization and stripping

10. After 37°C incubation, put the dishes on ice immediately and wash twice with cold PBS (+), pH 7.4 to stop endocytosis;
11. Add 2ml Stripping Buffer (MesNa, 30 min X 2 times, 50mM in NT buffer) to strip the membrane-bound biotin with gentle shaking.
12. Wash cells twice with cold PBS, pH 7.4. (For some highly-expressed proteins, concentration of MesNa and incubation times may be increased for desired stripping efficiency through optimization.) ;

C. Cell lysis and binding to streptavidin-agarose

13. Add 400 ~ 500 µl of regular lysis buffer with freshly added Proteinase Inhibitor Cocktail (Sigma);
14. Vigorously shake the plate on ice for 10-15 min, harvest cells to an Eppendorf (EP) tube by using a cell scraper. Squeeze cells with a pipet tip by pipetting in order to help break down cell membrane;

15. Rotate the EP tubes for 40 min at 4°C for further lysis;
16. Centrifuge the tubes at 13200 rpm for 20 min at 4°C;
17. Transfer the supernatant to a new EP tube;
18. Measure protein concentrations to normalize loading amount of proteins. 300 ~ 500 µg of proteins may be applied to bind streptavidin-agarose beads;
19. 40 µl of Streptavidin-Agarose beads (Pierce) is added to each tube. Rotate for 1.5 ~ 4 h at 4°C;
20. After rotation, centrifuge at 13,200 rpm for 1 min at 4°C. Wash the beads with 1ml of regular lysis buffer for 3 times (don't lose beads);
21. Wash the beads with 1ml of PBS (pH7.4).
22. Now all the membrane proteins are bound to beads, so the target protein has to be released for the following immunoblot detection. The remaining volume of PBS in beads is estimated and add 10 µl of 5X Laemmli sample buffer with freshly added beta-mercaptomethanol (reducing agent, final concentration is 5%);
23. Incubate the mixture for 30min at 50°C to denature the released proteins. During the incubation, tap the bottom of tubes 3 times to make sure that all beads are accessible to the Laemmli sample buffer;
24. After denaturing is done, spin down the samples. Then Western Blot is followed.

D. Data analysis

Relative OAT1 internalized is calculated as % of the total initial cell-surface hOAT1 or hOAT4 pool.

(6) Site-directed mutagenesis

1. Design the primer pair containing the site(s) you want to mutate according to the manual of Site-Directed Mutagenesis Kit (Stratagene);

Note: Check the secondary structure of primers on the website of IDT (Integrated DNA Technologies, Iowa) or other websites providing the free software for the DNA structural analysis.

2. Primer synthesis (two complimentary oligonucleotides) provided by IDT;
3. Dissolve the primers in ddH₂O and dilute to the concentration of 125 ng/ul for use;
4. Set up a reaction of 25 µl total volume (the manual of Site-Directed Mutagenesis Kit);
5. Run PCR after choose programs for mutation;

Note: PCR condition is based on the manual of Site-Directed Mutagenesis Kit.

6. Add 0.5 µl of Dpn I restriction enzyme to the reaction tube, and incubate for at least 1 hour at 37°C to digest the parental DNA strands;
7. Dilute PCR products with purified water at 1:5 ratio before performing transformation;
8. Conduct transformation (see the protocol of transformation);
9. Grow the transformed bacteria in the incubator overnight at 37°C;
10. Select two different colonies from the LB agar plate;
11. Purify plasmids using Spin Mini-Prep kit (QIAGEN);
12. Sequence the purified plasmids to confirm the correct mutations at the DNA core facility of UMDNJ, Piscataway, NJ;

13. Analyze the sequencing data by using “Laser gene” software (DNASTAR, Inc.) (see the manual of Laser gene).

(7) Transformation

1. Thaw DH5 α competent cells on ice for 10min without pipetting;
2. Transfer 10 μ l of competent cells into an ice-chilled “2059” tube on ice;
3. Add 1 μ l of plasmid DNA (10 ~ 100 ng/ μ l) to competent cells. Mix the contents thoroughly but gently by stirring the cells while adding the DNA with the pipette tip;
4. Incubate the tubes for 30 minutes on ice;
5. Incubate the competent cells for 45 seconds at 42 °C in a water bath;
6. Put the tubes on ice and incubate for 2 min;
7. Add 190 μ l of SC medium to each tube;
8. Incubate the tubes in an incubator at 225 rpm for 1h at 37 °C;
9. Seed 50 ~ 100 μ l of cell suspension from each tube on a prewarmed LB plate with 100 μ g/ml ampicillin;

Note: A different antibiotic may be used if the selection resistance of the plasmid is not ampicillin, for example, kanamycin.

10. Incubate the plates for 16 ~ 24 hours in an incubator at 37 °C;
11. Check the growth of bacteria by observing the morphology of colonies.

(8) Immunostaining for colocalization

A. Cell fixation

1. 1×10^5 COS-7 Cells expressing hOAT1-C-myc are cultured on cover glass (thickness 0.15, suitable for laser) in a 24-well plate;
2. Incubate cells with 1 μ M transferrin-tetramethylrhodamine conjugate (Molecular Probes) in DMEM medium at 4 °C for 1 h;
3. Incubate cells at 37 °C for a designated period of time (allow internalization to occur);
4. Wash cells with PBS twice;
5. Add freshly prepared 4% paraformaldehyde in PBS, and incubate for 20 min at room temperature avoiding light.

B. Cell permeabilization

6. Incubate the cells with freshly prepared 0.1 % Triton X-100 in PBS for 5 min at room temperature;
7. Wash once with PBS;
8. Incubate the cells with 0.1 % Triton X-100 in PBS for 5 min at room temperature;
9. Wash once with PBS;
10. Incubate the cells with 0.1 % Triton X-100 in PBS for 5 min at room temperature;
11. Wash twice with PBS.

C. Fluorescent probe labeling

12. Incubate the cells with freshly prepared 5% goat serum in PBS for 1 ~ 2 h at room temperature;
13. Incubate the cells with primary antibodies in freshly prepared 2.5% goat serum in PBS for 2h at room temperature or overnight at 4 °C;

Note: Two antibodies against two antigens must be from different species. Use 2 $\mu\text{g}/\text{ml}$ of 9E10 mAb, 1.5 $\mu\text{g}/\text{ml}$ of rabbit anti-myc pAb (Sigma), and 1:250 dilution of anti-EEA1 mAb (BD Biosciences) for colocalization analysis.

14. Wash four times with PBS;
15. Incubate the cells with fluorescence-labelled secondary antibodies in 2.5% goat serum in PBS for 2 h at room temperature;
16. Note: Two fluorescence-labelled antibodies must recognize two different immunoglobulins, such as mouse IgG and rabbit IgG. Use anti-mouse and anti-rabbit IgG at 1:1000 dilution for hOAT1 detection, and anti-mouse IgG at 1:500 dilution for EEA1 detection.
17. Wash four times with PBS for 5 min each time with gentle rotation.

D. Antifading reagents and mounting

18. Put a small drop of anti-fading reagent on the microscope slide, and transfer the glass cover on which the cells grow to the drop of anti-fading reagent on the microscope slide with the side of cells facing down;
19. Note: Slowly lay down glass cover to prevent air bubbles.
20. Dry the microscope slides covered with foil for 15 ~ 20 min at room temperature in a chemical hood with strong air flow;
21. Seal the glass cover with a small amount of nail polish;
22. Dry the microscope slides covered with foil for 10 ~ 15 min at room temperature in a chemical hood with strong air flow.

E. Confocal microscopy

23. Check the immunostaining efficiency of specimens under a fluorescent microscope;
 24. Samples are visualized with a Zeiss LSM-510 laser-scanning microscope (Carl Zeiss Inc., Thornwood, NY).
- (9) Total expression analysis of hOAT1 mutants following treatments with protease inhibitors and chemical chaperons
1. Plate 2×10^5 cells on each well of a 12-well plate, and grow for 24 hours.
 2. Transfect 2 μ g plasmid DNA of each hOAT1 mutant with Lipofectamine 2000, change media after 6 h of transfection.
 3. After 48 h of transfection, Cells were incubated in serum-free DMEM media containing proteasomal inhibitor MG132, lysosomal inhibitors leupeptin/pepstatin A, chemical chaperones 4PBA or glycerol individually or in combination.
 4. After the incubation for a designated period of time, wash the cells twice with ice-cold PBS, and lyse cells with 150 μ l of RIPA lysis buffer.
 5. Shake the plate on ice for 30 min, and collect cell lysate.
 6. Pipet the cell lysate with a 100 μ l pipet tip reaching the bottom of the EP tube to break cells effectively.
 7. Rotate the EP tubes on a shaker for 30 min at 4 $^{\circ}$ C and then centrifuge at 13,000 rpm for 20 min.
 8. Transfer the supernatant and measure the protein concentration of the total lysate samples using Bradford method.

9. Transfer 30 ~ 40 μ g of proteins to a new EP tube, and add equal volume of 2X urea sample buffer containing 5% beta-mercaptomethanol (final concentration).
10. Denature the samples for 60 min at RT with tapping every 10 min.
11. Load each denatured sample to a well of minigel, and analyze by SDS-PAGE and immunoblotting.

(10) SDS-PAGE and immunoblotting

A. Gel running

1. At least 400 ml of 1x running buffer is used and can be re-used.
2. Set 200V to run 30 min for 7.5% gel, running time can be adjusted by purpose.

B. Transfer

3. Use 100% methanol to pre-wet the PVDF membrane for 30 seconds, and transfer to Transfer buffer for at least 30min;
4. Use 1200-1500 ml of transfer buffer;
5. Set 100V to transfer for at least 30min (for large proteins, transfer time should be longer).

C. Primary antibody incubation

6. After transfer step, transfer the PVDF membrane to a small container and block with 5 % non-fat milk in PBST keeping the protein side up for 1hour at room temperature with gently shaking;
7. Rinse the membrane with PBST once, add primary antibody (in 2.5 % milk in PBST), and incubate overnight;

8. Wash membrane three times with PBST, 5 min each time;
9. Incubate with secondary antibody (anti-mouse or rat IgG) at a ratio of 1:5000 ~ 1:10000 for 1 h at RT;
10. Extensively wash with PBST for more than three times, each time 10 ~ 15 min.

D. Development of membrane

11. Adjust the focus of the FluorChem 8800 imaging system;
12. Open the software on the computer, click “Acquire”, click “Movie setup”, set “Sensitivity” as Medium;, set Exposure time at 3 ~ 5 seconds, total frames at 30, click “copy to next” until the frame is 30. Then click “GO”;
13. For the marker, take another photo by choosing “reflective”, the exposure time is typically 18 milliseconds.

E. Reprobe with another primary antibody

14. The membrane can be re-probed by stripping the antibody on the membrane with Restore® Western Blot Stripping Buffer (Pierce). Incubate the membrane with stripping buffer for 40 min at 37°C;
15. Wash three times with PBST, 5 ~ 10min each time;
16. Incubate the membrane with another primary antibody overnight.

3.3 Results

3.3.1 Regulation of hOAT4 internalization by NHERF1

Na/H exchange regulatory factor 1 (NHERF1) belongs to a PDZ protein family, NHERF family. It is a cytoplasmic scaffolding protein that is shown to participate in

protein targeting and the assembly of protein complexes (43). NHERF1 contains two tandem PDZ domains at the N-terminal side and an ERM-binding domain at its C-terminal region. The ERM-binding domain can bind to the actin-associated proteins including merlin, ezrin, radixin, and moesin, and tether the protein complex to cytoskeleton elements (37, 43). Epidermal growth factor receptor (EGFR) was found to be regulated by NHERF1. EGFR was stabilized at the cell surface by NHERF1 and the internalization of EGF-EGFR complex was delayed by NHERF1 (44).

Previously we observed that the function of hOAT4 was enhanced by transfection of NHERF1 because of the increased surface expression level of hOAT4 (40). In this study, we observed that the steady-state surface expression level of hOAT4 was increased by overexpression of NHERF1, as seen in Fig. 3-1.

By means of the biotinylation-based internalization approach we used to characterize the hOAT4 internalization, we found that the internalization of hOAT4 in COS-7 cells was significantly inhibited by overexpression of NHERF1 (Fig. 3-2). These results indicate that an increased hOAT4 at the cell surface and a consequent increase in hOAT4-mediated uptake of estrone sulfate after overexpression of NHERF1 was due to the delay of hOAT4 internalization by NHERF1. Therefore, the endocytosis and function of hOAT4 protein and can be modulated by the interaction between this transporter and PDZ proteins such as NHERF1.

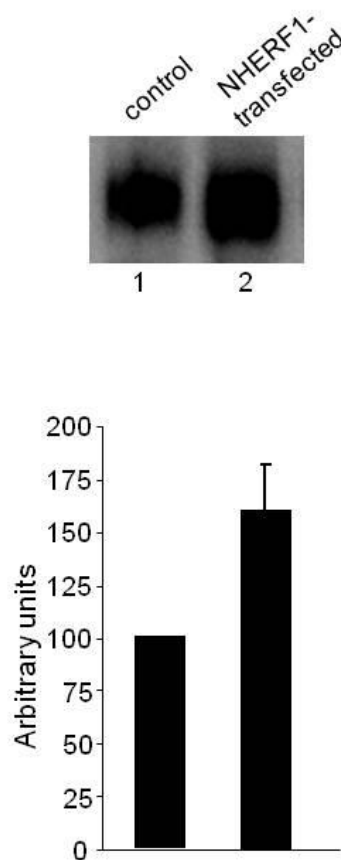


Figure 3-1 Effect of NHERF1 transfection on the steady-state surface expression of hOAT4 in COS-7 cells. Top panel: Steady-state surface expression of hOAT4 in cells transfected with or without NHERF-1 mutant was determined by biotinylation analyses. Bottom panel: Densitometry analysis of results from top panel as well as other experiments. Surface expression of hOAT4 in cell transfected with NHERF-1 mutant was expressed as % of total cell surface hOAT4 pool in control cells. Values are mean \pm S.E. (n = 3). (*Pharmaceutical Research*. 2010, 27 (4): 589~596)

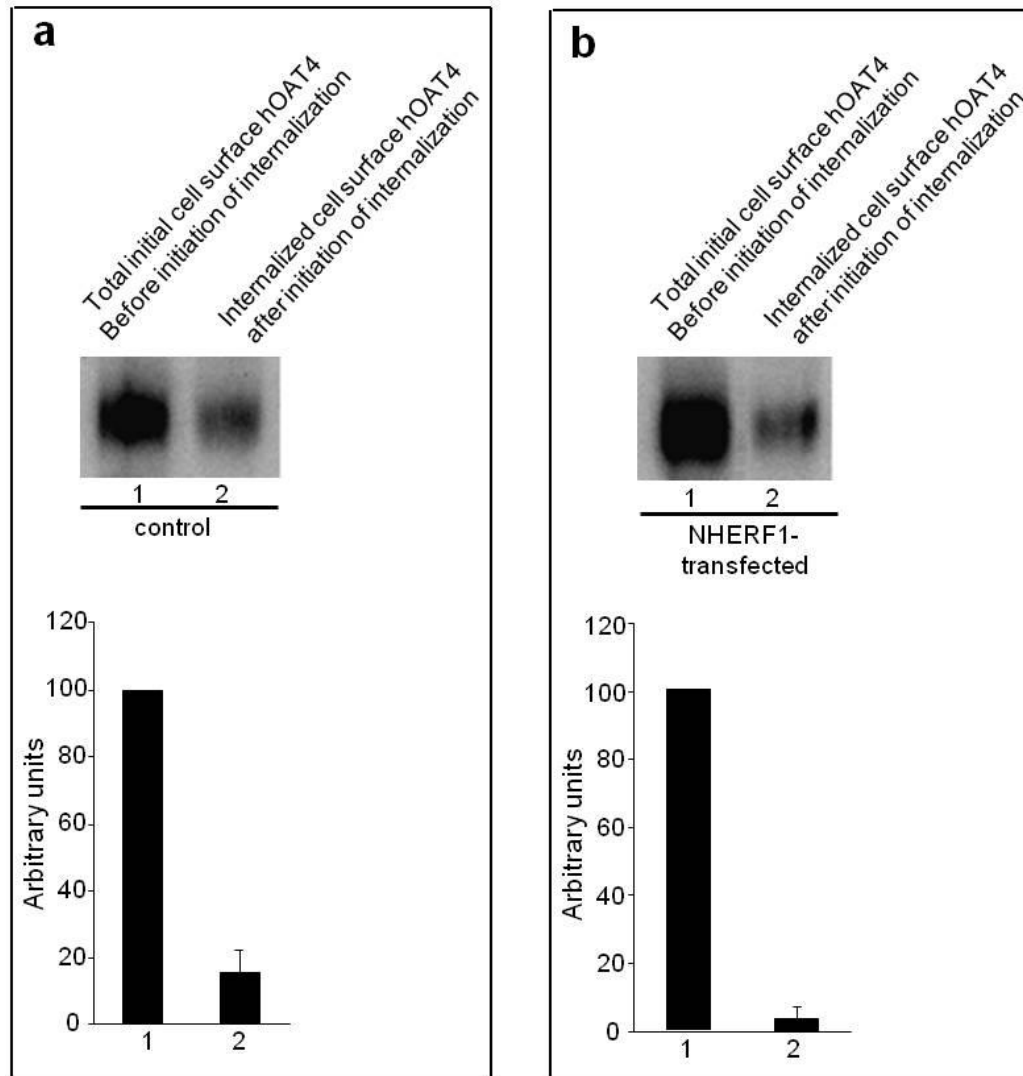


Figure 3-2 . Effect of NHERF1 transfection on the internalization of hOAT4 in COS-7 cells. a. Top panel: Cells were transfected with control plasmid (pcDNA vector). 48 h later, hOAT4 internalization (15 min) was analyzed as described in “Materials and Methods” section followed by Western blotting using anti-myc antibody (1:100). Bottom panel: Densitometry analysis of results from top panel as well as other experiments. Internalized hOAT4 was expressed as % of total initial cell surface hOAT4 pool. Values are mean \pm S.E. (n = 3). b. Top panel: Cells were transfected with cDNA encoding NHERF-1. 48 h later, hOAT4 internalization (15 min) was analyzed as

described in “Materials and Methods” section followed by Western blotting using anti-myc antibody (1:100). Bottom panel: Densitometry analysis of results from top panel as well as other experiments. Internalized hOAT4 was expressed as % of total initial cell surface hOAT4 pool. Values are mean \pm S.E. (n = 3). (*Pharmaceutical Research*. 2010, 27 (4): 589~596)

3.3.2 Role of the dileucine motif (L6L7) at the amino terminus of hOAT1

Dileucine (LL)-based motives have been demonstrated to play important roles in various cellular processes including endocytosis of transmembrane proteins (20, 41), transport of proteins from the ER to the plasma membrane (42), and sorting of transmembrane proteins to the lysosome (41). Because the structural elements of hOAT1 that dictate the trafficking of this transporter have not been identified yet, we hypothesize that the dileucine (Leu6Leu7) located at the amino-terminus of hOAT1 may play a role in the membrane trafficking of hOAT1 protein.

3.3.2.1 The role of LL6 in the function of hOAT1

As shown in Fig. 3-3, the location of the dileucine motif (L6L7) of hOAT1 is at the amino-terminus that is in the intracellular side of the protein. By substituting L6 and L7 with alanine (A) individually or simultaneously, we attempted to determine the possible role of this dileucine motif in the function of hOAT1.

Firstly, we tested the effect of mutation of these leucine residues on the hOAT1-mediated PAH transport in COS-7 cells. Figure 3-4 indicates that individual substitution of Leu6 and Leu7 with alanine resulted in a 20% and 75% reduction in PAH transport mediated

by hOAT1 respectively, and simultaneous substitution of these two leucine residues with alanine caused a complete loss of PAH transport mediated by hOAT1.

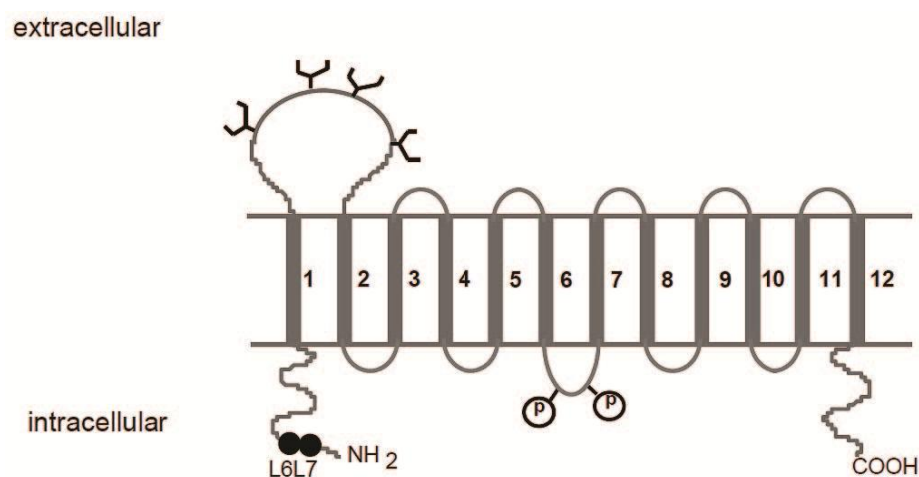


Figure 3-3 Predicted transmembrane topology of hOAT1. Twelve transmembrane domains are numbered from 1 to 12. Potential glycosylation sites are denoted by tree-like structures. Potential phosphorylation sites are labeled as P. Positions of the mutation is indicated by •. (*International Journal of Biochemistry and Molecular Biology*, 2011, 2(1): 31~38)

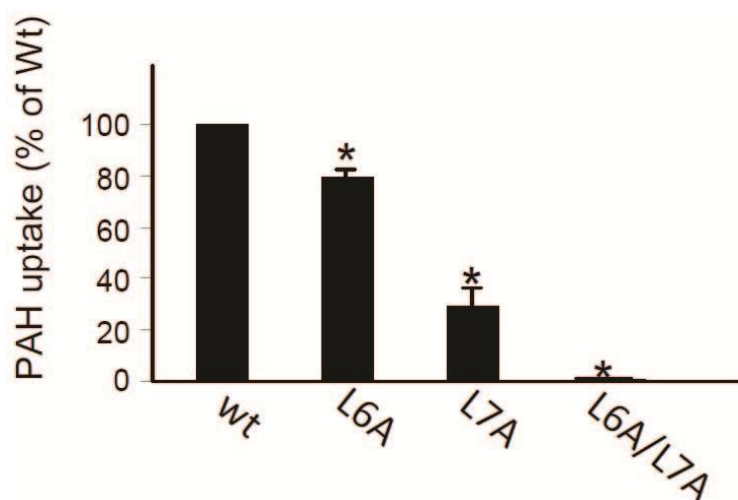


Figure 3-4 ³H-labeled PAH uptake by hOAT1 wild type (Wt) and its alanine-substituted mutants L6A, L7A, and L6A/L7A. Transport of PAH (20 μ M, 3 min) in COS-7 cells expressing hOAT1 Wt, L6A, L7A, and L6A/L7A was measured. Uptake activity was expressed as a percentage of the uptake measured in Wt. The results represent data from three experiments, with triplicate measurements for each mutant. Asterisks indicate values significantly different ($p < 0.05$) from that of Wt. (*International Journal of Biochemistry and Molecular Biology*, 2011, 2(1): 31~38)

3.3.2.2 Effect of mutation of L6A/L7A on hOAT1 expression

Based on the results of the uptake experiment shown in Fig. 3-4, we chose the L6A/L7A mutant for the following study because the transport activity of this mutant was completely lost. Both cell surface and total expression of L6A/L7A hOAT1 were determined by means of immunoblotting method for the purpose of determining the reason for the complete loss of transport activity of L6A/L7A hOAT1.

As shown in Fig. 3-5, the expression of L6A/L7A hOAT1 at the cell surface was completely abolished by the mutation, and the mutant also had no detectable 80 kDa band in the total cell extract with a remarkably reduced 60 kDa band. Our previous studies demonstrated that the 80 kDa band corresponds to the mature form of hOAT1 and the 60 kDa band corresponds to the immature form of hOAT1 (45, 46). As the loading control for immunoblotting, the expression of the house-keeping protein, β -actin, did not change in both wildtype and mutant samples.

These observations indicate that the complete abolished surface expression of L6A/L7A hOAT1 was due to the complete loss of mature form of L6A/L7A hOAT1, because only

mature hOAT1 proteins is presented to the cell surface and transport PAH across the plasma membrane. And the complete loss of transport activity of L6A/L7A hOAT1 resulted from the abolished surface expression of this mutant.

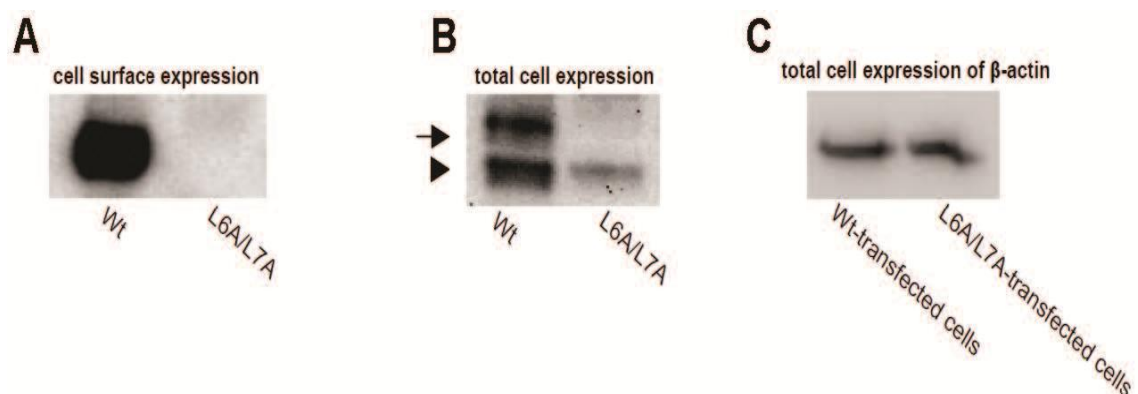


Figure 3-5 Cell surface and total cell expression of hOAT1 Wt and its mutant L6A/L7A.

a. Immunoblotting analysis of cell surface expression of hOAT1 Wt and its mutant L6A/L7A. Cells were biotinylated, and the labeled cell surface proteins were precipitated with streptavidin beads, separated by SDS-PAGE, followed by immunoblotting with anti-myc antibody (1:100). b. Immunoblotting analysis of total cell expression of hOAT1 Wt and its mutant L6A/L7A. Cells were lysed, and their proteins were separated by SDS-PAGE, followed by immunoblotting with anti-myc antibody (1:100). Mature form (cell surface form) was shown as arrow and immature form (ER-resident form) was shown as arrowhead. c. Immunoblotting analysis of β -actin, a house-keeping protein, in cells transfected with hOAT1 Wt and its mutant L6A/L7A. (*International Journal of Biochemistry and Molecular Biology*, 2011, 2(1): 31~38)

3.3.2.3 Effect of protease inhibitors on the expression of mutant L6A/L7A hOAT1

We further investigated the mechanism underlying the loss of expression of the mutant L6A/L7A hOAT1 by treating cells with various protease inhibitors. Cell has two major mechanisms to degrade proteins: one is through the proteasome pathway, and the other is through the lysosome pathway. The proteasome is responsible for the degradation of most cytosolic and nuclear proteins as well as some membrane proteins (47-51), and remove misfolding and misaggregated proteins in the ER (52-55). The lysosome is responsible for the degradation of membrane proteins and extracellular materials that internalize into cell by endocytosis or other mechanisms (56-60).

There are a variety of protease inhibitors that can specifically inhibit either pathway of degradation. MG132 has been commonly used to inhibit the protein degradation by the proteasome (61-65), and leupeptin and pepstatin A are inhibitors widely used to inhibit the lysosome proteolysis (66-70). We previously found (45, 46) that hOAT1 protein in the total cell lysate run as two separate bands of 60 kDa and 80 kDa apparent sizes, and the 60 kDa band was sensitive to the treatment of endoglycosidase H (endo H), but the 80 kDa band was resistant to the endo H treatment. Therefore, the 60 kDa band corresponds to the core-glycosylated immature form of hOAT1 that resides in the ER, and the 80 kDa band corresponds to the fully-glycosylated mature form of this transporter that is targeted to the cell surface.

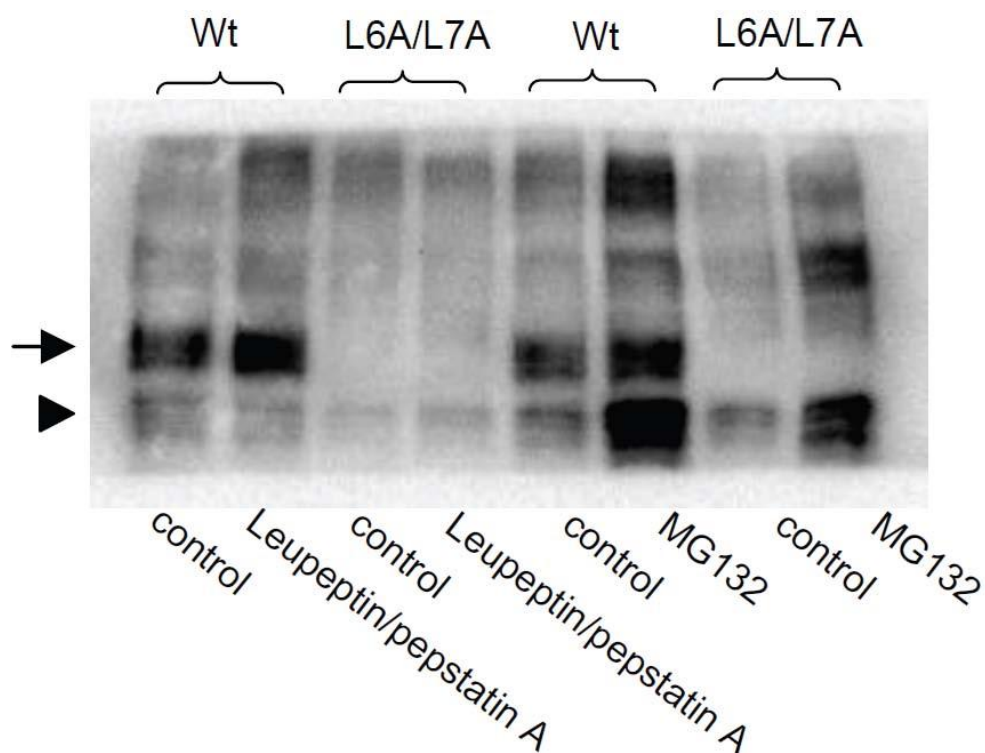


Figure 3-6 Effect of protease inhibitors on the total expression of hOAT1 Wt and its mutant L6A/L7A. Immunoblot analysis of total cell expression of hOAT1 Wt and L6A/L7A in cells treated with or without lysosomal inhibitors leupeptin/pepstatin A (50 μ g/ml for 16 hrs) or proteasomal inhibitor MG132 (10 μ M for 6 hrs). Treated cells were then lysed, followed by immunoblotting using anti-myc antibody (1:100). Mature form (cell surface form) was shown as arrow and immature form (ER-resident form) was shown as arrowhead. (*International Journal of Biochemistry and Molecular Biology*, 2011, 2(1): 31~38)

In Fig. 3-6, we can see that treatment of cells expressing wildtype hOAT1 with the lysosomal inhibitors, leupeptin and pepstatin A, only increased the intensity of 80 kDa band without significant effect on the 60 kDa band in the total cell extract. Treatment of cells expressing the mutant L6A/L7A hOAT1 with leupeptin and pepstatin A had no

effect on the expression of mature form of this protein (80 kDa) in the total cell extracts and slightly increased the intensity of 60 kDa band corresponding to the immature hOAT1 protein.

Treatment of cells expressing wildtype hOAT1 with a proteasomal inhibitor MG132 led to the accumulation of both the immature form (60 kDa) and mature form (80 kDa) of this protein in the total cell extracts. The MG132 treatment of cells expressing L6A/L7A hOAT1 led to the significant accumulation of only the 60 kDa immature form of hOAT1 protein without any effect on the 80 kDa band in the total cell extracts. Similar results were observed at higher concentration of these protease inhibitors (data not shown). In addition, the higher molecular weight bands in MG132-treated samples may represent the polyubiquitinated species because of inhibition of proteasome.

3.3.2.4 Cellular localization of mutant L6A/L7A hOAT1

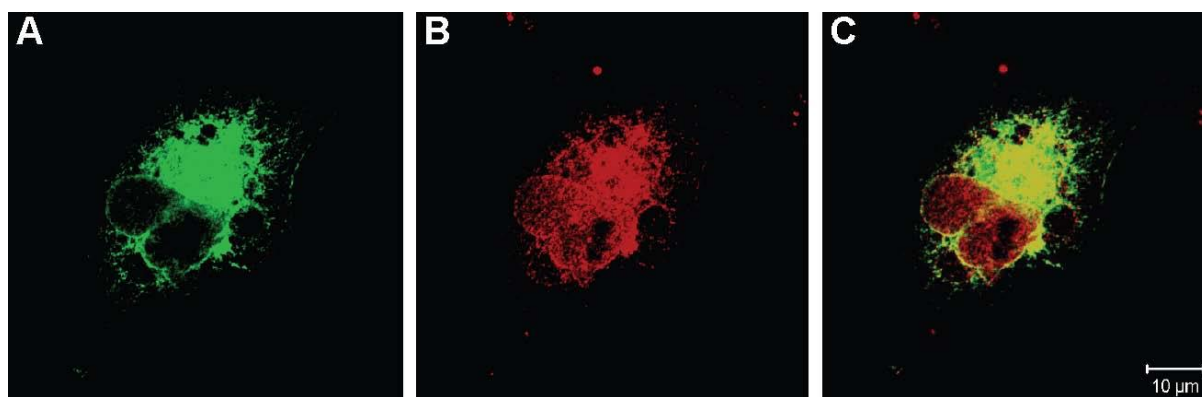


Figure 3-7 Immunolocalization of L6A/L7A hOAT1. L6A/L7A-transfected cells were immunostained for L6A/L7A, and an ER marker calnexin. a, Fluorescence image of L6A/L7A (green). b, Fluorescence images of calnexin (red). c, Merged image (yellow) of

a and b. Bar = $\sim 10 \mu\text{m}$. (*International Journal of Biochemistry and Molecular Biology*, 2011, 2(1): 31~38)

The significant increase in the amount of 60 kDa immature form of mutant L6A/L7A hOAT1 after treatment of the proteasomal inhibitor MG132 suggested that the immature L6A/L7A hOAT1 may accumulate in the ER after inhibition of the proteasome-mediated proteolysis. To determine the cellular localization of L6A/L7A hOAT1 after MG132 treatment, an immunolocalization experiment was performed using confocal microscopy. As demonstrated in Fig. 3-7, L6A/L7A hOAT1 (green) significantly colocalized with calnexin (red), an ER marker, after treatment of L6A/L7A hOAT1 expressing cells with $10 \mu\text{M}$ MG132 for 6 h.

3.3.2.5 Effect of chemical chaperones on the expression of mutant L6A/L7A hOAT1

Chemical chaperons such as sodium 4-phenylbutyrate (4PBA) and glycerol have been shown to promote ER exit and maturation of some plasma membrane proteins (71, 72). With the purpose of promoting the ER exit and maturation of L6A/L7A hOAT1, we treated L6A/L7A hOAT1 expressing cells with 4PBA or glycerol in combination with MG132. Our result in Fig. 3-8 indicates that treatments of both 4PBA and glycerol resulted in an increase only in the 60 kDa immature form of L6A/L7A hOAT1 without considerable effect on the 80 kDa mature form of this mutant.

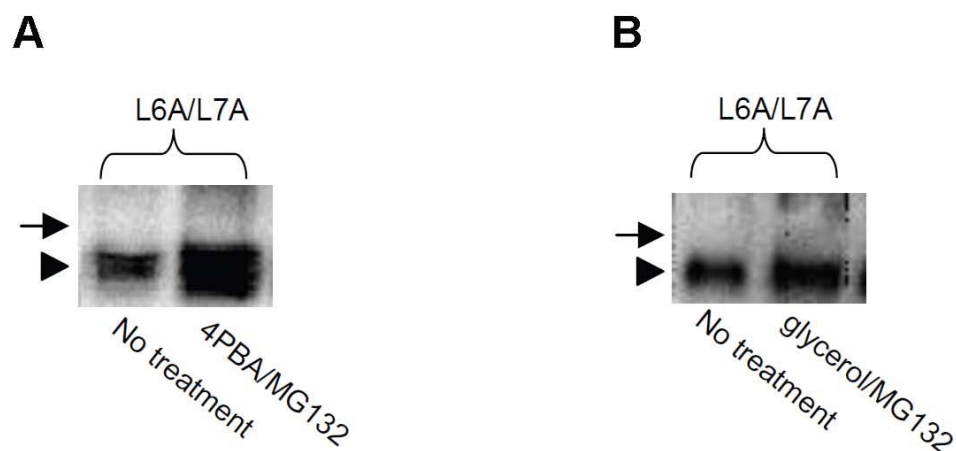


Figure 3-8 Effect of chemical chaperones on the expression of L6A/L7A. a. Effect of 4PBA on the expression of L6A/L7A. L6A/L7A-expressing cells were treated with or without 4PBA (1mM, 24h) in the presence of MG132 (10 μ M). Treated cells were then lysed, followed by immunoblotting with anti-myc antibody (1:100). b. Effect of glycerol on the expression of L6A/L7A. L6A/L7A-expressing cells were treated with or without glycerol (5%, 24h) in the presence of MG132 (10 μ M). Treated cells were then lysed, followed by immunoblotting with anti-myc antibody (1:100). Mature form (cell surface form) was shown as arrow and immature form (ER-resident form) was shown as arrowhead. (*International Journal of Biochemistry and Molecular Biology*, 2011, 2(1): 31~38)

3.4 Discussion

3.4.1 PDZ-binding motif and NHERF1

Previously, Miyazaki et al reported (39) that the PDZ protein NHERF1 interacted with hOAT4 and the association between them enhanced hOAT4-mediated transport of

estrone-3-sulfate in human embryonic kidney 293 (HEK293) cells, and the effect of NHERF1 on hOAT4 function was abolished by deleting the PDZ-binding motif at the carboxyl-terminus of hOAT4. We also observed (40) a similar effect of NHERF1 on hOAT4 function in LLC-PK1 cells. Transit transfection of LLC-PK1 cells expressing hOAT4 with NHERF1 enhanced estrone sulfate transport mediated by hOAT4 and concomitantly increased the surface expression of hOAT4 without an effect on hOAT4 total expression.

These studies suggest that the protein-protein interaction between hOAT4 and NHERF1 stabilized the hOAT4 protein at the plasma membrane and may modulate the trafficking of hOAT4 from and to the cell surface, and the PDZ-binding motif is required for the association between hOAT4 and NHERF1.

To directly address the question whether the hOAT4 endocytosis is affected by the protein-protein interaction between hOAT4 and NHERF1, we examined the internalization of hOAT4 in COS-7 cells transfected with empty vector or NHERF1. As we speculated, overexpression of NHERF1 significantly delayed the internalization of hOAT4 (Fig. 3-2). How this PDZ protein modulated hOAT4 internalization and stabilization at the cell surface remains unclear. Some studies of other membrane proteins whose membrane trafficking processes are modulated by NHERF1 may provide some clues to the regulatory mechanism underlying the effect of NHERF1 on the surface stabilization and endocytosis of hOAT4.

NHERF1 has two tandem PDZ domains in the amino terminal side and a ERM binding domain at the carboxyl terminal side (37). Wang *et al* reported (43) that overexpression of NHERF1 inhibited the parathyroid hormone (PTH)-induced internalization of

parathyroid hormone receptor PTH1R in both Chinese hamster ovary cells and MC4 osteoblast cells. To determine which PDZ domain of NHERF1 was involved in the regulation of PTH1R endocytosis, they employed three NHERF1 mutants, one having a mutation in PDZ domain 1 (PDZ 1), one having a mutation in PDZ domain 2 (PDZ 2), and one having mutations in both PDZ domains. After transit transfection with these NHERF1 mutants, both single mutations in either PDZ 1 or PDZ 2 decreased the PTH1R internalization and interacted with this receptor. In contrast, the NHERF1 mutant harboring double mutations in both PDZ domains did not affect the PTH1R internalization, and did not associate with PTH1R protein. These results suggest that interaction of PTH1R with either PDZ domain of NHERF1 is sufficient to inhibit the PTH1R internalization by stabilizing the receptor at the plasma membrane. They also found that the ERM domain of NHERF1 was required for the stabilization of PTH1R at the plasma membrane, indicating that the effect of NHERF1 on membrane retention and endocytosis of PTH1R required one PDZ domain and the ERM binding domain.

In order to elucidate the molecular mechanism by which NHERF1 modulated the membrane retention and internalization of hOAT4, more studies are needed in the future.

3.4.2 Dileucine motif

Dileucine (LL)-based motives have been demonstrated to play critical roles in a variety of cellular processes including endocytosis of membrane proteins (20, 73-78), intracellular sorting of membrane proteins (41, 79, 80), and rate of protein phosphorylation (81). We previously found that hOAT1 proteins traffic between the cell surface and the intracellular endosomes under basal and PKC-activation conditions (82). However, the structural elements that regulate the hOAT1 trafficking have not been

identified yet. By examining the sequence of hOAT1, we found that there is a dileucine motif (L6L7) located at the amino terminus of this transporter. Given that dileucine-based motives have been shown to participate in the endocytosis of a number of membrane proteins, we hypothesized that this dileucine motif at the N-terminus of hOAT1 might be involved in hOAT1 endocytosis.

Firstly we replaced L6 and L7 with alanine (A) individually and simultaneously by means of site-directed mutagenesis approach. The transport activities of these hOAT1 mutants, L6A, L7A, and L6A/L7A, were reduced significantly compared with that of wild-type hOAT1. Unexpectedly, the simultaneous mutations of both leucine residues (L6A/L7A) resulted in a complete loss of function (Fig. 3-4). L6A/L7A hOAT1 was selected for the subsequent experiments. Our surface biotinylation result shows that the complete loss of function of L6A/L7A hOAT1 was due to the absence of mature form (80 kD) of this mutant at the cell surface (Fig. 3-5A) and in total cellular extract (Fig. 3-5B). It seems that the L6L7 motif does not play a role in the hOAT1 trafficking from the cell surface, and may be involved in its stability.

To investigate the mechanism underlying the loss of mature form of L6A/L7A hOAT1, we analyzed the degradation of this mutant by treating COS-7 cells expressing this mutant with both proteasomal and lysosomal inhibitors. Our results indicate that proteasome-mediated degradation is the major degradation pathway of the immature L6A/L7A hOAT1 (60 kD), and proteasomal inhibition by a proteasomal inhibitor MG132 increased only the amount of 60 kD immature L6A/L7A hOAT1 without an effect on the 80 kD mature L6A/L7A hOAT1 (Fig. 3-6).

Because our previous report (45) showed that the 60 kD immature hOAT1 that is unglycosylated resides in the ER and the 80 kD mature hOAT1 is fully glycosylated and targeted to the plasma membrane, the mutations in L6L7 may cause a folding defect in hOAT1 protein and the L6A/L7A hOAT1 mutant may be recognized by the quality control system in the ER as a non-native protein and targeted for proteasome-mediated degradation. Consequently, the maturation and transport of the mutant from the ER is significantly compromised, and the immature L6A/L7A hOAT1 is trapped in the ER as indicated by the colocalization of L6A/L7A hOAT1 with calnexin, an ER marker, in COS-7 cells (Fig. 3-7).

Chemical chaperons such as 4-phenylbutyrate (4PBA) and glycerol have been shown to rescue some surface protein mutants that are retained in the ER and promote the delivery of the mutants to the plasma membrane (71, 72). In the present study, we treated L6A/L7A hOAT-expressing cells with both 4PBA and glycerol. We observed that the maturation of L6A/L7A hOAT1 could not be enhanced by these chemicals, because the escape of the immature mutant from the ER could not be promoted by the treatments of 4PBA and glycerol (Fig. 3-8). Hence, the L6L7 motif might function as an ER exit motif, and the mutant harboring mutations in this motif may be recognized by the quality control machinery for the ER exit for further modifications and targeted for the proteasome-mediated degradation. Another possibility is that the folding defect due to the mutation in L6A/L7A may be so severe that it could not be stabilized and helped to escape the ER by the chemical chaperons. In conclusion, our current study is the first study showing that the dileucine L6L7 at the amino terminus of hOAT1 plays a critical role in the stability and maturation of this transporter.

4 Regulation of OATs by ubiquitination

4.1 Introduction

Ubiquitination is an important posttranslational modification of proteins by means of covalent conjugation of ubiquitin to target proteins. Ubiquitin is a highly conserved protein expressed in all eukaryotic cells (83). The last residue of ubiquitin, Gly76, can be conjugated to the ϵ -amino group of a lysine residue in a target protein. While originally the function of ubiquitination was discovered to target cytosolic proteins for proteasome degradation, ubiquitination has now been demonstrated to participate in other critical cellular processes including membrane trafficking, DNA repair, and transcription (83). The membrane proteins regulated by ubiquitination include sodium channel (84), water channel (85), dopamine transporter (86, 87), and glycine transporter (9), and so on.

The molecular mechanism by which PKC regulates the internalization of OAT proteins remains unclear. Recent studies regarding the PKC-induced endocytosis of other transmembrane proteins have proposed a critical role of ubiquitination of surface membrane proteins in their endocytosis and lysosomal degradation. Miranda *et al* reported (86) that PKC activation-induced endocytosis of dopamine transporter is dependent on ubiquitination. The endocytosis of water channel aquaporin-2 (AQP2) has been shown to be enhanced by ubiquitination (85). Glutamate transporter GLT1 (88) and glycine transporter GLYT1 (9) have also been shown to undergo PKC-induced internalization, and their ubiquitination was stimulated by PKC activation. Blocking the

PKC-induced ubiquitination of these transporters significantly impaired the PKC-dependent internalization of these transporters.

It is not known that whether OAT proteins also undergo ubiquitination, and whether the membrane trafficking of OAT proteins is regulated by ubiquitination. In this study, we aimed at answering these intriguing questions using various approaches.

4.2 Materials and Methods

4.2.1 Materials and Instruments

4.2.1.1 Cell

COS-7 cell was purchased from American Type Culture Collection (Manassas, VA).

4.2.1.2 Chemicals

Dulbecco's modified Eagle's medium was purchased from Cellgro (Manassas, VA). Fetal bovine serum, protease inhibitor cocktail, Triton X-100 and Sodium 2-mercaptoethanesulfonate (MesNa) were purchased from Sigma (St. Louis, MO). LipofectAmine 2000™ reagent, 1 M Tris-HCl (pH 7.5 and pH 8.0) and geneticin (G418) were purchased from Invitrogen (Carlsbad, CA). SuperSignal West Dura extended duration substrate kit, NHS-SS-biotin and streptavidin-agarose beads were purchased from Thermo Scientific (Waltham, MA). p-[³H]Aminohippuric acid (PAH) was from NEN Life Science Products (Hercules, CA).

4.2.2 Experimental Procedures

(1) Cell culture

COS-7 cells and COS-7 cells stably expressing hOAT1-C-myc are grown at 37 °C and 5% CO₂ in Dulbecco's modified Eagle's medium (Cellgro, USA) supplemented with 10% fetal bovine serum (Sigma), 100 units/ml penicillin, and 100 mg/ml streptomycin.

(2) Transfection

1. Plate 5×10^5 COS-7 cells in a 35 mm dish and grow for 24 h;
2. For each 35 mm dish, mix 4 µg of plasmid DNA in 250 µl of Opti-MEM®I reduce serum medium in a sterile EP tube, and mix 10 µl of Lipofectamine 2000 transfection reagent in 250 µl of Opti-MEM®I reduce serum medium in a sterile EP tube. Incubate for 5 min at room temperature;
3. Combine the diluted DNA and diluted Lipofectamine 2000, mix gently and incubate for 20 min at room temperature;
4. Mix the DNA-Lipofectamine 2000 complexes with culture medium by adding 100 µl of complexes to 2 ml of culture medium for each 35 mm dish, and mix gently;
5. Remove the medium in the dish containing cells and add the medium with the DNA- Lipofectamine 2000 complexes into the dish;
6. Incubate the cells for 24 ~ 72 h in a cell culture incubator at 37 °C;

Note: To reduce the toxicity of Lipofectamine 2000, the medium with the DNA- Lipofectamine 2000 complexes may be replaced by the medium without the complexes 4 ~ 6 h after transfection.

(3) Uptake assay

1. Plate $5 \sim 7 \times 10^4$ COS-7 cells expressing hOAT1-C-myc into collagen-coated 48-well plate in triplicate evenly;
2. Preparation of uptake solution:
3. PAH: 19 μM cold PAH + 1 μM hot [^3H] PAH, totally 20 μM . (long-time stored cold PAH may be degraded that lead to a lowered uptake value)
4. Stock solution: cold PAH: 50 mM, hot [^3H] PAH: varies from batch to batch
5. Estrone sulfate: 50nM for both cold and hot [^3H] Estrone sulfate
6. Stock solution: Cold estrone sulfate: 100 μM , hot estrone sulfate: varies from batch to batch.
7. Put the plate on bench for 5 min at room temperature (allow the media to reach room temperature);
8. Aspirate the medium, add 120 μl of uptake solution, for PAH let stand 3 min, or for Estrone Sulfate 3 or 4 min, rotating the plate slowly on a shaker at room temperature;

9. Stop uptake by adding 500 μ l of ice-cold PBS (+) (freshly add 1 mM CaCl_2 and 1 mM MgCl_2) at a rate of three wells/min. Aspirate the uptake solution and PBS (+), and wash each well once with 500 μ l of ice-cold PBS (+);
10. Aspirate PBS (+) completely, add 200 μ l of 0.2 N NaOH to lyse cells, rotating rigorously for more than 40 min at room temperature;
11. Label the scintillation vials, add 200 μ l of 0.2 N HCl for neutralization. Pipette up and down the cell lysate and transfer all the lysate into the scintillation vials;
12. Add 3 ml of scintillation liquid, mix and cap;
13. Insert 1.44M floating disk into machine, use program "01" label. The counting is carried out at a rate of approximately 75 seconds /vial;
14. Analyze data using Microsoft Excel software.

(4) Cell surface biotinylation

1. Plate 5×10^5 cells on each well of a 6-well plate or a 35 mm dish, and grow for 24 hours;
2. Place the 6-well plate on ice for a couple of minutes;
3. Aspirate the medium and wash cells with 2 ml of cold PBS(+) (pH8.0) [supplemented with both 1mM Ca^{2+} (CaCl_2) and 1mM Mg^{2+} (MgCl_2)] two times to remove any proteins in the culture medium and cool down the cells rapidly;

4. Add 1ml of freshly prepared 0.5 mg/ml NHS-SS-Biotin (Pierce) in PBS(+) (pH8.0);
5. Incubate the cells on ice for twice, each time for 20 min with gently shaking on an orbital shaker ;
6. Remove biotin solution and wash cells with 2 ml of 100mM Glycine in PBS(+) (pH8.0) once;
7. Incubate the cells with 2 ml of cold 100mM Glycine in PBS(+) (pH8.0) for 20 ~ 30 min, with gently shaking on a orbital shaker;
8. Extensively wash the cells twice with 2ml of cold PBS (+) (pH8.0);
9. Add 400 ~ 500 μ l of regular lysis buffer with freshly added Proteinase Inhibitor Cocktail (Sigma);
10. Vigorously shake the plate on ice for 10-15 min, harvest cells to an Eppendorf (EP) tube by using a cell scraper. Squeeze cells with a pipet tip by pipetting in order to help break down cell membrane;
11. Rotate the EP tubes for 40 min at 4°C for further lysis;
12. Centrifuge the tubes at 13200 rpm for 20 min at 4°C;
13. Transfer the supernatant to a new EP tube;
14. Measure protein concentrations to normalize loading amount of proteins.
300 ~ 500 μ g of proteins may be applied to bind streptavidin-agarose beads;
15. 40 μ l of Streptavidin-Agarose beads (Pierce) is added to each tube. Rotate for 1.5 ~ 4 h at 4°C;

16. After rotation, centrifuge at 13,200 rpm for 1 min at 4°C. Wash the beads with 1ml of regular lysis buffer for 3 times (don't lose beads);
17. Wash the beads with 1ml of PBS (pH7.4);
18. Now all the membrane proteins are bound to beads, so the target protein has to be released for the following immunoblot detection. The remaining volume of PBS in beads is estimated and add 10 µl of 5X Laemmli sample buffer with freshly added beta-mercaptomethanol (reducing agent, final concentration is 5%);
19. Incubate the mixture for 30min at 50°C to denature the released proteins. During the incubation, tap the bottom of tubes 3 times to make sure that all beads are accessible to the Laemmli sample buffer;
20. After denaturing is done, spin down the samples. Then Western Blot is followed.

(5) Internalization assay

A. Cell surface biotinylation

1. Plate 5×10^5 cells on each well of a 6-well plate or a 35 mm dish, and grow for 24 hours;
2. Place the 6-well plate on ice for a couple of minutes;
3. Aspirate the medium and wash cells with 2 ml of cold PBS(+) (pH8.0) [supplemented with both 1mM Ca^{2+} (CaCl_2) and 1mM Mg^{2+} (MgCl_2)] two times to remove any proteins in the culture medium and cool down the cells rapidly;

4. Add 1ml of freshly prepared 0.5 mg/ml NHS-SS-Biotin (Pierce) in PBS(+) (pH8.0);
5. Incubate the cells on ice for 20 min with gently shaking on an orbital shaker;
6. Remove biotin solution and wash cells with 2 ml of 100mM Glycine in PBS(+) (pH8.0) once;
7. Incubate the cells with 2 ml of cold 100mM Glycine in PBS(+) (pH8.0) for 20 ~ 30 min, with gently shaking on a orbital shaker;
8. Extensively wash the cells twice with 2ml of cold PBS (+) (pH8.0);
9. After quenching of Glycine, each 35mm-dish is incubated in prewarmed PBS(+), pH7.4 or serum-free medium at 37°C for a designated period of time. (Based on my experience, 3 minutes is enough for a 35mm-dish to reach the endocytosis-allowable temperature, so the actual time is 3 minutes longer than the designated time, eg. if 5 min is the designated time, the actual time of incubation is 8 min.);

B. Internalization and stripping

10. After 37°C incubation, put the dishes on ice immediately and wash twice with cold PBS (+), pH 7.4 to stop endocytosis;
11. Add 2ml Stripping Buffer (MesNa, 30 min X 2 times, 50mM in NT buffer) to strip the membrane-bound biotin with gentle shaking.
12. Wash cells twice with cold PBS, pH 7.4. (For some highly-expressed proteins, concentration of MesNa and incubation times may be increased for desired stripping efficiency through optimization.) ;

C. Cell lysis and binding to streptavidin-agarose

13. Add 400 ~ 500 μ l of regular lysis buffer with freshly added Proteinase Inhibitor Cocktail (Sigma);
14. Vigorously shake the plate on ice for 10-15 min, harvest cells to an Eppendorf (EP) tube by using a cell scraper. Squeeze cells with a pipet tip by pipetting in order to help break down cell membrane;
15. Rotate the EP tubes for 40 min at 4°C for further lysis;
16. Centrifuge the tubes at 13200 rpm for 20 min at 4°C;
17. Transfer the supernatant to a new EP tube;
18. Measure protein concentrations to normalize loading amount of proteins.
300 ~ 500 μ g of proteins may be applied to bind streptavidin-agarose beads;
19. 40 μ l of Streptavidin-Agarose beads (Pierce) is added to each tube. Rotate for 1.5 ~ 4 h at 4°C;
20. After rotation, centrifuge at 13,200 rpm for 1 min at 4°C. Wash the beads with 1ml of regular lysis buffer for 3 times (don't lose beads);
21. Wash the beads with 1ml of PBS (pH7.4).
22. Now all the membrane proteins are bound to beads, so the target protein has to be released for the following immunoblot detection. The remaining volume of PBS in beads is estimated and add 10 μ l of 5X Laemmli sample buffer with freshly added beta-mercaptoethanol (reducing agent, final concentration is 5%);

23. Incubate the mixture for 30min at 50°C to denature the released proteins.

During the incubation, tap the bottom of tubes 3 times to make sure that all beads are accessible to the Laemmli sample buffer;

24. After denaturing is done, spin down the samples. Then Western Blot is followed.

D. Data analysis

Relative OAT1 internalized is calculated as % of the total initial cell-surface hOAT1 or hOAT4 pool.

(6) SDS-PAGE and immunoblotting

A. Gel running

1. At least 400 ml of 1x running buffer is used and can be re-used.
2. Set 200V to run 30 min for 7.5% gel, running time can be adjusted by purpose.

B. Transfer

3. Use 100% methanol to pre-wet the PVDF membrane for 30 seconds, and transfer to Transfer buffer for at least 30min;
4. Use 1200-1500 ml of transfer buffer;
5. Set 100V to transfer for at least 30min (for large proteins, transfer time should be longer).

C. Primary antibody incubation

6. After transfer step, transfer the PVDF membrane to a small container and block with 5 % non-fat milk in PBST keeping the protein side up for 1 hour at room temperature with gently shaking;
7. Rinse the membrane with PBST once, add primary antibody (in 2.5 % milk in PBST), and incubate overnight;
8. Wash membrane three times with PBST, 5 min each time;
9. Incubate with secondary antibody (anti-mouse or rat IgG) at a ratio of 1:5000 ~ 1:10000 for 1 h at RT;
10. Extensively wash with PBST for more than three times, each time 10 ~ 15 min.

D. Development of membrane

11. Adjust the focus of the FluorChem 8800 imaging system;
17. Open the software on the computer, click “Acquire”, click “Movie setup”, set “Sensitivity” as Medium; set Exposure time at 3 ~ 5 seconds, total frames at 30, click “copy to next” until the frame is 30. Then click “GO”;
18. For the marker, take another photo by choosing “reflective”, the exposure time is typically 18 milliseconds.

E. Reprobe with another primary antibody

19. The membrane can be re-probed by stripping the antibody on the membrane with Restore® Western Blot Stripping Buffer (Pierce). Incubate the membrane with stripping buffer for 40 min at 37°C;

20. Wash three times with PBST, 5 ~ 10min each time;
 21. Incubate the membrane with another primary antibody overnight.
- (7) Isolation of plasma membrane fraction
1. Plate 1×10^6 cells/dish in a 60 mm dish, grow for 24h;
 2. Place cells on ice, aspirate the medium and wash cells with cold PBS, pH 7.4 twice;
 3. Add 700 μ l of isolation buffer with freshly added PIC;
 4. Scrape the cells and transfer to an EP tube;
 5. Sonicate the cells with appropriate times and cycles to disrupt cells with our sonicator. Use 10 seconds at 45% output, two times. (to check the sonication efficiency, take 10 μ l of liquid from the EP tube for observation under microscope, should have no intact cells);
 6. Centrifuge at 1,000 g for 10min at 4°C to remove insoluble components;
 7. Transfer the supernatant (membrane fraction and intracellular parts) to a new EP tube;
 8. Precool the Ultracentrifuge machine in Dr. Sinko's lab for 10 min. Centrifuge the supernatant at 17,000g (approx. 11500 rpm, rotor JA-18.1) for 20 min at 4°C.
 9. Remove or transfer the supernatant (intracellular components);
 10. Dissolve the pellet (plasma membrane fraction) in 60 μ l of isolation buffer by pipetting up and down, and transfer to an EP tube.

(8) Immunoprecipitation (cultured cells)

1. Plate 5×10^5 cells in a well of six-well plate, and grow for 24 ~ 48 h;
2. Wash cells twice with ice-cold PBS (pH7.4);
3. Lysed the cells with 400 ~ 500 μ l of lysis buffer I with 150 mM NaCl and 1% of proteinase inhibitor cocktail (PIC);
4. Vigorously shake the plate on ice for 10-15 min, harvest cells to an Eppendorf (EP) tube by using a cell scraper. Squeeze cells with a pipet tip by pipetting in order to help break down cell membrane;
5. Rotate the EP tubes for 40 min at 4 °C for further lysis;
6. Centrifuge the tubes at 13200 rpm for 20 min at 4 °C;
7. Transfer the supernatant to a new EP tube;
8. Measure protein concentrations to normalize loading amount of proteins;
9. 300 ~ 400 μ g of protein sample is precleared with 20 μ l of protein A or protein G agarose slurry (Thermo Scientific) in lysis buffer I with 150 mM NaCl and 1% of PIC (total volume is 400 ~500 μ l) for 1.5-2 h with rotation at 4 °C;
10. Meanwhile, 3 ~ 4 μ g of antibody or 1.5-2 μ l of normal mouse IgG (Santa Cruz Biotechnology) as negative control are incubated with 20 μ l of protein A or protein G agarose slurry for 1.5-2 h in lysis buffer I with 150 mM NaCl and 1% of PIC (total volume is 400 ~ 500 μ l) with end-over-end mixing.

The antibody-bound protein A agarose beads are rinsed once with lysis buffer I with 150 mM NaCl to remove the unbound antibody;

Note: Protein A and protein G have different binding affinity to certain types of immunoglobulins. For example, protein G has higher affinity for mouse IgG1 than protein A. Ant-c-myc monoclonal antibody 9E10 is mouse IgG1, so protein G agarose should be better than protein A agarose for 9E10 IP experiments.

11. Precleared protein sample from “step 9” is centrifuged at 13,000 rpm for 1 min at 4 °C, and the supernatant is incubated with the antibody-bound protein A agarose beads at 4 °C overnight with end-over-end mixing in order to form antigen-antibody complex;
12. Wash the agarose beads with 600 µl of lysis buffer I with 500 mM NaCl for four times, and 1 ml of ice-cold PBS (pH7.4) once;
13. The sample is denatured by adding 30 µl of 2X urea sample buffer containing 8% of beta-mercaptoethanol, and incubating for 30 min at 50°C with tapping;
14. SDS-PAGE and Western blot.

(9) Extraction of proteins from rat kidney slices

1. Blow oxygen into the 50 ml tube containing ice-cold modified Cross and Taggart saline buffer (MCT buffer) (95 mM NaCl, 80 mM mannitol, 5 mM KCl, 0.74 mM CaCl₂, and 9.5 mM Na₂PO₄, pH 7.4).

2. Put one freshly removed rat kidney into the freshly oxygenated MCT buffer from step “1” with oxygen bubbling.
3. Transfer the kidney into a small box containing ice-cold MCT buffer with oxygen bubbling, and then cut the kidney into small slices with a new blade in the box.
4. Incubate the slices with 15 ml of vehicle (DMSO) or 1 μ M PMA in prewarmed MCT buffer for 30 min at 37 °C on a heat block.
5. After 37 °C incubation, transfer the kidney slices to a “2059” tube in which there is 2 ml of ice-cold PBS (pH 7.4) with 1% PIC and 20 mM NEM.
6. Note: the PBS volume is based on 1g tissue/5ml PBS.
7. Homogenize the kidney slices in the tube using the mechanic homogenizer in our lab until there is no visible particle.
8. Store the homogenate in a “– 80 °C” freezer until use.

(10) Immunoprecipitation (rat kidney tissue)

1. Measure protein concentrations of homogenized tissue samples to normalize loading amount of proteins;
2. 100 ~ 200 μ g of protein sample is precleared with 20 μ l of protein A-agarose slurry (Thermo Scientific) in 500 μ l of RIPA buffer (10 mM pH 7.4 Tris-HCl, 150 mM NaCl, 1% Triton X-100, 1 mM EDTA, 1% sodium deoxycholate, and 0.1% SDS) and 1% of PIC (total volume is 400 ~500 μ l) for 1.5-2 h with rotation at 4 °C;

3. Meanwhile, 3 ~ 4 μg of antibody or 3 ~ 4 μg of normal rabbit IgG (Millipore) as negative control are incubated with 20 μl of protein A agarose slurry for 1.5-2 h in RIPA buffer and 1% of PIC (total volume is 400 ~ 500 μl) with end-over-end mixing. The antibody-bound protein A agarose beads are rinsed once with RIPA buffer to remove the unbound antibody;
4. Precleared protein sample from “step 2” is centrifuged at 13,000 rpm for 1 min at 4 $^{\circ}\text{C}$, and the supernatant is incubated with the antibody-bound protein A agarose beads at 4 $^{\circ}\text{C}$ overnight with end-over-end mixing in order to form antigen-antibody complex;
5. Wash the agarose beads with 600 μl of RIPA buffer for four times, and 1 ml of ice-cold PBS (pH7.4) once;
6. The sample is denatured by adding 30 μl of 2X urea sample buffer containing 8 % of beta-mercaptoethanol, and incubating for 30 min at 50 $^{\circ}\text{C}$ with tapping;
7. SDS-PAGE and Western blot.

(11) Ubiquitination assay

1. Plate 5 x10⁵ COS-7 cells expressing hOAT1-C-myc or hOAT3-C-myc in a well of six-well plate, and grow for 24 ~ 48 h;
2. Treat the cells with DMSO or 1 μM PMA in serum-free DMEM medium for 30 min at 37 $^{\circ}\text{C}$;
3. Wash cells twice with ice-cold PBS (pH7.4);

4. Lysed the cells with 400 ~ 500 μ l of lysis buffer I with 150 mM NaCl, freshly added 1% of proteinase inhibitor cocktail (PIC) and 20 mM NEM (deubiquitination inhibitor);
5. Vigorously shake the plate on ice for 10-15 min, harvest cells to an Eppendorf (EP) tube by using a cell scraper. Squeeze cells with a pipet tip by pipetting in order to help break down cell membrane;
6. Rotate the EP tubes for 40 min at 4°C for further lysis;
7. Centrifuge the tubes at 13200 rpm for 20 min at 4 °C;
8. Transfer the supernatant to a new EP tube;
9. Measure protein concentrations to normalize loading amount of proteins;
10. 300 ~ 400 μ g of protein sample is precleared with 20 μ l of protein A-agarose slurry (Thermo Scientific) in lysis buffer I with 150 mM NaCl and 1% of PIC (total volume is 400 ~500 μ l) for 1.5-2 h with rotation at 4 °C;
11. Meanwhile, 3 ~ 4 μ g of antibody or 1.5-2 μ l of normal mouse IgG (Santa Cruz Biotechnology) as negative control are incubated with 20 μ l of protein A or protein G agarose slurry for 1.5-2 h in lysis buffer I with 150 mM NaCl and 1% of PIC (total volume is 400 ~ 500 μ l) with end-over-end mixing. The antibody-bound protein A agarose beads are rinsed once with lysis buffer I with 150 mM NaCl to remove the unbound antibody;
12. Precleared protein sample from “step 9” is centrifuged at 3000x g for 1 min at 4 °C, and the supernatant is incubated with the antibody-bound protein A

agarose beads at 4 °C overnight with end-over-end mixing in order to form antigen-antibody complex;

13. Wash the agarose beads with 600 µl of lysis buffer I with 500 mM NaCl for four times, and 1 ml of ice-cold PBS (pH7.4) once;
14. The sample is denatured by adding 30 µl of 2X urea sample buffer containing 8 % of beta-mercaptoethanol, and incubating for 30 min at 50°C with tapping;
15. SDS-PAGE;
16. Western blot to detect ubiquitinated hOAT1 and hOAT3 with anti-ubiquitin antibody.

(12) Ubiquitination assay combined with biotinylation

1. Plate 1×10^6 cells on each well of a 60 mm dish, and grow for 24 hours;
2. Place the dishes on ice for a couple of minutes;
3. Aspirate the medium and wash cells with 3 ml of cold PBS(+) (pH8.0) [supplemented with both 1mM Ca^{2+} (CaCl_2) and 1mM Mg^{2+} (MgCl_2)] two times to remove any proteins in the culture medium and cool down the cells rapidly;
4. Add 2 ml of freshly prepared 0.5 mg/ml NHS-SS-Biotin (Pierce) in PBS(+) (pH8.0);
5. Incubate the cells on ice for twice, each time for 20 min with gently shaking on an orbital shaker ;

6. Remove biotin solution and wash cells with 3 ml of 100mM Glycine in PBS(+) (pH8.0) once;
7. Incubate the cells with 3 ml of cold 100mM Glycine in PBS(+) (pH8.0) for 20 ~ 30 min, with gently shaking on a orbital shaker;
8. Extensively wash the cells twice with 3 ml of cold PBS (+) (pH8.0);
9. Add 500 μ l of lysis buffer I with freshly added Proteinase Inhibitor Cocktail (Sigma) and 20 mM NEM;
10. Vigorously shake the plate on ice for 10-15 min, harvest cells to an Eppendorf (EP) tube by using a cell scraper. Squeeze cells with a pipet tip by pipetting in order to help break down cell membrane;
11. Rotate the EP tubes for 40 min at 4°C for further lysis;
12. Centrifuge the tubes at 13200 rpm for 20 min at 4°C;
13. Transfer the supernatant to a new EP tube;
17. Measure protein concentrations to normalize loading amount of proteins.
750 μ g of protein sample is precleared with 30 μ l of protein G-agarose slurry (Thermo Scientific) in lysis buffer I with 150 mM NaCl and 1% of PIC (total volume is 600 μ l) for 1.5-2 h with rotation at 4 °C;
18. Meanwhile, 6 μ g of anti-myc antibody 9E10 are incubated with 30 μ l of protein G agarose slurry for 1.5-2 h in lysis buffer I with 150 mM NaCl and 1% of PIC (total volume is 600 μ l) with end-over-end mixing. The antibody-bound protein G agarose beads are rinsed once with lysis buffer I with 150 mM NaCl to remove the unbound antibody;

19. Precleared protein sample from “step 9” is centrifuged at 3000x g for 1 min at 4 °C, and the supernatant is incubated with the antibody-bound protein A agarose beads at 4 °C overnight with end-over-end mixing in order to form antigen-antibody complex;
20. Wash the agarose beads with 600 µl of lysis buffer I with 500 mM NaCl for four times, and 1 ml of ice-cold PBS (pH7.4) once;
14. **Elution:** Incubate the beads with 40 µl of regular lysis buffer containing 1% SDS for 15 min at 37 °C with tapping. Add 360 µl of prewarmed regular lysis buffer without SDS to dilute SDS to 0.1% at room temperature and mix well.
15. Centrifuge for 1 min at 3000x g at room temperature and transfer the supernatant to a new Eppendorf tube . After incubation of the tube for 5 min on ice, 30 µl of Streptavidin-Agarose beads (Pierce) is added to each tube. Rotate for overnight at 4°C;
16. Centrifuge the samples at 3000x g for 1 min at 4°C. Wash the beads with 1 ml of regular lysis buffer for 3 times (don't lose beads) and 1 ml of PBS (pH7.4);
21. The sample is denatured by adding 30 µl of 2X urea sample buffer containing 8 % of beta-mercaptoethanol, and incubating for 30 min at 50 °C with tapping;
22. SDS-PAGE;

23. Western blot to detect ubiquitinated hOAT1 and hOAT3 with anti-ubiquitin antibody or anti-myc antibody.

(13) Site-directed mutagenesis

1. Design the primer pair containing the site(s) you want to mutate according to the manual of Site-Directed Mutagenesis Kit (Stratagene);

Note: Check the secondary structure of primers on the website of IDT (Integrated DNA Technologies, Iowa) or other websites providing the free software for the DNA structural analysis.

2. Primer synthesis (two complimentary oligonucleotides) provided by IDT;
3. Dissolve the primers in ddH₂O and dilute to the concentration of 125 ng/ul for use;
4. Set up a reaction of 25 µl total volume (the manual of Site-Directed Mutagenesis Kit);
5. Run PCR after choose programs for mutation;
6. Note: PCR condition is based on the manual of Site-Directed Mutagenesis Kit.
7. Add 0.5 µl of Dpn I restriction enzyme to the reaction tube, and incubate for at least 1 hour at 37°C to digest the parental DNA strands;
8. Dilute PCR products with purified water at 1:5 ratio before performing transformation;
9. Conduct transformation (see the protocol of transformation);

10. Grow the transformed bacteria in the incubator overnight at 37°C;
11. Select two different colonies from the LB agar plate;
12. Purify plasmids using Spin Mini-Prep kit (QIAGEN);
13. Sequence the purified plasmids to confirm the correct mutations at the DNA core facility of UMDNJ, Piscataway, NJ;
14. Analyze the sequencing data by using “Laser gene” software (DNASTAR, Inc.) (see the manual of Laser gene).

(14) Transformation

1. Thaw DH5α competent cells on ice for 10min without pipetting;
2. Transfer 10 µl of competent cells into an ice-chilled “2059” tube on ice;
3. Add 1 µl of plasmid DNA (10 ~ 100 ng/µl) to competent cells. Mix the contents thoroughly but gently by stirring the cells while adding the DNA with the pipette tip;
4. Incubate the tubes for 30 minutes on ice;
5. Incubate the competent cells for 45 seconds at 42 °C in a water bath;
6. Put the tubes on ice and incubate for 2 min;
7. Add 190 µl of SC medium to each tube;
8. Incubate the tubes in an incubator at 225 rpm for 1h at 37 °C;
9. Seed 50 ~ 100 µl of cell suspension from each tube on a prewarmed LB plate with 100 µg/ml ampicillin;

10. Note: A different antibiotic may be used if the selection resistance of the plasmid is not ampicillin, for example, kanamycin.
11. Incubate the plates for 16 ~ 24 hours in an incubator at 37 °C;
12. Check the growth of bacteria by observing the morphology of colonies.

(15) Conjugation of antibody to protein G agarose resin

A. Binding of antibody to protein G agarose

1. Wash protein G agarose beads twice with PBS (pH 7.4);

Note: Use 200 µl of protein G agarose slurry for each antibody coupling.

2. Prepare 50 µg of antibody for coupling. Adjust the volume to 500 µl containing both PBS (PIC added freshly) and antibody. Use 100 µl of settled beads to bind antibody (5 µg antibody/10 µl of settled protein G agarose);
3. Incubate on a rotator for 60 min at RT, ensuring that the slurry remains suspended during incubation;
4. Wash the resin three times with PBS.

B. Crosslinking the bound antibody to protein G immobilized on agarose resin

1. Dissolve the crosslinking reagent DMP (Pierce) in crosslinking buffer (0.2 M triethanolamine, pH 8.0) to prepare a 60 mM solution;

Note: Prepare 60 mM solution of DMP freshly because DMP is easily hydrolyzed.

2. Remove PBS completely from the antibody-bound resin, and add 485 μ l of the crosslinking buffer and 15 μ l of 60 mM DMP solution to the volume of 500 μ l.

Note: The DMP is added at 30X molar excess to protein G on the agarose beads at the working concentration of 1.8 mM.

3. Incubate the EP tube containing the buffer and resin for 60 min at RT on a rotator;
4. Add 25 μ l of 1 M Tris-HCl (pH 7.5) at 50 mM final concentration to the sample to stop the reaction, mix well and incubate for 15 min at RT on a rotator;
5. Centrifuge the EP tube at 5000 x g for 1 min;
6. Remove the supernatant and wash the resin twice with 1ml of 50 mM Tris-HCl (pH 7.5);
7. Wash the resin twice with 1 ml of PBS;
8. Store the antibody-crosslinked resin in PBS with 0.05 N NaN_3 at 4 °C until use.

Note: Prepare 60 mM DMP solution in crosslinking buffer (DMP molecular weight is 259.17): Weigh 7.8 mg DMP, add crosslinking buffer to 500 μ l, and mix well.

- (16) Sequential immunoprecipitation with anti-Myc and anti-ubiquitin antibodies

A. First IP with anti-Myc antibody (9E10)

1. Treat the cells in 10 cm dish with 1 μ M PMA for 30 min at 37 °C and solubilized the cells with 500 μ l of lysis buffer I with 3% PIC and 40 mM NEM (deubiquitination inhibitor).
2. Collect cell lysate and determine protein concentrations, and then use 1.8 mg of proteins to preclear with 60 μ l protein G agarose beads.
3. Incubate 50 μ g 9E10 antibodies with 200 μ l protein G agarose slurry for 1h at RT and wash twice with PBS.
4. Transfer precleared sample to 12.5 μ g of 9E10 antibody bound on protein G agarose beads (50 μ l, from step “3”) to bind c-myc hOAT1.
5. Incubate overnight at 4 °C.
6. Wash the immunoprecipitates 3 times with lysis buffer I with 500 mM NaCl and once with PBS, and completely remove supernatants from the beads.

B. Elution:

7. Add 50 μ l of modified RIPA buffer with 1% SDS, incubate the tube at 37 °C (water bath) for 5 min, tapping 3 times during the incubation.
8. After the elution step, centrifuge the elution samples for 1 min at 1500g at RT, and transfer the supernatant to a new EP tube. Then dilute the eluted sample with 9-time volume of prewarmed modified RIPA buffer (no SDS) at RT to neutralize the denaturing effect of SDS.

9. Measure proteins concentrations of eluted sample after dilution to 0.1% SDS and use modified RIPA buffer to correct protein concentration. (Modified RIPA buffer also has high absorbance using Bradford method).

C. Second IP with anti-ubiquitin antibody (FK2)

10. Transfer 500 μ l of the supernatant to an Amicon Ultra-4 centrifugal filter, and centrifuge for 20 min at 14,000g to concentrate to 30 ~ 35 μ l for the second IP with anti-Ub antibody (FK2), and combine 10 concentrated samples for FK2 and IgG IP (1.5 mg x 10 protein).
11. Transfer the concentrated hOAT1 sample to the 20 (1.5 mg protein) or 60 μ l (1.5 mg x 10 protein) of FK₂- or IgG-crosslinked agarose beads, and add 450 μ l of modified RIPA buffer for the second IP, and incubate overnight at 4 $^{\circ}$ C;
12. Wash the immunoprecipitates 4 times with modified RIPA buffer with 500 mM NaCl and once with PBS, and add 35 μ l of 2x urea sample buffer with 8% beta-ME (final concentration) to denature for 30 min at 50 $^{\circ}$ C;

D. **Gel staining**

13. After SDS-PAGE, transfer the gel to a clean box with purified water, gently shake the box and discard the water, wash 3 times with purified water, each time 5 min
14. Stain with 25 ml of Coomassie blue (Pierce) for 2h.
15. After staining, wash the gel with purified water, change water 3 times, each time 30 min, and destain overnight with purified water.

(17) Protein identification by LC-MS/MS

1. The gel bands of interest were reduced, carboxymethylated with iodoacetamide, digest with trypsin using standard protocols.
2. Peptides were extracted, solubilized in 0.1% trifluoroacetic acid, and analyzed by nanoLC-MS/MS using a RSLC system (Dionex, Sunnyvale CA) interfaced with a Velos-LTQ-Orbitrap (ThermoFisher, San Jose, CA). Samples were loaded onto a self-packed 100 μ m x 2cm trap packed with Magic C18AQ, 5 μ m 200 Å (Michrom Bioresources Inc, Auburn, CA) and washed with Buffer A(0.2% formic acid) for 5 min with flowrate of 10 μ l/min.
3. The trap was brought in-line with the homemade analytical column (Magic C18AQ, 3 μ m 200 Å, 75 μ m x 50cm) and peptides fractionated at 300 nL/min with a 90 min linear gradient of 2 to 45% Buffer B (0.2% formic acid, acetonitrile).
4. Mass spectrometry data was acquired using a data-dependent acquisition procedure with a cyclic series of a full scan acquired in Orbitrap with resolution of 60,000 followed by MSMS scans(acquired in linear ion trap) of 20 most intense ions with a repeat count of two and the dynamic exclusion duration of 60 sec.
5. The LC-MS/MS data was searched against the ENSEMBL human database using a local version of the Global Proteome Machine (GPM USB, Beavis Informatics Ltd, Winnipeg, Canada) with carbamidoethyl on cysteine as fixed modification and ubiquitinylation on lysine (+114 Da) as well as

oxidation of methionine and tryptophan as variable modifications using a 10 ppm precursor ion tolerance and a 0.4 Da fragment ion tolerance.

4.3 Results

4.3.1 *In vitro* PMA-induced ubiquitination of OAT1

To analyze whether hOAT1 is ubiquitinated under basal and PKC-activation condition, we treated the CO-7 cells expressing both transporters with vehicle (DMSO) and 1 μ m PMA for 30 min at 37 °C, and solubilized with lysis buffer. hOAT1-C-myc protein was immunoprecipitated with anti-myc antibody 9E10 and immunoblotted with anti-ubiquitin antibody P4D1, and reprobed with anti-myc antibody 9E10. As seen in Fig. 4-1, a smeared pattern of ubiquitinated proteins was displayed by immunoblotting with anti-ubiquitin antibody in PMA-treated cells, and a weak smeared band was seen in untreated cells. The molecular size of the smeared band in PMA-treated cells is in the range of 100 ~ 220 kDa.

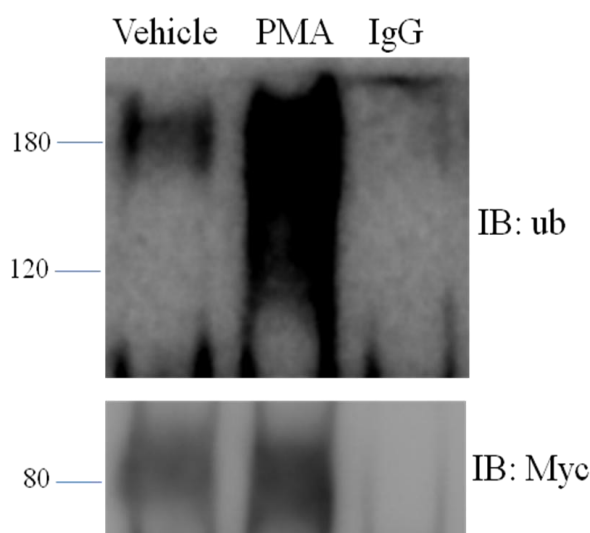


Figure 4-1 PKC-dependent ubiquitination of hOAT1 in COS-7 cells stably expressing hOAT1-C-myc. COS-7 cells stably expressing hOAT1-C-myc were incubated with

vehicle (DMSO) or 1 μ M PMA for 30 min at 37 $^{\circ}$ C, and solubilized with lysis buffer. hOAT1-C-myc protein was immunoprecipitated with anti-myc antibody 9E10 and immunoblotted with anti-ubiquitin antibody P4D1, and reprobbed with anti-myc antibody 9E10.

To test whether hOAT1 can be ubiquitinated by ectopically expressed ubiquitin, hOAT1-C-myc COS-7 cells were transiently transfected with HA-tagged ubiquitin (HA-ubiquitin), and treated with 1 μ M PMA for 30 min at 37 $^{\circ}$ C. The cells were solubilized with lysis buffer. hOAT1-C-myc protein was immunoprecipitated with anti-myc antibody 9E10 and immunoblotted with anti-HA antibody, and reprobbed with anti-myc antibody 9E10. In Fig. 4-2, a similar smeared band is revealed by anti-HA antibody in PMA-treated cells and a weak smeared band is in untreated cells, indicative of the conjugation of HA-ubiquitin to hOAT1-C-myc. This result indicates that similar to endogenous ubiquitin, hOAT1 protein was also ubiquitinated by ectopically expressed ubiquitin, and the ubiquitination of hOAT1 was stimulated by PKC activation.

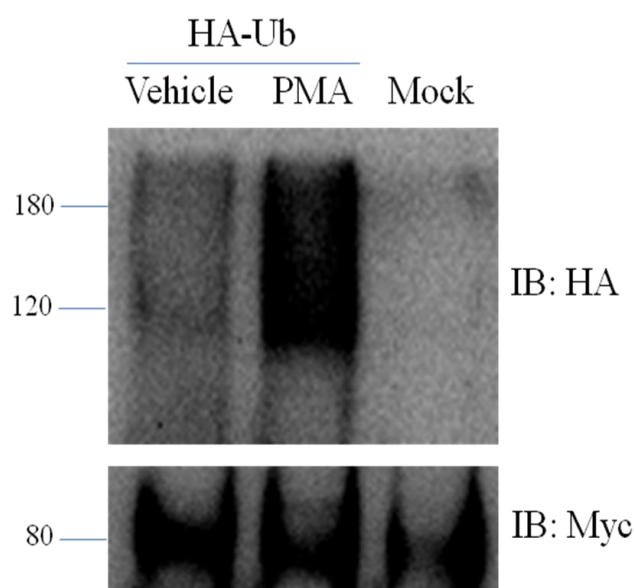


Figure 4-2 PKC-dependent ubiquitination of hOAT1 in COS-7 cells stably expressing hOAT1-C-myc following transfection of empty vector and HA-tagged ubiquitin (HA-Ub). After 48h transfection of HA-Ub, COS-7 cells stably expressing hOAT1-C-myc were incubated with vehicle (DMSO) or 1 μ M PMA for 30 min at 37 $^{\circ}$ C, and solubilized with lysis buffer. hOAT1-C-myc protein was immunoprecipitated with anti-myc antibody 9E10 and immunoblotted with anti-HA antibody, and reprobed with anti-myc antibody 9E10.

By measuring the time kinetics of PKC-induced ubiquitination of hOAT1 in COS-7 cell, we determined whether the ubiquitination of hOAT1 is time-dependent. We incubated COS-7 cells expressing hOAT1-C-myc with vehicle or 1 μ M PMA for the indicated times at 37 $^{\circ}$ C, solubilized the cells with lysis buffer, immunoprecipitated hOAT1 with anti-myc antibody and immunoblotted with anti-ubiquitin antibody P4D1, and reprobed with anti-myc antibody 9E10.. As shown in Fig. 4-3, the ubiquitination of hOAT1 in COS-7 cells treated with PMA at 37 $^{\circ}$ C reached a maximum at around 15 ~ 30 min, and decreased with continued incubation of cells with PMA (data not shown).

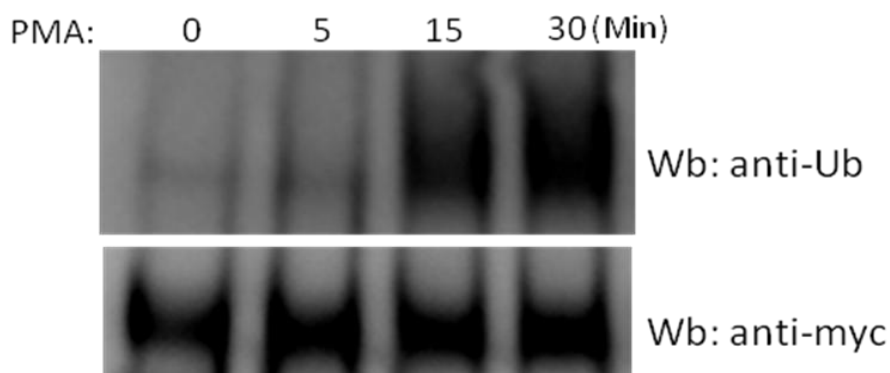


Figure 4-3 Time-dependence of ubiquitination of hOAT1 in COS-7 cells stably expressing hOAT1-C-myc. COS-7 cells stably expressing hOAT1-C-myc were incubated with vehicle (DMSO) or 1 μ M PMA for the indicated times at 37 $^{\circ}$ C, and solubilized with lysis buffer. hOAT1-C-myc protein was immunoprecipitated with anti-myc antibody 9E10 and immunoblotted with anti-ubiquitin antibody P4D1, and reprobed with anti-myc antibody 9E10. Bottom panel: The same immunoblot as the one in the top panel was reprobed by anti-myc antibody 9E10.

4.3.2 PMA-induced ubiquitination of rat OAT1 in rat kidney slices

After we found that hOAT1 can be ubiquitinated in expression system, we also examined whether OAT1 is ubiquitinated in rat kidney. Preparation of protein samples from rat kidney slices was based on a reported procedure (89). Briefly, rat kidney slices were incubated with vehicle or 1 μ M PMA for 30 min at 37 $^{\circ}$ C, and homogenized. Rat OAT1 proteins in the homogenates were immunoprecipitated with rabbit anti-human OAT1 antibody. Subsequently ubiquitinated proteins were immunoblotted with anti-ubiquitin antibody P4D1. In Fig. 4-4, a similar smeary band as that in the cells treated with PMA was detected in the rat kidney slices treated with PMA, indicating that the ubiquitination of rat OAT1 occurred *in vivo*.

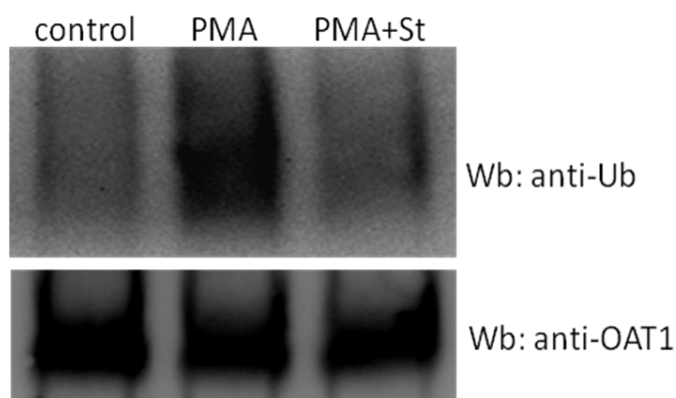
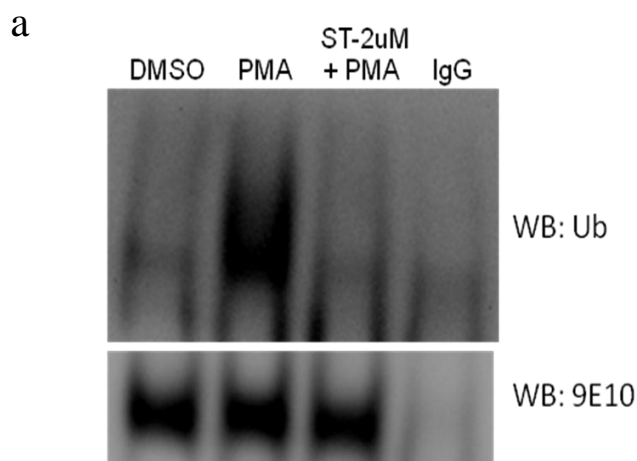


Figure 4-4 In vivo PMA-induced ubiquitination of rat OAT1. Rat kidney slices were treated with PKC activator PMA (1 μ M) in the presence and absence of PKC inhibitor staurosporin (2 μ M) for 30 min. Treated slices were then homogenized, immunoprecipitated with anti-OAT1 antibody, followed by immunoblotting with anti-ubiquitin antibody P4D1. Bottom panel: The same immunoblot was reprobed by anti-OAT1 antibody.

4.3.3 PMA-induced ubiquitination of OAT1 is sensitive to PKC inhibitor treatment

In order to determine that the effect of PMA treatment on ubiquitination of hOAT1 is specifically mediated by PKC activation rather than the other effects of PMA treatment occurring in the cell, two experiments using a PKC inhibitor, staurosporine, were conducted. After pretreatment of staurosporine, the cells expressing hOAT1 were treated by PMA in the presence or absence of staurosporine. As shown in Fig. 4-5, our results indicate that staurosporine treatment completely abolished the effect of PMA on ubiquitination of hOAT1 in COS-7 cells. This suggests that the effect of PMA on hOAT1 ubiquitination is specific to PKC activation induced by PMA treatment.



b

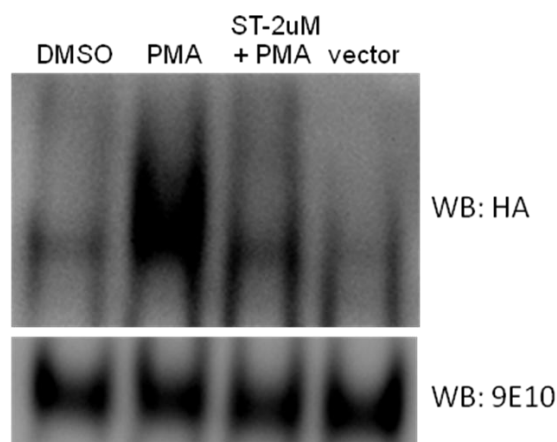


Figure 4-5 Blocking of PMA-induced ubiquitination of OAT1 by staurosporine treatment.

a. Endogenous ubiquitin. b. Transfected HA-ubiquitin. OAT1-expressing COS-7 cells were treated with PKC activator PMA (1 μ M) in the presence and absence of PKC inhibitor staurosporin (2 μ M) for 30 min. Treated cells were then lysed, immunoprecipitated with anti-myc antibody 9E10, followed by immunoblotting with anti-ubiquitin antibody P4D1. Bottom panel: The same immunoblot as the one in the top panel was reprobed by anti-myc antibody 9E10..

4.3.4 PMA-induced ubiquitination of cell surface OAT1

It is established that ubiquitination of membrane proteins at the cell surface plays a role in the internalization (84, 90-92) and/or endosomal sorting for degradation by lysosome (93-96). PKC-dependent ubiquitination of dopamine transporter (87), water channel (85), and glutamate transporter (88) is reported to occur at the cell surface. To determine whether the ubiquitination of hOAT1 occurs at the cell surface, we used a previously described approach (85) to isolate cell surface hOAT1 in COS-7 cells treated with vehicle

or PMA. Briefly, COS-7 cells were biotinylated and treated with vehicle or PMA, and lysed. hOAT1-C-myc was immunoprecipitated with anti-Myc antibody, released from the protein G beads by 1% SDS, and then the released hOAT1 proteins were subject to streptavidin pulldown to recover biotinylated hOAT1 and detected by Western blot.

The immunoblotting of immunoprecipitated hOAT1-C-myc with anti-ubiquitin antibody presented in Fig. 4-6 indicates PKC-induced ubiquitination of hOAT1 proteins at the cell surface.

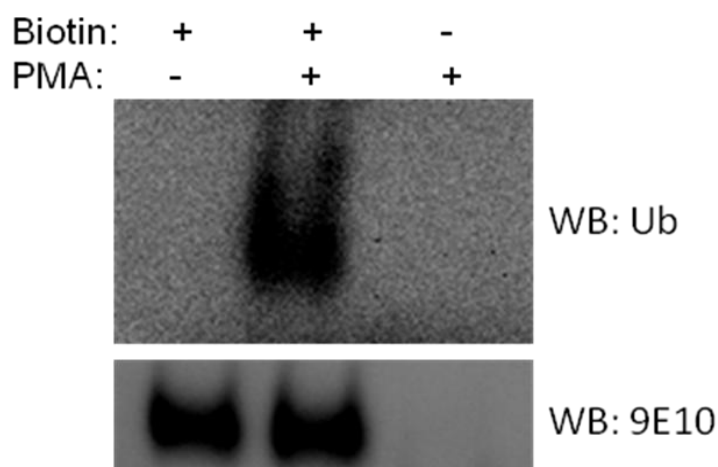


Figure 4-6 PKC-dependent ubiquitination of hOAT1 occurs at the plasma membrane. COS-7 cells stably expressing hOAT1-C-myc were biotinylated and incubated with vehicle (DMSO) or 1 μ M PMA for 30 min at 37 $^{\circ}$ C, and the biotinylated hOAT1-C-myc protein was isolated as in “Materials and methods”. hOAT1-C-myc protein was immunoprecipitated with anti-myc antibody 9E10 and immunoblotted with anti-ubiquitin antibody P4D1, and reprobed with anti-myc antibody 9E10.

4.3.5 Affinity purification and mass spectrometric analysis of ubiquitinated OAT1 proteins

Until now we cannot rule out the possibility that the ubiquitin detected in the above experiments was incorporated to a protein associated with hOAT1 that was co-immunoprecipitated with hOAT1. To address this issue, we utilized a strategy to purify the ubiquitinated hOAT1 proteins by sequentially immunoprecipitating hOAT1-C-myc with anti-myc antibody and then the ubiquitinated hOAT1-C-myc with anti-ubiquitin antibody. After sequential immunoprecipitation, the band of ubiquitinated hOAT1-C-myc in the gel was cut for mass spectrometric analysis.

Importantly, there was no considerable difference in the immunoreactivity of hOAT1-C-myc-ubiquitin conjugates between these two antibodies. Therefore, the result indicates that the ubiquitin detected in these experiments was incorporated to hOAT1-C-myc protein instead of a protein associated with this transporter. The result of mass spectrometry confirmed that only hOAT1 and ubiquitin were identified in the band corresponding to ubiquitinated forms of hOAT1 proteins. This indicates that the ubiquitin reactivity did not come from a protein associated with hOAT1. And Table 4-1 shows that Lys48-linked ubiquitin chains were detected in the sample of mass spectrometry, which reveals the existence of Lys48-linked polyubiquitin chains conjugated to hOAT1 molecules.

Identification	Peptides	Charge
Ubiquitin		
PMA	R.LIFAG K ^{48*} QLEDGR.T	+2
	R.LIFAG K ^{48*} QLEDGR.T	+3
* Denotes Gly-Gly modification of the ϵ -amino group of the lysine side chain.		

Table 4-1 Ubiquitinated peptides of ubiquitin analyzed by mass spectrometry. Modified amino acids are shown in bold. Periods represent the beginning and end of the peptide cut by trypsin.

4.3.6 Effects of ubiquitin mutants on PMA-induced ubiquitination of OAT1

Because we already observed the lysine-48 linkage on the ubiquitin molecule attached to hOAT1 protein from our mass spectrometric analysis, we further investigated the effects of different HA-tagged ubiquitin mutants on the PMA-dependent ubiquitination of hOAT1 protein. As indicated in Fig. 4-9, in line with our mass spectrometry result, the K48R mutant of ubiquitin significantly inhibited the PMA-dependent ubiquitination of hOAT1 and a K63R mutant of ubiquitin did not decrease the effect of PMA on hOAT1 ubiquitination. The delta G mutant of ubiquitin whose C-terminal glycine was deleted cannot be conjugated to the substrate protein due to the lack of the last glycine residue. As a result, the delta G ubiquitin completely abolished the PMA-dependent ubiquitination of hOAT1, which implies that our experimental system was suitable for the evaluation of the effects of various ubiquitin mutants on hOAT1 ubiquitination. Our results of this

experiment support that the K48-linked ubiquitin chains constitute a major type of polyubiquitin chains conjugated to hOAT1 proteins following PMA treatment.

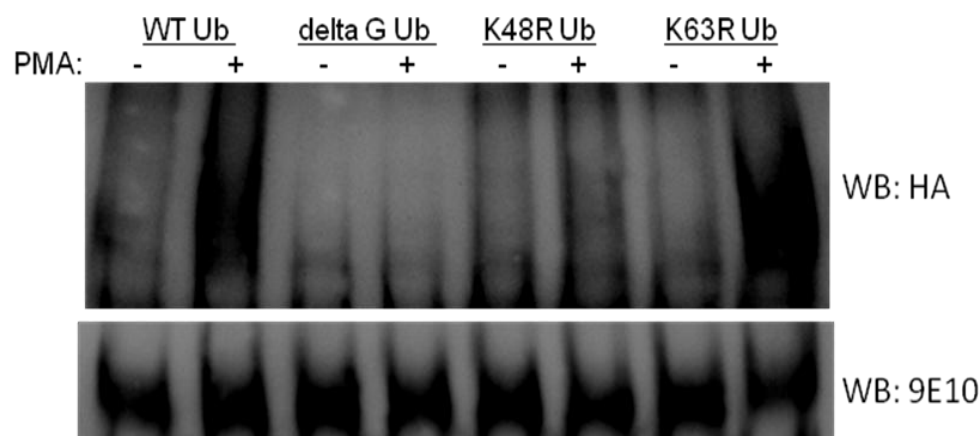


Figure 4-7 Effects of ubiquitin mutants on PMA-induced ubiquitination of OAT1. 4 μ g of cDNAs for HA-tagged wild type ubiquitin (WtUb), ubiquitin mutants Ub Δ G, Ub-K48R and Ub-K63R were transfected into COS-7 cells expressing OAT1 respectively, followed by treatment with or without PMA for 30 min. Treated cells were lysed. OAT1 was immunoprecipitated by anti-myc antibody 9E10, followed by immunoblotting with anti-HA antibody 12CA5. Bottom panel: The same immunoblot as the one in the top panel was reprobed by anti-myc antibody 9E10.

4.3.7 Effect of K48R ubiquitin mutant on PMA-induced reduction of cell surface OAT1

Previously, our group found that the cell surface expression of hOAT1 protein were down-regulated by PMA treatment and the internalization of hOAT1 proteins were accelerated in the presence of PMA (82). We hypothesized that the PMA-dependent ubiquitination of hOAT1 may play a role in the PMA-induced down-regulation of surface hOAT1. By means of forced expression of K48R ubiquitin mutant in COS-7 cells

expressing hOAT1 to overcome the effect of the presence of endogenous ubiquitin, we conducted an experiment to examine the effect of transfection of K48R ubiquitin mutant on the PMA-induced reduction of surface hOAT1 in COS-7 cells. In Fig. 4-10, our result shows that transfection of K48R ubiquitin considerably inhibited the effect of PMA on the surface expression of hOAT1, which suggests that K48-linked polyubiquitin chains attached to hOAT1 is important for the PMA-induced down-regulation of surface hOAT1 proteins.

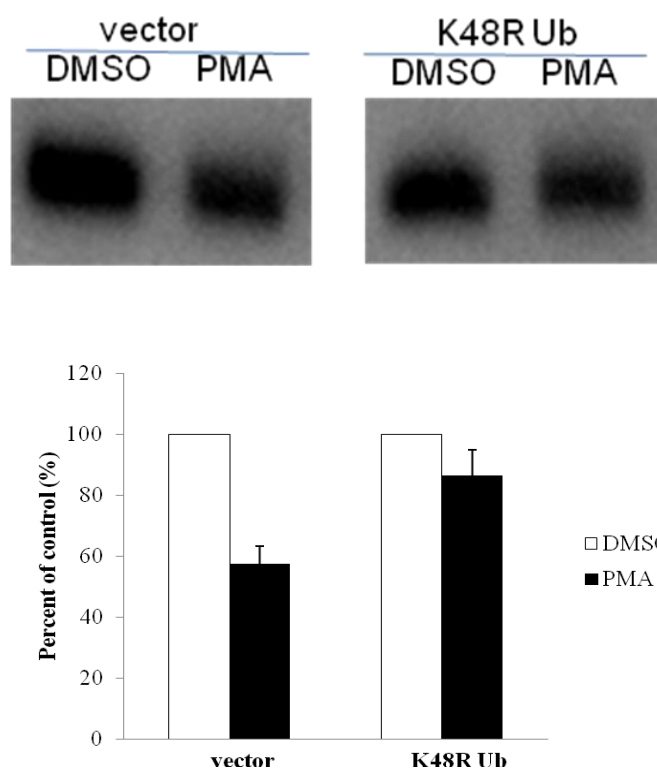


Figure 4-8 Effect of K48R ubiquitin mutant on PMA-induced reduction of cell surface OAT1. OAT1-expressing cells were transfected with Ub-K48R (or vector as control), followed by treatment with or without PMA (1 μ M) for 30 min. Treated cells underwent cell surface biotinylation. Biotinylated proteins were isolated with streptavidin beads and analyzed by immunoblotting with an anti-myc antibody 9E10. b. Densitometry plot of

results of different experiments. Surface OAT1 in PMA-treated cells was expressed as % of surface OAT1 in control cells. Values are mean \pm S.E. (n = 3).

4.3.8 Effect of K48R ubiquitin mutant on PKC-regulated internalization of OAT1

Our previous study already discovered that in COS-7 cells, hOAT1 proteins traffics constitutively between the cell surface and intracellular compartments including early endosome, and PKC-activation by PMA treatment enhanced the endocytosis of hOAT1 (82). Because in the current study, short-term PMA treatment has been shown to induce ubiquitination of hOAT1 in COS-7 cell, we hypothesize that the PMA-induced ubiquitination of hOAT1 may play a role in the PKC-regulated endocytosis of hOAT1. To determine a possible cause-effect relationship between the increase in ubiquitination and endocytosis induced by PMA treatment, we used the K48R ubiquitin mutant to inhibit the PMA-dependent ubiquitination of hOAT1 and attempted to determine the effect of inhibition of PMA-dependent hOAT1 ubiquitination on the PMA-dependent endocytosis of hOAT1 in COS-7 cell. As shown in Fig. 4-11, consistent with the result of surface expression of hOAT1 after transfection of K48R ubiquitin mutant shown above, the PMA-induced increase of hOAT1 internalization was remarkably inhibited by transfection of K48R ubiquitin mutant compared with empty vector transfected cells. This result suggests that PMA-induced hOAT1 ubiquitination is required for the effect of PMA on the endocytosis of hOAT1.

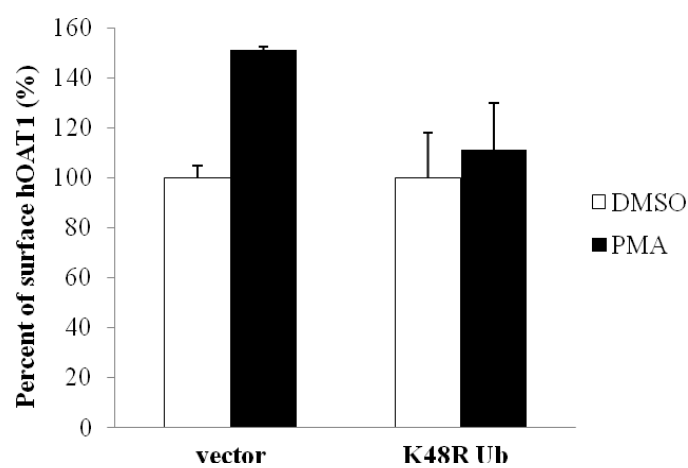
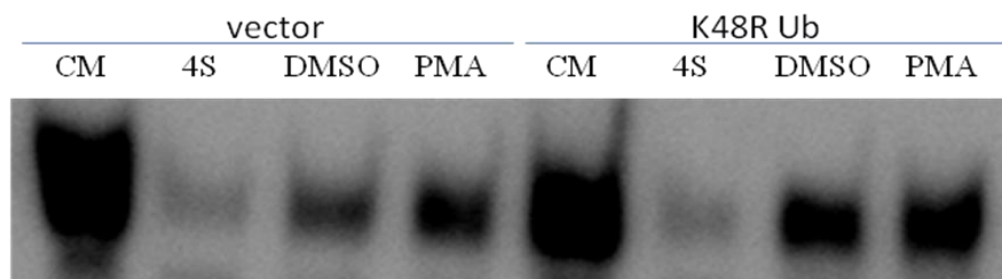


Figure 4-9 Effect of K48R ubiquitin mutant on PKC-regulated internalization of OAT1. COS-7 cells were transfected with OAT1 (1 μ g) and Ub-K48R (4 μ g) (or vector as control). OAT1 internalization (15 Min) was then determined as described in “Materials and Methods” section, followed by immunoblotting using anti-myc antibody 9E10. b. Densitometry plot of results from different experiments. Internalized surface OAT1 in PMA-treated cells was expressed as % of internalized surface OAT1 in control cells. Values are mean \pm S.E. (n = 3).

4.3.9 Multiple lysine substitutions of OAT1 inhibit PMA-induced ubiquitination

It is important to find out the possible role of PKC-induced ubiquitination of hOAT1 in its internalization and/or lysosomal degradation. Using site-directed mutagenesis

approach, we generated a series of mutants in which multiple lysine residues in the intracellular domain of hOAT1 were simultaneously substituted to arginine. By analyzing the ubiquitination of these hOAT1 mutants in COS-7 cells treated with vehicle or PMA, we found a mutant, named N5KR, in which five lysine residues (Lys163, Lys297, Lys303, Lys315 and Lys321) located in the intracellular loops excluding the C-terminus were simultaneously replaced by arginine displayed significantly reduced ubiquitination after PKC activation compared to that of wild-type hOAT1 (Fig. 4-12). This result suggests that these lysine residues are potential ubiquitination sites of hOAT1.

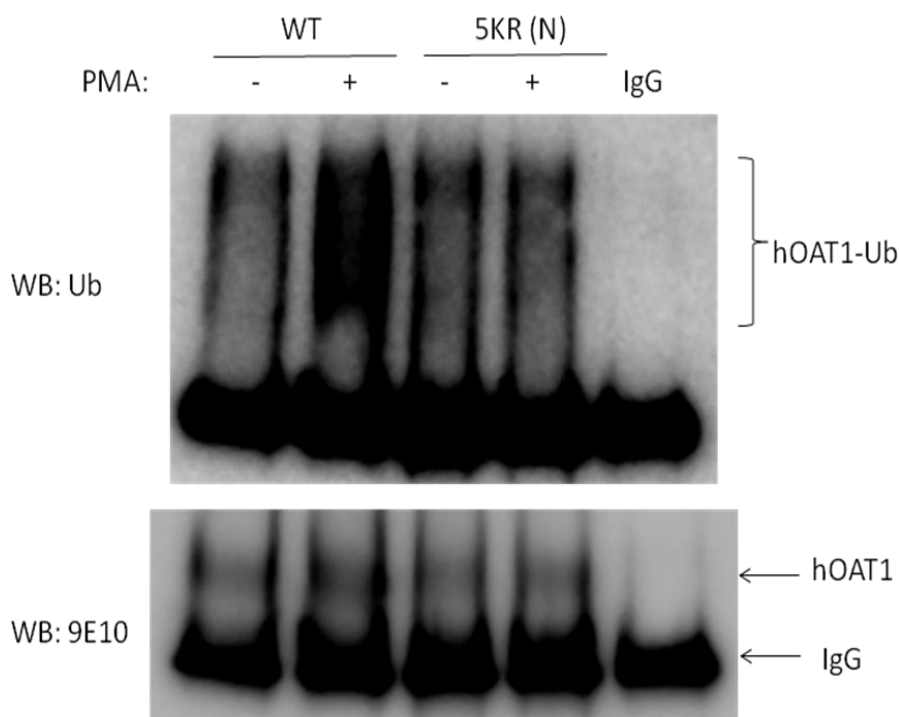
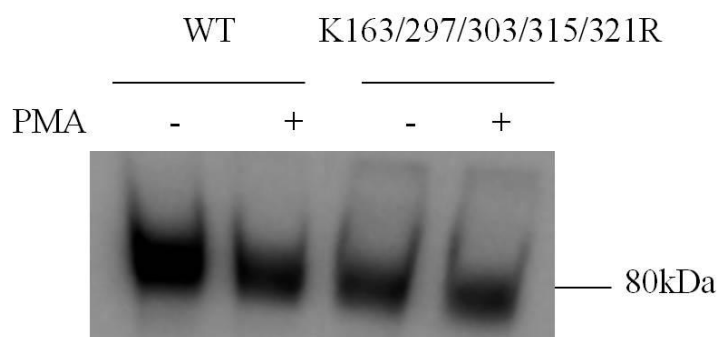


Figure 4-10 Effect of multiple lysine mutation on PKC-induced ubiquitination of hOAT1. After 48h transfection of wild-type and N5KR hOAT1-C-myc, COS-7 cells were incubated with vehicle (DMSO) or 1 μ M PMA for 30 min at 37 $^{\circ}$ C, and solubilized with lysis buffer. hOAT1-C-myc protein was immunoprecipitated with anti-myc antibody

9E10 and immunoblotted with anti-ubiquitin antibody P4D1, and reprobed with anti-myc antibody 9E10.

4.3.10 Down-regulation of OAT1 by PKC activation is decreased by multilycine mutation

Generation of the hOAT1 mutant that is minimally ubiquitinated in response to PKC activation allowed us to analyze the effect of PKC-induced ubiquitination of hOAT1 on the PKC-induced down-regulation of this transporter. Surface expression of hOAT1 has been shown to be down-regulated by PKC activation in COS-7 cells and other cell models. COS-7 cells expressing wild-type or N5KR hOAT1-C-myc were incubated with vehicle (DMSO) or 1 μ M PMA for 30 min at 37 °C. Surface hOAT1 proteins were subject to surface biotinylation and immunoblot with anti-myc antibody 9E10. As shown in Fig. 4-13, PMA-induced down-regulation of cell surface N5KR hOAT1 was significantly less than that of wild-type hOAT1. This observation implies a role of PKC-induced ubiquitination of hOAT1 in the down-regulation of this transporter by PKC activation.



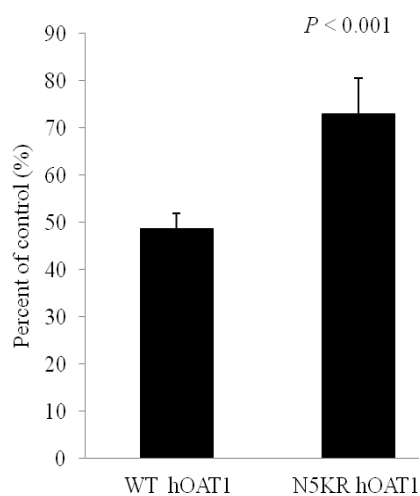
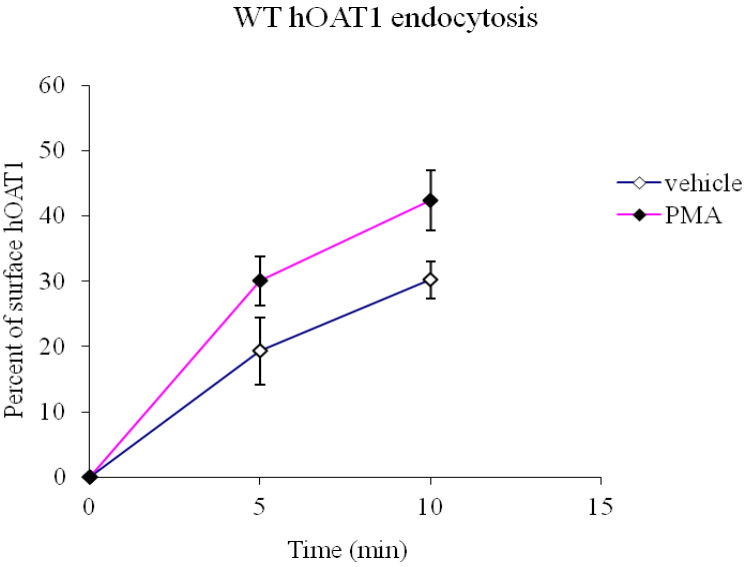
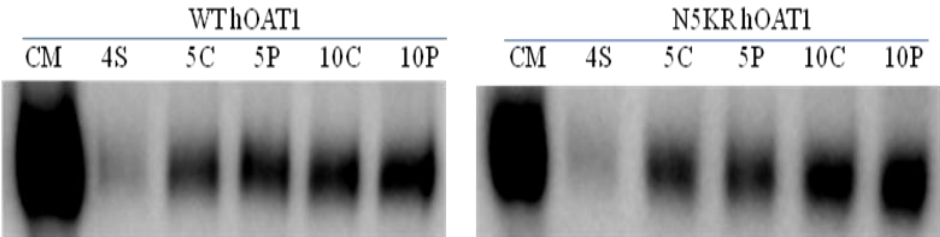


Figure 4-11 Effect of multiple lysine mutation on PKC-induced down-regulation of surface OAT1. After 48h transfection of wild-type and N5KR hOAT1-C-myc, COS-7 cells were incubated with vehicle (DMSO) or 1 μ M PMA for 30 min at 37 $^{\circ}$ C. Surface OAT1 proteins were subject to surface biotinylation and immunoblot with anti-myc antibody 9E10. (Data provided by Jinwei Wu)

4.3.11 Multiple lysine substitutions of OAT1 inhibit PMA-induced internalization

To examine the effect of multiple lysine substitutions of hOAT1 on PMA-induced endocytosis, we compared the internalization rates of wild-type and the ubiquitination-deficient N5KR mutant of hOAT1 in COS-7 cells. We observed (Fig. 4-14) that substitutions of the intracellular five lysines with arginine in hOAT1 protein inhibited the effect of PMA on the internalization of hOAT1 in COS-7 cells. Our result confirms a role of PMA-dependent ubiquitination of hOAT1 in the increase of hOAT1 endocytosis following exposure to PMA.



N5KR hOAT1 endocytosis

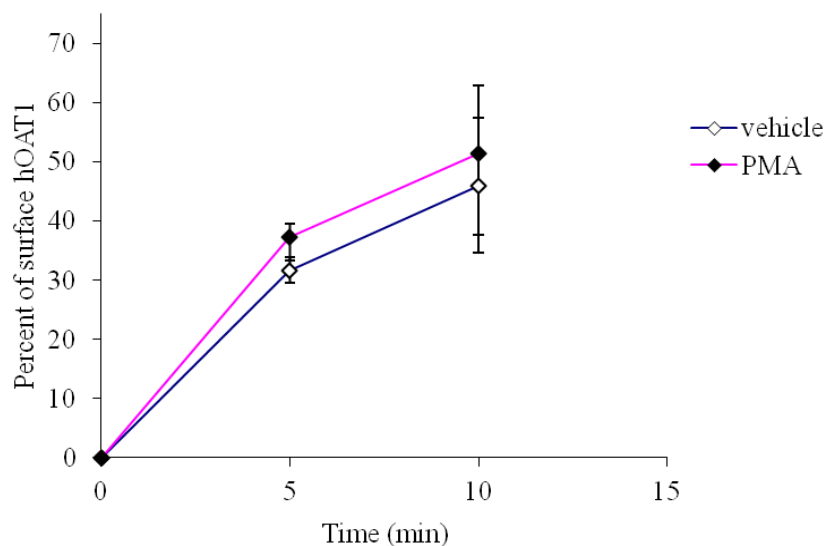


Figure 4-12 Effect of multiple lysine mutation on PKC-induced endocytosis of OAT1. After 48h transfection of wild-type and N5KR hOAT1-C-myc, COS-7 cells were incubated with vehicle (DMSO) or 1 μ M PMA for 30 min at 37 °C. Surface OAT1 proteins were subject to internalization assay and immunoblot with anti-myc antibody 9E10.

4.3.12 Effect of PKC activation on the degradation of surface OAT1

The degradation of some membrane proteins has been demonstrated to be promoted by PKC activation (85, 87, 97). It is likely that the degradation of hOAT1 and hOAT3 may also be regulated by PKC, because the transport activity and endocytosis of both transporters have been shown to be regulated by PKC (82, 98, 99). We analyzed the degradation rates of hOAT1 and hOAT3 at the cell surface in the absence or presence of PMA for 2 ~ 8 hours using a biotinylation method described in the methods section.

Interestingly, our data indicated that PMA treatment enhanced the degradation of both transporters significantly (Fig. 4-15 and 4-16).

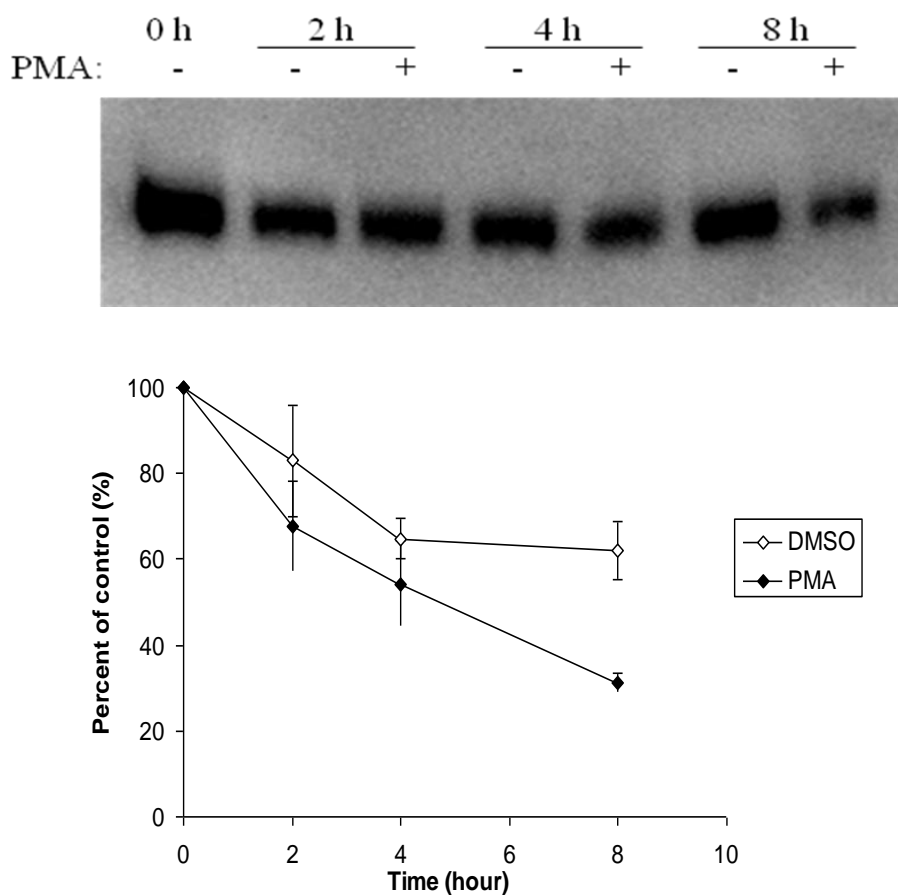


Figure 4-13 Effect of PKC activation on the degradation of surface OAT1. Cell surface proteins of COS-7 cells expressing OAT1 were biotinylated, and incubated with vehicle (DMSO) or 1 μ M PMA for designated periods of time at 37 °C to allow degradation to occur. Surface OAT1 proteins were subject to pulldown by streptavidin beads and immunoblot with anti-myc antibody 9E10.

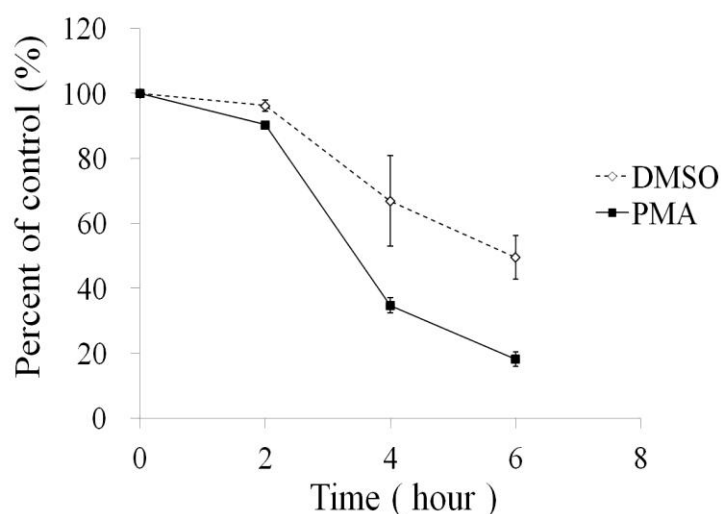


Figure 4-14 Effect of PKC activation on the degradation of surface OAT3. Cell surface proteins of COS-7 cells expressing OAT3 were biotinylated, and incubated with vehicle (DMSO) or 1 μ M PMA for designated periods of time at 37 $^{\circ}$ C to allow degradation to occur. Surface OAT1 proteins were subject to pulldown by streptavidin beads and immunoblot with anti-myc antibody 9E10.

4.3.13 Effect of K48R ubiquitin mutant on PKC-regulated degradation of surface OAT1

Because we observed that prolonged treatment with PMA in COS-7 cells expressing hOAT1 enhanced the degradation of surface hOAT1 proteins as demonstrated above, we speculated that the PMA-induced ubiquitination of hOAT1 may be involved in the PMA-induced degradation of surface hOAT1. In fact, ubiquitination of membrane proteins including transporters and receptors has been shown to play an important role in the degradation of these membrane proteins, such as interferon receptor-alpha (94), prolactin receptor (93), water channel (85), and sodium channel (87).

Our result shown in Fig. 4-16 indicates that expression of K48R ubiquitin mutant significantly delayed the PMA-induced degradation of surface hOAT1 in COS-7 cells. This finding suggests that PMA-induced hOAT1 ubiquitination is required for the effect of PMA treatment on the degradation of surface hOAT1.

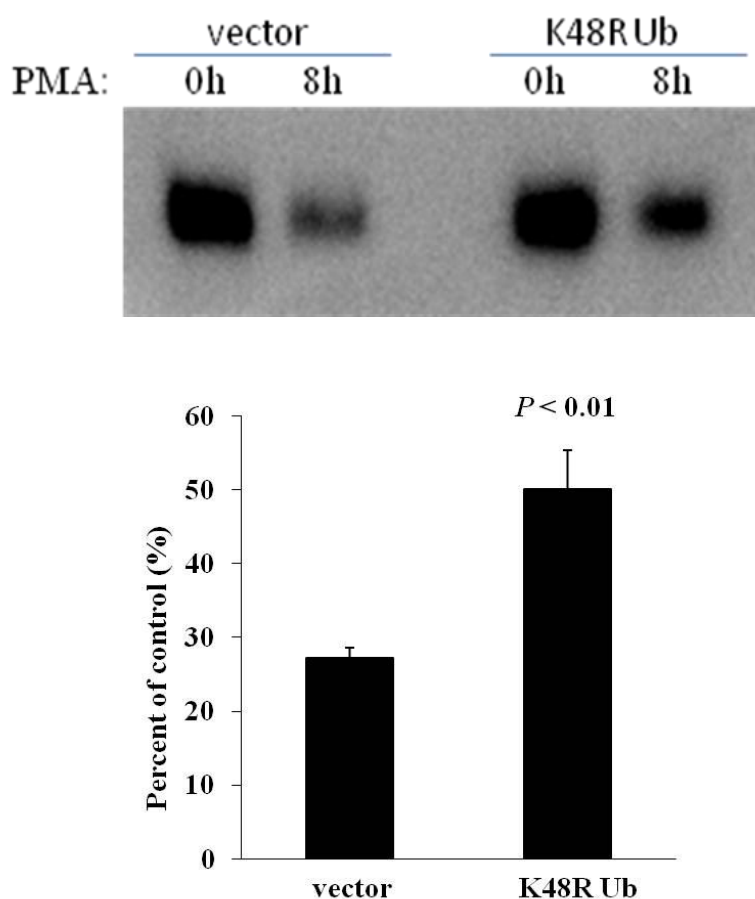
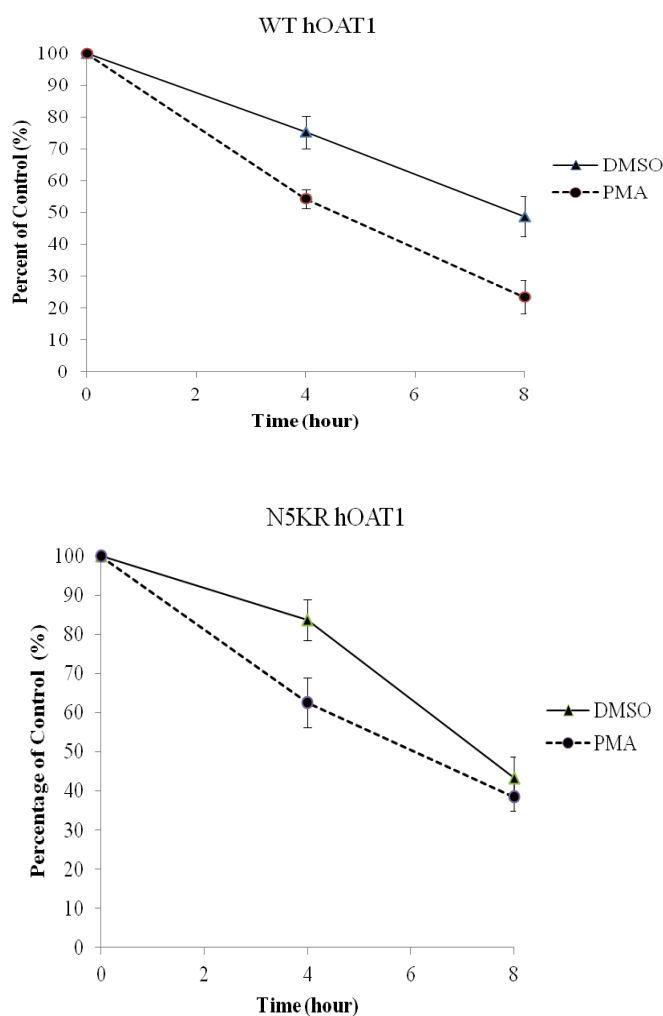


Figure 4-15 Effect of K48R ubiquitin mutant on PKC-regulated degradation of surface OAT1. After 48 h transfection of with OAT1 (1 μ g) and Ub-K48R (4 μ g) (or vector as control), cell surface proteins of the cells were biotinylated, and incubated with vehicle (DMSO) or 1 μ M PMA for 8 h at 37 $^{\circ}$ C to allow degradation to occur. Surface OAT1 proteins were subject to pulldown by streptavidin beads and immunoblot with anti-myc antibody 9E10.

4.3.14 Multiple lysine substitutions of OAT1 inhibit PMA-induced degradation of surface hOAT1

Similar to the effect of K48R ubiquitin mutant on the PMA-induced degradation of surface hOAT1, multiple lysine substitutions of hOAT1 with arginine (N5KR hOAT1 mutant) delayed the degradation of surface hOAT1 in the presence of PMA, as shown in Fig. 4-17. Consequently, our data suggest that PMA-induced ubiquitination of hOAT1 plays an important role in the PMA-induced degradation of surface hOAT1.



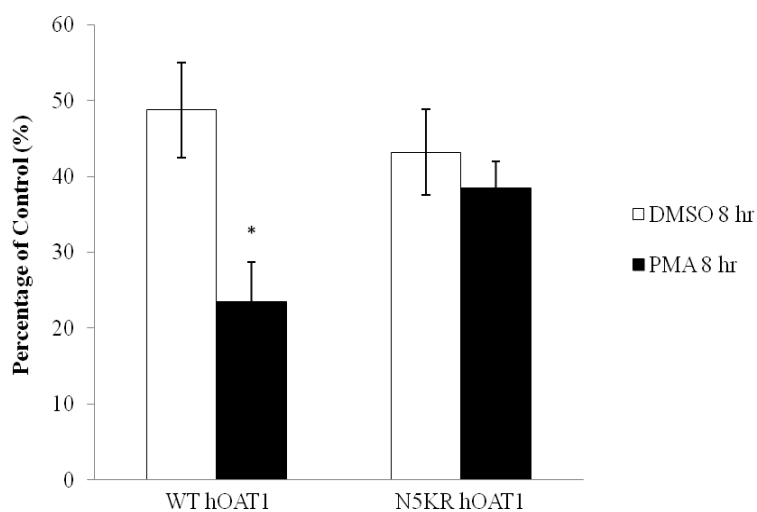


Figure 4-16 Effect of multiple lysine substitutions on PKC-induced degradation of surface OAT1. After 48 h transfection of with wildtype OAT1 or N5KR OAT1, cell surface proteins of the cells were biotinylated, and incubated with vehicle (DMSO) or 1 μ M PMA for 4 and 8 h at 37 $^{\circ}$ C to allow degradation to occur. Surface OAT1 proteins were subject to pulldown by streptavidin beads and immunoblot with anti-myc antibody 9E10. (Data provided by Jinwei Wu)

4.4 Discussion

While originally the function of ubiquitination was discovered to target cytosolic proteins for proteasome degradation, ubiquitination has now been demonstrated to participate in other critical cellular processes including membrane trafficking, post-internalization sorting, proteasomal degradation, DNA repair, and transcription (83). The membrane proteins regulated by ubiquitination include sodium channel (84), water channel (85), dopamine transporter (86, 87), and glycine transporter (9), interferon-alpha receptor (94), and so on.

The molecular mechanism by which PKC regulates the internalization of OAT proteins remains unclear. Recent studies regarding the PKC-induced endocytosis of other transmembrane proteins have proposed a critical role of ubiquitination of membrane proteins in their endocytosis, post-internalization targeting, and lysosomal degradation. Miranda *et al* reported (86) that PKC activation-induced endocytosis of dopamine transporter is dependent on ubiquitination of this protein.

In the current study, we discovered that PMA treatment induces ubiquitination of hOAT1 and hOAT3 in COS-7 cells as well as rat OAT1 in rat kidney slices. We further characterized the PMA-dependent ubiquitination of hOAT1 in COS-7 cells. We found that the PMA-dependent hOAT1 ubiquitination is time-dependent, sensitive to PKC inhibitor, occurs at the cell surface, and precedes the endocytosis of hOAT1. We further investigated the roles of PMA-dependent ubiquitination of hOAT1 in PKC-regulated endocytosis and degradation of hOAT1 in COS-7 cells. We adopted two different approaches to determine the effect of inhibition of PMA-dependent ubiquitination of hOAT1 on PKC-regulated endocytosis and degradation of hOAT1. One is forced expression of ubiquitin mutants to overcome the effect of endogenous ubiquitin. The other is substitution of lysine residues residing in the intracellular portion of hOAT1 protein with arginine, because these lysine residues are potential ubiquitin acceptors. Our data demonstrate that PMA-dependent ubiquitination of hOAT1 is essential for the regulation of endocytosis and degradation of hOAT1 by PKC activation.

In the data of mass spectrometric analysis of ubiquitinated hOAT1 molecules, while the coverage of hOAT1-derived peptides is not enough to allow the identification of the lysine residues located in the intracellular portion of hOAT1 that serve as the ubiquitin

acceptors, sufficient information regarding the peptides originated from ubiquitin molecules that are conjugated to hOAT1 was obtained successfully. In the affinity purified sample of ubiquitinated hOAT1 proteins, we only identified hOAT1 and ubiquitin, which indicates that the immunoreactivity to anti-ubiquitin antibody of the immunoprecipitated hOAT1 proteins did not come from a protein associated with hOAT1. The intracellular side of hOAT1 protein contains ten lysine residues. Six of them are located in the intracellular loops and four of them are located in the carboxyl-terminus. By checking the molecular size of the smeary band of hOAT1-ubiquitin conjugates revealed by anti-ubiquitin antibody, we found that the apparent molecular mass of hOAT1-ubiquitin conjugates is greater than expected from hOAT1 that undergoes multiple monoubiquitination on every intracellular lysine residue ($80 \text{ kD} + 8 \text{ kD} \times 10 = 160 \text{ kD}$). This analysis suggests that hOAT1 might be polyubiquitinated. In line with the analysis of molecular size, our mass spectrometric data confirmed the existence of lysine-48 linked polyubiquitin chains conjugated to hOAT1. It is worth to note that we also observed the peptides of ubiquitin whose Lys-48 residue was cut by trypsin after in-gel digestion. This finding suggests the presence of multi-ubiquitination.

It has been shown that different types of ubiquitination (mono- versus polyubiquitination via different types of linkages) have different physiologic outcome for the ubiquitinated substrate. For example, while monoubiquitination is required for downregulation of the EGF receptor (95, 100), K63 chains have been shown to contribute to endocytosis of the TrkA nerve growth factor receptor (101). While IFNAR1 internalization requires both K48 and K63 linkages (94), PRLr internalization relies mainly on K63-conjugated chains (93). To identify the specific types of OAT1 ubiquitination, we performed mass

spectrometric analysis, one of the most powerful approaches to identify post-translational modifications of numerous proteins. For such purpose, we developed sequential immunoprecipitation procedures ensuring that the high purity of ubiquitinated OAT1 was used. The mass spectroscopic results indeed confirmed that ubiquitin and OAT1 were the two predominant proteins detected in our sample, providing evidence that ubiquitin was conjugated OAT1 rather than to an OAT-associated protein. Furthermore, our mass spectroscopic analysis identified several peptide fragments from ubiquitin protein, which covered all seven lysine residues. Only K48-linked ubiquitin was detected. These results indicate that OAT1 is ubiquitinated mainly through a K48-linked polyubiquitin chain. Although the limited coverage of OAT1 peptides using mass spectroscopy did not allow us to identify the lysine residues on OAT1 that serve as ubiquitin acceptors, we are currently underway to use site-directed mutagenesis approach to identify these residues.

In the present study, some important questions remain to be answered. These question include: 1) which E3 ligase conjugates ubiquitin moiety to hOAT1 and hOAT3; 2) the ubiquitination sites of hOAT1 and hOAT3; 3) whether other regulatory mechanisms other than PKC activation are involved in hOAT1 and hOAT3 ubiquitination; 4) how ubiquitination regulates the endocytosis and degradation of OATs transporters; 5) how ubiquitination of OATs transporters is related to drug disposition mediated by this family of transporters in animals and humans. To address thses important questions, more studies are warranted.

5 References

1. N. Mizuno and Y. Sugiyama. Drug transporters: their role and importance in the selection and development of new drugs. *Drug Metab Pharmacokinet.* 17:93-108 (2002).
2. R.B. Kim. Transporters and drug discovery: why, when, and how. *Mol Pharm.* 3:26-32 (2006).
3. N. Anzai, Y. Kanai, and H. Endou. Organic anion transporter family: current knowledge. *J Pharmacol Sci.* 100:411-426 (2006).
4. F. Zhou and G. You. Molecular insights into the structure-function relationship of organic anion transporters OATs. *Pharm Res.* 24:28-36 (2007).
5. C. Srimaroeng, J.L. Perry, and J.B. Pritchard. Physiology, structure, and regulation of the cloned organic anion transporters. *Xenobiotica.* 38:889-935 (2008).
6. M.K. Loder and H.E. Melikian. The dopamine transporter constitutively internalizes and recycles in a protein kinase C-regulated manner in stably transfected PC12 cell lines. *J Biol Chem.* 278:22168-22174 (2003).
7. L.D. Jayanthi, D.J. Samuvel, and S. Ramamoorthy. Regulated internalization and phosphorylation of the native norepinephrine transporter in response to phorbol esters. Evidence for localization in lipid rafts and lipid raft-mediated internalization. *J Biol Chem.* 279:19315-19326 (2004).
8. S. Shigematsu, R.T. Watson, A.H. Khan, and J.E. Pessin. The adipocyte plasma membrane caveolin functional/structural organization is necessary for the efficient endocytosis of GLUT4. *J Biol Chem.* 278:10683-10690 (2003).
9. E. Fernandez-Sanchez, J. Martinez-Villarreal, C. Gimenez, and F. Zafra. Constitutive and regulated endocytosis of the glycine transporter GLYT1b is controlled by ubiquitination. *J Biol Chem.* 284:19482-19492 (2009).
10. A. Swiatecka-Urban, M. Duhaime, B. Coutermarsh, K.H. Karlson, J. Collawn, M. Milewski, G.R. Cutting, W.B. Guggino, G. Langford, and B.A. Stanton. PDZ domain interaction controls the endocytic recycling of the cystic fibrosis transmembrane conductance regulator. *J Biol Chem.* 277:40099-40105 (2002).
11. Z. Zhao, X. Li, J. Hao, J.H. Winston, and S.A. Weinman. The CIC-3 chloride transport protein traffics through the plasma membrane via interaction of an N-terminal dileucine cluster with clathrin. *J Biol Chem.* 282:29022-29031 (2007).
12. D. Wang and M.W. Quick. Trafficking of the plasma membrane gamma-aminobutyric acid transporter GAT1. Size and rates of an acutely recycling pool. *J Biol Chem.* 280:18703-18709 (2005).
13. B.D. Grant and J.G. Donaldson. Pathways and mechanisms of endocytic recycling. *Nat Rev Mol Cell Biol.* 10:597-608 (2009).

14. F.R. Maxfield and T.E. McGraw. Endocytic recycling. *Nat Rev Mol Cell Biol.* 5:121-132 (2004).
15. C. Le Roy and J.L. Wrana. Clathrin- and non-clathrin-mediated endocytic regulation of cell signalling. *Nat Rev Mol Cell Biol.* 6:112-126 (2005).
16. G. You, K. Kuze, R.A. Kohanski, K. Amsler, and S. Henderson. Regulation of mOAT-mediated organic anion transport by okadaic acid and protein kinase C in LLC-PK(1) cells. *J Biol Chem.* 275:10278-10284 (2000).
17. F. Zhou, M. Hong, and G. You. Regulation of human organic anion transporter 4 by progesterone and protein kinase C in human placental BeWo cells. *Am J Physiol Endocrinol Metab.* 293:E57-61 (2007).
18. F.M. Brodsky, C.Y. Chen, C. Knuehl, M.C. Towler, and D.E. Wakeham. Biological basket weaving: formation and function of clathrin-coated vesicles. *Annu Rev Cell Dev Biol.* 17:517-568 (2001).
19. M. Marchetti, M.N. Monier, A. Fradagrada, K. Mitchell, F. Baychelier, P. Eid, L. Johannes, and C. Lamaze. Stat-mediated signaling induced by type I and type II interferons (IFNs) is differentially controlled through lipid microdomain association and clathrin-dependent endocytosis of IFN receptors. *Mol Biol Cell.* 17:2896-2909 (2006).
20. U. Schmidt, S. Briese, K. Leicht, A. Schurmann, H.G. Joost, and H. Al-Hasani. Endocytosis of the glucose transporter GLUT8 is mediated by interaction of a dileucine motif with the beta2-adaptin subunit of the AP-2 adaptor complex. *J Cell Sci.* 119:2321-2331 (2006).
21. J. Smith, R. Yu, and P.M. Hinkle. Activation of MAPK by TRH requires clathrin-dependent endocytosis and PKC but not receptor interaction with beta-arrestin or receptor endocytosis. *Mol Endocrinol.* 15:1539-1548 (2001).
22. A. Jiang, K. Lehti, X. Wang, S.J. Weiss, J. Keski-Oja, and D. Pei. Regulation of membrane-type matrix metalloproteinase 1 activity by dynamin-mediated endocytosis. *Proc Natl Acad Sci U S A.* 98:13693-13698 (2001).
23. C. Morisco, C. Marrone, J. Galeotti, D. Shao, D.E. Vatner, S.F. Vatner, and J. Sadoshima. Endocytosis machinery is required for beta1-adrenergic receptor-induced hypertrophy in neonatal rat cardiac myocytes. *Cardiovasc Res.* 78:36-44 (2008).
24. H. Huang, X. Feng, J. Zhuang, O. Frohlich, J.D. Klein, H. Cai, J.M. Sands, and G. Chen. Internalization of UT-A1 urea transporter is dynamin dependent and mediated by both caveolae- and clathrin-coated pit pathways. *Am J Physiol Renal Physiol.* 299:F1389-1395.
25. J.A. Gray, D.J. Sheffler, A. Bhatnagar, J.A. Woods, S.J. Hufeisen, J.L. Benovic, and B.L. Roth. Cell-type specific effects of endocytosis inhibitors on 5-hydroxytryptamine(2A) receptor desensitization and resensitization reveal an arrestin-, GRK2-, and GRK5-independent mode of regulation in human embryonic kidney 293 cells. *Mol Pharmacol.* 60:1020-1030 (2001).

26. A. Mashukova, M. Spehr, H. Hatt, and E.M. Neuhaus. Beta-arrestin2-mediated internalization of mammalian odorant receptors. *J Neurosci.* 26:9902-9912 (2006).
27. K. Xiao, J. Garner, K.M. Buckley, P.A. Vincent, C.M. Chiasson, E. Dejana, V. Faundez, and A.P. Kowalczyk. p120-Catenin regulates clathrin-dependent endocytosis of VE-cadherin. *Mol Biol Cell.* 16:5141-5151 (2005).
28. N. Bayer, D. Schober, M. Huttinger, D. Blaas, and R. Fuchs. Inhibition of clathrin-dependent endocytosis has multiple effects on human rhinovirus serotype 2 cell entry. *J Biol Chem.* 276:3952-3962 (2001).
29. R. Yumoto, H. Nishikawa, M. Okamoto, H. Katayama, J. Nagai, and M. Takano. Clathrin-mediated endocytosis of FITC-albumin in alveolar type II epithelial cell line RLE-6TN. *Am J Physiol Lung Cell Mol Physiol.* 290:L946-955 (2006).
30. A. Salikhova, L. Wang, A.A. Lanahan, M. Liu, M. Simons, W.P. Leenders, D. Mukhopadhyay, and A. Horowitz. Vascular endothelial growth factor and semaphorin induce neuropilin-1 endocytosis via separate pathways. *Circ Res.* 103:e71-79 (2008).
31. S. Venkatesan, J.J. Rose, R. Lodge, P.M. Murphy, and J.F. Foley. Distinct mechanisms of agonist-induced endocytosis for human chemokine receptors CCR5 and CXCR4. *Mol Biol Cell.* 14:3305-3324 (2003).
32. A. Benmerah, M. Bayrou, N. Cerf-Bensussan, and A. Dautry-Varsat. Inhibition of clathrin-coated pit assembly by an Eps15 mutant. *J Cell Sci.* 112 (Pt 9):1303-1311 (1999).
33. E.M. van Damand W. Stoorvogel. Dynamin-dependent transferrin receptor recycling by endosome-derived clathrin-coated vesicles. *Mol Biol Cell.* 13:169-182 (2002).
34. N.A. Wolff, K. Thies, N. Kuhnke, G. Reid, B. Friedrich, F. Lang, and G. Burckhardt. Protein kinase C activation downregulates human organic anion transporter 1-mediated transport through carrier internalization. *J Am Soc Nephrol.* 14:1959-1968 (2003).
35. B.R. Cobb, F. Ruiz, C.M. King, J. Fortenberry, H. Greer, T. Kovacs, E.J. Sorscher, and J.P. Clancy. A(2) adenosine receptors regulate CFTR through PKA and PLA(2). *Am J Physiol Lung Cell Mol Physiol.* 282:L12-25 (2002).
36. M.G. Kazanietz, M.J. Caloca, O. Aizman, and S. Nowicki. Phosphorylation of the catalytic subunit of rat renal Na⁺, K⁺-ATPase by classical PKC isoforms. *Arch Biochem Biophys.* 388:74-80 (2001).
37. Y. Kato, C. Watanabe, and A. Tsuji. Regulation of drug transporters by PDZ adaptor proteins and nuclear receptors. *Eur J Pharm Sci.* 27:487-500 (2006).
38. B. Broneand J. Eggermont. PDZ proteins retain and regulate membrane transporters in polarized epithelial cell membranes. *Am J Physiol Cell Physiol.* 288:C20-29 (2005).
39. H. Miyazaki, N. Anzai, S. Ekaratanawong, T. Sakata, H.J. Shin, P. Jutabha, T. Hirata, X. He, H. Nonoguchi, K. Tomita, Y. Kanai, and H. Endou. Modulation of

- renal apical organic anion transporter 4 function by two PDZ domain-containing proteins. *J Am Soc Nephrol.* 16:3498-3506 (2005).
40. F. Zhou, W. Xu, K. Tanaka, and G. You. Comparison of the interaction of human organic anion transporter hOAT4 with PDZ proteins between kidney cells and placental cells. *Pharm Res.* 25:475-480 (2008).
 41. S. Vergarajauregui and R. Puertollano. Two di-leucine motifs regulate trafficking of mucolipin-1 to lysosomes. *Traffic.* 7:337-353 (2006).
 42. M.T. Duvernay, F. Zhou, and G. Wu. A conserved motif for the transport of G protein-coupled receptors from the endoplasmic reticulum to the cell surface. *J Biol Chem.* 279:30741-30750 (2004).
 43. B. Wang, A. Bisello, Y. Yang, G.G. Romero, and P.A. Friedman. NHERF1 regulates parathyroid hormone receptor membrane retention without affecting recycling. *J Biol Chem.* 282:36214-36222 (2007).
 44. C.S. Lazar, C.M. Cresson, D.A. Lauffenburger, and G.N. Gill. The Na⁺/H⁺ exchanger regulatory factor stabilizes epidermal growth factor receptors at the cell surface. *Mol Biol Cell.* 15:5470-5480 (2004).
 45. K. Tanaka, W. Xu, F. Zhou, and G. You. Role of glycosylation in the organic anion transporter OAT1. *J Biol Chem.* 279:14961-14966 (2004).
 46. F. Zhou, W. Xu, M. Hong, Z. Pan, P.J. Sinko, J. Ma, and G. You. The role of N-linked glycosylation in protein folding, membrane targeting, and substrate binding of human organic anion transporter hOAT4. *Mol Pharmacol.* 67:868-876 (2005).
 47. C.L. Ward, S. Omura, and R.R. Kopito. Degradation of CFTR by the ubiquitin-proteasome pathway. *Cell.* 83:121-127 (1995).
 48. L. Sepp-Lorenzino, Z. Ma, D.E. Lebowitz, A. Vinitsky, and N. Rosen. Herbimycin A induces the 20 S proteasome- and ubiquitin-dependent degradation of receptor tyrosine kinases. *J Biol Chem.* 270:16580-16587 (1995).
 49. T.J. Jensen, M.A. Loo, S. Pind, D.B. Williams, A.L. Goldberg, and J.R. Riordan. Multiple proteolytic systems, including the proteasome, contribute to CFTR processing. *Cell.* 83:129-135 (1995).
 50. D. Peroz, S. Dahimene, I. Baro, G. Loussouarn, and J. Merot. LQT1-associated mutations increase KCNQ1 proteasomal degradation independently of Derlin-1. *J Biol Chem.* 284:5250-5256 (2009).
 51. D. Zhang, Q. Hou, M. Wang, A. Lin, L. Jarzylo, A. Navis, A. Raissi, F. Liu, and H.Y. Man. Na,K-ATPase activity regulates AMPA receptor turnover through proteasome-mediated proteolysis. *J Neurosci.* 29:4498-4511 (2009).
 52. E.M. Holand W. Scheper. Protein quality control in neurodegeneration: walking the tight rope between health and disease. *J Mol Neurosci.* 34:23-33 (2008).
 53. X. Wang, H. Su, and M.J. Ranek. Protein quality control and degradation in cardiomyocytes. *J Mol Cell Cardiol.* 45:11-27 (2008).

54. M. Niand A.S. Lee. ER chaperones in mammalian development and human diseases. *FEBS Lett.* 581:3641-3651 (2007).
55. D.N. Hebertand M. Molinari. In and out of the ER: protein folding, quality control, degradation, and related human diseases. *Physiol Rev.* 87:1377-1408 (2007).
56. R. Glozman, T. Okiyoned, C.M. Mulvihill, J.M. Rini, H. Barriere, and G.L. Lukacs. N-glycans are direct determinants of CFTR folding and stability in secretory and endocytic membrane traffic. *J Cell Biol.* 184:847-862 (2009).
57. B.W. van Balkom, M. Boone, G. Hendriks, E.J. Kamsteeg, J.H. Robben, H.C. Stronks, A. van der Voorde, F. van Herp, P. van der Sluijs, and P.M. Deen. LIP5 interacts with aquaporin 2 and facilitates its lysosomal degradation. *J Am Soc Nephrol.* 20:990-1001 (2009).
58. J.C. Hou, D. Williams, J. Vicogne, and J.E. Pessin. The glucose transporter 2 undergoes plasma membrane endocytosis and lysosomal degradation in a secretagogue-dependent manner. *Endocrinology.* 150:4056-4064 (2009).
59. C.M. Balut, Y. Gao, S.A. Murray, P.H. Thibodeau, and D.C. Devor. ESCRT-dependent targeting of plasma membrane localized KCa3.1 to the lysosomes. *Am J Physiol Cell Physiol.* 299:C1015-1027.
60. A.R. Subramanya, J. Liu, D.H. Ellison, J.B. Wade, and P.A. Welling. WNK4 diverts the thiazide-sensitive NaCl cotransporter to the lysosome and stimulates AP-3 interaction. *J Biol Chem.* 284:18471-18480 (2009).
61. S. Gastaldello, S. D'Angelo, S. Franzoso, M. Fanin, C. Angelini, R. Betto, and D. Sandona. Inhibition of proteasome activity promotes the correct localization of disease-causing alpha-sarcoglycan mutants in HEK-293 cells constitutively expressing beta-, gamma-, and delta-sarcoglycan. *Am J Pathol.* 173:170-181 (2008).
62. L. Guoand Y. Wang. Glutamate stimulates glutamate receptor interacting protein 1 degradation by ubiquitin-proteasome system to regulate surface expression of GluR2. *Neuroscience.* 145:100-109 (2007).
63. A.K. Holzerand S.B. Howell. The internalization and degradation of human copper transporter 1 following cisplatin exposure. *Cancer Res.* 66:10944-10952 (2006).
64. H. Nakagawa, A. Tamura, K. Wakabayashi, K. Hoshijima, M. Komada, T. Yoshida, S. Kometani, T. Matsubara, K. Mikuriya, and T. Ishikawa. Ubiquitin-mediated proteasomal degradation of non-synonymous SNP variants of human ABC transporter ABCG2. *Biochem J.* 411:623-631 (2008).
65. K. Wakabayashi, H. Nakagawa, A. Tamura, S. Koshiba, K. Hoshijima, M. Komada, and T. Ishikawa. Intramolecular disulfide bond is a critical check point determining degradative fates of ATP-binding cassette (ABC) transporter ABCG2 protein. *J Biol Chem.* 282:27841-27846 (2007).
66. H.M. Jones, K.L. Hamilton, G.D. Papworth, C.A. Syme, S.C. Watkins, N.A. Bradbury, and D.C. Devor. Role of the NH2 terminus in the assembly and

- trafficking of the intermediate conductance Ca^{2+} -activated K^{+} channel hIK1. *J Biol Chem.* 279:15531-15540 (2004).
67. J. Ozols. Degradation of hepatic stearyl CoA delta 9-desaturase. *Mol Biol Cell.* 8:2281-2290 (1997).
 68. C.N. Wang, T.C. Hobman, and D.N. Brindley. Degradation of apolipoprotein B in cultured rat hepatocytes occurs in a post-endoplasmic reticulum compartment. *J Biol Chem.* 270:24924-24931 (1995).
 69. R.H. Moore, A. Tuffaha, E.E. Millman, W. Dai, H.S. Hall, B.F. Dickey, and B.J. Knoll. Agonist-induced sorting of human beta2-adrenergic receptors to lysosomes during downregulation. *J Cell Sci.* 112 (Pt 3):329-338 (1999).
 70. J. Ahlberg, A. Berkenstam, F. Henell, and H. Glaumann. Degradation of short and long lived proteins in isolated rat liver lysosomes. Effects of pH, temperature, and proteolytic inhibitors. *J Biol Chem.* 260:5847-5854 (1985).
 71. H. Hayashi and Y. Sugiyama. 4-phenylbutyrate enhances the cell surface expression and the transport capacity of wild-type and mutated bile salt export pumps. *Hepatology.* 45:1506-1516 (2007).
 72. R.C. Rubenstein, M.E. Egan, and P.L. Zeitlin. In vitro pharmacologic restoration of CFTR-mediated chloride transport with sodium 4-phenylbutyrate in cystic fibrosis epithelial cells containing delta F508-CFTR. *J Clin Invest.* 100:2457-2465 (1997).
 73. L. Colgan, H. Liu, S.Y. Huang, and Y.J. Liu. Dileucine motif is sufficient for internalization and synaptic vesicle targeting of vesicular acetylcholine transporter. *Traffic.* 8:512-522 (2007).
 74. Y. Miyashita and M. Ozawa. Increased internalization of p120-uncoupled E-cadherin and a requirement for a dileucine motif in the cytoplasmic domain for endocytosis of the protein. *J Biol Chem.* 282:11540-11548 (2007).
 75. D. Herring, R. Huang, M. Singh, L.C. Robinson, G.H. Dillon, and N.J. Leidenheimer. Constitutive GABAA receptor endocytosis is dynamin-mediated and dependent on a dileucine AP2 adaptin-binding motif within the beta 2 subunit of the receptor. *J Biol Chem.* 278:24046-24052 (2003).
 76. K. Nakamura and M. Ascoli. A dileucine-based motif in the C-terminal tail of the lutropin/choriogonadotropin receptor inhibits endocytosis of the agonist-receptor complex. *Mol Pharmacol.* 56:728-736 (1999).
 77. I. Hamer, C.R. Haft, J.P. Paccaud, C. Maeder, S. Taylor, and J.L. Carpentier. Dual role of a dileucine motif in insulin receptor endocytosis. *J Biol Chem.* 272:21685-21691 (1997).
 78. M.J. Francis, E.E. Jones, E.R. Levy, R.L. Martin, S. Ponnambalam, and A.P. Monaco. Identification of a di-leucine motif within the C terminus domain of the Menkes disease protein that mediates endocytosis from the plasma membrane. *J Cell Sci.* 112 (Pt 11):1721-1732 (1999).

79. W. Wang, H.H. Loh, and P.Y. Law. The intracellular trafficking of opioid receptors directed by carboxyl tail and a di-leucine motif in Neuro2A cells. *J Biol Chem.* 278:36848-36858 (2003).
80. S.J. Kiland C. Carlin. EGF receptor residues leu(679), leu(680) mediate selective sorting of ligand-receptor complexes in early endosomal compartments. *J Cell Physiol.* 185:47-60 (2000).
81. H.O. Awwad, E.E. Millman, E. Alpizar-Foster, R.H. Moore, and B.J. Knoll. Mutating the dileucine motif of the human beta(2)-adrenoceptor reduces the high initial rate of receptor phosphorylation by GRK without affecting postendocytic sorting. *Eur J Pharmacol.* 635:9-15.
82. Q. Zhang, M. Hong, P. Duan, Z. Pan, J. Ma, and G. You. Organic anion transporter OAT1 undergoes constitutive and protein kinase C-regulated trafficking through a dynamin- and clathrin-dependent pathway. *J Biol Chem.* 283:32570-32579 (2008).
83. M. Miranda and A. Sorkin. Regulation of receptors and transporters by ubiquitination: new insights into surprisingly similar mechanisms. *Mol Interv.* 7:157-167 (2007).
84. M.B. Butterworth, R.S. Edinger, H. Ova, D. Burg, J.P. Johnson, and R.A. Frizzell. The deubiquitinating enzyme UCH-L3 regulates the apical membrane recycling of the epithelial sodium channel. *J Biol Chem.* 282:37885-37893 (2007).
85. E.J. Kamsteeg, G. Hendriks, M. Boone, I.B. Konings, V. Oorschot, P. van der Sluijs, J. Klumperman, and P.M. Deen. Short-chain ubiquitination mediates the regulated endocytosis of the aquaporin-2 water channel. *Proc Natl Acad Sci U S A.* 103:18344-18349 (2006).
86. M. Miranda, K.R. Dionne, T. Sorkina, and A. Sorkin. Three ubiquitin conjugation sites in the amino terminus of the dopamine transporter mediate protein kinase C-dependent endocytosis of the transporter. *Mol Biol Cell.* 18:313-323 (2007).
87. M. Miranda, C.C. Wu, T. Sorkina, D.R. Korstjens, and A. Sorkin. Enhanced ubiquitylation and accelerated degradation of the dopamine transporter mediated by protein kinase C. *J Biol Chem.* 280:35617-35624 (2005).
88. I.M. Gonzalez-Gonzalez, N. Garcia-Tardon, C. Gimenez, and F. Zafra. PKC-dependent endocytosis of the GLT1 glutamate transporter depends on ubiquitylation of lysines located in a C-terminal cluster. *Glia.* 56:963-974 (2008).
89. S.A. Barros, C. Srimaroeng, J.L. Perry, R. Walden, N. Dembla-Rajpal, D.H. Sweet, and J.B. Pritchard. Activation of protein kinase C ζ increases OAT1 (SLC22A6)- and OAT3 (SLC22A8)-mediated transport. *J Biol Chem.* 284:2672-2679 (2009).
90. T. Hatanaka, Y. Hatanaka, and M. Setou. Regulation of amino acid transporter ATA2 by ubiquitin ligase Nedd4-2. *J Biol Chem.* 281:35922-35930 (2006).
91. S. Diestel, D. Schaefer, H. Cremer, and B. Schmitz. NCAM is ubiquitylated, endocytosed and recycled in neurons. *J Cell Sci.* 120:4035-4049 (2007).

92. P. van Kerkhof, M. Sachse, J. Klumperman, and G.J. Strous. Growth hormone receptor ubiquitination coincides with recruitment to clathrin-coated membrane domains. *J Biol Chem.* 276:3778-3784 (2001).
93. B. Varghese, H. Barriere, C.J. Carbone, A. Banerjee, G. Swaminathan, A. Plotnikov, P. Xu, J. Peng, V. Goffin, G.L. Lukacs, and S.Y. Fuchs. Polyubiquitination of prolactin receptor stimulates its internalization, postinternalization sorting, and degradation via the lysosomal pathway. *Mol Cell Biol.* 28:5275-5287 (2008).
94. K.G. Kumar, H. Barriere, C.J. Carbone, J. Liu, G. Swaminathan, P. Xu, Y. Li, D.P. Baker, J. Peng, G.L. Lukacs, and S.Y. Fuchs. Site-specific ubiquitination exposes a linear motif to promote interferon-alpha receptor endocytosis. *J Cell Biol.* 179:935-950 (2007).
95. K. Haglund, S. Sigismund, S. Polo, I. Szymkiewicz, P.P. Di Fiore, and I. Dikic. Multiple monoubiquitination of RTKs is sufficient for their endocytosis and degradation. *Nat Cell Biol.* 5:461-466 (2003).
96. J.M. Bomberger, R.L. Barnaby, and B.A. Stanton. The deubiquitinating enzyme USP10 regulates the post-endocytic sorting of cystic fibrosis transmembrane conductance regulator in airway epithelial cells. *J Biol Chem.* 284:18778-18789 (2009).
97. A.L. Sheldon, M.I. Gonzalez, E.N. Krizman-Genda, B.T. Susarla, and M.B. Robinson. Ubiquitination-mediated internalization and degradation of the astroglial glutamate transporter, GLT-1. *Neurochem Int.* 53:296-308 (2008).
98. P. Duan, S. Li, and G. You. Angiotensin II inhibits activity of human organic anion transporter 3 through activation of protein kinase Calpha: accelerating endocytosis of the transporter. *Eur J Pharmacol.* 627:49-55.
99. S. Li, P. Duan, and G. You. Regulation of human organic anion transporter 3 by peptide hormone bradykinin. *J Pharmacol Exp Ther.* 333:970-975.
100. Y. Mosesson, K. Shtiegman, M. Katz, Y. Zwang, G. Vereb, J. Szollosi, and Y. Yarden. Endocytosis of receptor tyrosine kinases is driven by monoubiquitylation, not polyubiquitylation. *J Biol Chem.* 278:21323-21326 (2003).
101. T. Geetha, J. Jiang, and M.W. Wooten. Lysine 63 polyubiquitination of the nerve growth factor receptor TrkA directs internalization and signaling. *Mol Cell.* 20:301-312 (2005).

6 Curriculum Vitae

QIANG ZHANG

Education

Doctor of Philosophy in Pharmaceutical Sciences

Jan. 2005 – May, 2012

Rutgers University, New Brunswick, New Jersey

Master of Science in Biochemistry and Molecular Biology

Sep. 2001 – Mar. 2004

East China University of Science and Technology, Shanghai, China

Bachelor of Science in Biochemistry

Sep. 1997 – Jul. 2001

East China University of Science and Technology, Shanghai, China

Work Experience


Jun. ~ Aug. 2011

Summer Intern, Clinical Pharmacology, Oncology Business Unit, Novartis Pharmaceuticals Corporation, Florham Park, New Jersey

Mar. ~ Dec. 2004

Scientist, R&D Department, Techwell Biopharmaceutical Co., Ltd, Shanghai, China,

Publications

1. **Qiang Zhang**, Jinwei Wu, Zui Pan, Guofeng You. The role of dileucine in the expression and function of human organic anion transporter 1 (hOAT1). *International Journal of Biochemistry and Molecular Biology*. 2011, 2(1): 31~38.
2. **Qiang Zhang**, Zui Pan, Guofeng You. Regulation of human organic anion transporter 4 by protein kinase C and NHERF-1: altering the endocytosis of the transporter. *Pharmaceutical Research*, 2010, 27(4): 589~596 (Selected for the cover of the issue of April, 2010).
3. **Qiang Zhang**, Mei Hong, Peng Duan, Zui Pan, Jianjie Ma, Guofeng You. Organic anion transporter OAT1 undergoes constitutive and protein kinase C-regulated trafficking through a dynamin- and clathrin-dependent pathway. *Journal of Biological Chemistry*, 2008, 283(47): 32570~32579 (, rated exceptional)
4. Hang Xiao, **Qiang Zhang**, Yong Lin, Bandaru Reddy, Chung S. Yang. Combination of atorvastatin and celecoxib synergistically induces cell cycle arrest and apoptosis in colon cancer cells. *International Journal of Cancer*, 2008, 122(9): 2115~2124

5. Feng Qian, Dongzhi Wei, **Qiang Zhang**, Shengli Yang. Modulation of P-glycoprotein function and reversal of multidrug resistance by (-)-epigallocatechin gallate in human cancer cells. *Biomedicine & Pharmacotherapy*, 2005, 59(3): 64~69
6. **Qiang Zhang**, Dongzhi Wei, Jianwen Liu. In vivo reversal of doxorubicin resistance by (-)-epigallocatechin gallate in a solid human carcinoma xenograft. *Cancer Letters*, 2004, 208(2): 179~186
7. Jiyu Li, Zhiwei Quan, **Qiang Zhang**, Jianwen Liu. Somatostatin enhanced chemosensitivity of gallbladder cancer cell in vitro. *Chinese Clinical Pharmacology & Therapeutics*, 2004, 9(2): 171~173 (Chinese)
8. Zhiwei Quan, Jiyu Li, **Qiang Zhang**, Jianwen Liu. Effect of somatostatin on the growth and cell cycle of human gallbladder cancer cell line. *Journal of Surgery Concepts & Practice*, 2003: 56~58 (Chinese)

Conference Abstracts

1. **Qiang Zhang**, Wonmo Suh, Guofeng You. Protein kinase C (PKC) regulates the trafficking and degradation of human organic anion transporter 3 (hOAT3) in COS-7 cell. AAPS Annual Meeting, Washington, D.C., Oct. 2011
2. **Qiang Zhang**, Jinwei Wu, Guofeng You. A di-leucine motif in the N-terminus of organic anion transporter 1 (OAT1) is essential for protein maturation in COS-7 cell. AAPS Annual Meeting, New Orleans, LA, Nov. 2010
3. **Qiang Zhang**, Zui Pan, Guofeng You. Organic anion transporter 4 (OAT4) undergoes constitutive and protein kinase C-regulated trafficking. AAPS Annual Meeting, Los Angeles, CA, Nov. 2009
4. **Qiang Zhang**, Guofeng You. Protein kinase C (PKC) regulates OAT1-mediated drug transport through clathrin-dependent pathway. AAPS Annual Meeting, Atlanta, GA, Nov. 2008
5. **Qiang Zhang**, Mei Hong, Guofeng You. The activity of human organic anion transporter hOAT1 is down regulated by activation of PKC through accelerating the endocytosis rate of the transporter. AAPS Annual Meeting, San Diego, CA, Nov. 2007